Institute of Neuroscience (IoNS)

Institute of information and communication technologies, electronics and applied mathematics (ICTEAM)

Using Robust and Optimal Control theory to understand handedness and bimanual coordination

David Córdova Bulens

Thesis submitted in partial fulfillment of the requirements for the Ph. D. Degree in Engineering Sciences

Thesis committee:
Philippe Lefèvre (UCL, advisor)
Frédéric Crevecoeur (UCL, advisor)
Jean-Louis Thonnard (UCL)
Olivier White (Université de Bourgogne, France)
Jeroen Smeets (Vrije Universiteit Amsterdam, Netherlands)
Steve Scott (Queen's University, Canada)
Raphaël Jungers (UCL, chair)

Louvain-la-Neuve, 2017.

Acknowledgements

Il y a 4 ans j'ai pris la décision de m'engager dans une thèse dans un domaine qui m'était totalement inconnu, les neurosciences. Ce fut le début d'une belle aventure qui m'a permis d'apprendre énormement et qui m'a beaucoup fait grandir. Tout le long de ce chemin, un grand nombre de personnes m'ont aidé à avancer et à croire que je pouvais y arriver, et je voulais les remercier dans les paragraphes qui suivent.

Pendant cette thèse j'ai eu la chance d'avoir trois promoteurs qui m'ont accompagné. Jean-Louis ton intérêt pour mon travail, l'optimisme sans faille dont tu fais preuve ainsi que ta vue d'ensemble sur le domaine m'ont toujours énormément aidé pour avancer. Frédéric, tes connaissances techniques et ta gentillesse m'ont toujours énormément aidé à progresser et à me sortir des divers problèmes auxquels j'ai fait face, tu m'as bien souvent offert des solutions quand je me sentais perdu. Philippe, ta précision, ainsi que ta capacité à rapidement analyser un problème afin de proposer des solutions efficaces ont toujours été d'une grande aide pour avancer tout le long de la thèse. Tous les trois, vous m'avez offert la possibilité d'explorer ce beau domaine que sont les neurosciences, en me faisant confiance et en me laissant la liberté d'explorer les questions que je souhaitais, tout en m'offrant continuellement votre soutien, ainsi que votre regard extrêmement pertinent. Ça a vraiment été un plaisir d'être encadré par vous et je vous en remercie énormément.

Je tenais aussi à remercier tous les membres de mon jury, le Prof. Olivier White, le Prof. Jeroen Smeets, le Prof. Steve Scott et le Prof. Raphaël Jungers pour leur gentillesse et leur regard extrêmement intéressé et intéressant sur mon travail, ils m'ont permis de grandement améliorer le contenu de ma thèse. Un grand merci aussi à Tyler Cluff pour m'avoir aidé dans mon travail en réalisant des expériences au Canada.

Je voudrais remercier Etienne, Isabelle, Nathalie, Marie-Christine, Cathy, Kira et Véronique pour leur gentillesse et pour toute leur aide, technique et admin-

istrative qui m'a facilité bien des tâches.

Je voulais remercier les anciens et actuels membres d'Eyelab. D'abord, Benoît, Vincent, Thibault, Caro et JJ qui m'ont extrêmement bien accueillis à mon arrivée dans le groupe et qui m'ont aidé à me lancer lors des premiers mois de la thèse. Je tiens évidemment à remercier Allan, avec qui j'ai partagé mon bureau pendant quatre ans et avec qui j'ai eu la chance de partager les bons moments ainsi que les moments difficiles de ma thèse, ça a toujours été un plaisir de discuter avec toi (et de t'écouter), je suis sûr que notre amitié continuera même si on ne partagera plus le même bureau dans l'avenir. Merci évidemment à Nicolas et Florian avec qui j'ai eu la chance de travailler et de discuter au cours de ces quatre années de thèse. Et je ne voudrais pas oublier toute la jeune génération, Laurent, Félicien, Antoine et Ghady que j'ai eu énormément de plaisir à rencontrer, je suis sûr que vous allez faire de l'excellent travail dans l'avenir.

Pendant ma thèse j'ai eu la chance de travailler dans deux instituts: l'ICTEAM et l'IoNS. Je voudrais remercier mes collègues du bâtiment Euler, Corentin, Matthew, PA, François G., Pierre-Yves C, Benjamin, Adrien, Romain, Emilie, Estelle, Aaron et j'en passe qui ont rendu toute mon expérience et la vie dans le bâtiment Euler extrêmement agréable. Je voudrais aussi remercier mes collègues de Woluwé, Cecile, Charlotte, Camille, Sylvie, Roxane, Julien, Sebastien, Emanuel, Diana et tous les autres avec qui c'était toujours un plaisir de discuter.

Je voulais aussi remercier du fond du cœur mes amis et en particulier Arnaud, Pierre, Claire, Maki, Aimeric, Thibault, François, Romain, Nash, Victor, Marine, Lena et Margay pour l'aide qu'ils m'ont apporté en participant à mes expériences mais surtout pour leur soutien et leur amitié. Vous avez toujours été là pour partager les bons moments et pour me soutenir dans les moments difficiles, et il y en a eu, et je vous en remercie de tout coeur. Je voulais aussi remercier Stéphanie qui m'a soutenu pendant une longue partie de ma thèse et qui m'a beaucoup aidé pour avancer et grandir. Je tiens aussi à remercier les Taitetus avec qui j'ai pris énormément de plaisir au cours de ces années, ainsi que tous mes autres amis qui m'ont aidé et avec qui j'ai partagé des choses tout au long de ces quatre années. Je dois aussi adresser un grand merci à toutes les personnes qui ont participé à mes expériences et que je n'aurais pas cité.

Et pour finir je souhaiterais remercier du fond du cœur ma famille, Maman, Lucho, Pablo et Chloé, Hector et Eli et Violette pour toute l'aide et le soutient qu'ils m'ont apporté. Je sais que je peux toujours compter sur vous, et vous avez toujours été là pour me soutenir.

Merci à tous.

Abstract

In this thesis, we study the neurophysiological basis of handedness or the individual preference for use of a hand, known as the dominant hand. Any motor task involves the decision of which arm to perform it with or how the two arms must coordinate. If using only one arm, humans show a preference to use their "dominant" arm, which is often more dexterous and skillful than the other one. Hand dominance also impacts bimanual coordination, as a different role is associated to each arm during a bimanual task. Such differences across the two arms cannot be explained based on anatomical aspects, since the two arms are equally strong and have the same freedom of movement. It has been reported that each arm has a specialized behavior, with the dominant arm having a better trajectory control and the non-dominant arm being more stable in front of perturbations. And yet it is still unclear why we have a dominant arm and what the neurophysiological basis of handedness is.

Amounting evidence has highlighted the importance of feedback when performing skilled movements, however, there is no control framework able to account for the differences in performance across limbs. Given the importance of feedback in motor control, we suspected that handedness was likely related to distinct feedback control strategies. In this thesis, we use optimal and robust control theory to model different feedback control strategies, and show that such distinct strategies can capture the differences in behavior observed across the two arms. We also study how the central nervous system coordinates the two arms during a bimanual task. Using optimal control theory, we highlight the impact of the joint configuration of the upper-limbs on how the two arms share the effort during a bimanual task. We show that the arm with the best spatial relationship between effort and target goal is the arm that produces the most significant effort during a bimanual task.

Altogether, the results of this thesis offer a new perspective on the differences in behavior across the two arms and highlight the fact that handedness arises from distinct feedback control strategies.

Contents

CHAPTER 1

Introduction

Consider the task of reaching for an object positioned close to your body. Before even starting the movement, the nervous system must decide which effector to use in order to reach towards the object. While this choice is influenced by parameters such as effort, success rate (Schweighofer et al., 2015) and by the biomechanics of our limbs (Cos et al., 2011), most individuals have a strong preference to use one arm over the other. This strong preference is commonly named "handedness". More precisely, handedness is defined as the tendency to use either the right or the left hand more frequently and more skilfully than the other. Often, the more regularly used arm, i.e. the dominant arm, is considered to be more skilled and dexterous than the other arm. For instance, most individuals will be able to easily write with their dominant hand but will face strong difficulties when writing with their non-dominant hand. Moreover, while the dominant hand is often considered more skilled in every aspect than the non-dominant hand, it has been shown that asymmetries in performance arise from specialization in the behavior of each arm (Sainburg, 2002). While such limb asymmetries in motor behavior have been observed in many animal species (Vallortigara and Rogers, 2005), humans appear special because of the large population level bias that exists for using the right arm over the other. Indeed, estimations based largely on self-report questionnaires have revealed that 9 out of 10 individuals have a strong preference for using their right-hand (Oldfield, 1971; Gilbert and Wysocki, 1992). Such a strong bias towards right-handedness is surprising given that the two arms are anatomically symmetrical and generally equal in terms of strength. The strong influence of handedness in our manual motor behavior as well as this strong bias towards right-handedness have been largely explored in the literature. However, despite the prominence of this feature in our behavior, no consensus exists on its origin. In this work we

will use the terms dominant and non-dominant hand for the sake of simplicity.

In this section we first will review the knowledge that has been gained about handedness, its influence on motor performance during unimanual movements and how it influences bimanual coordination. Second, because control theory is an important tool that will be used in the following chapters we introduce optimal control theory and how it has been used in the study of human motor control. Finally we present the aim of the work presented in this thesis.

1.1 Handedness

1.1.1 Origins of the bias towards right-handedness

It has been suggested that handedness finds its origin in genetics. Genetic based theories hypothesize the existence of particular genes responsible for the development of right-handedness (Annett, 1978, 1981, 1998; McManus, 1985). Firstly, Annett proposed the right-shift theory in which she hypothesizes that there is no gene directly responsible for right or left handedness. Instead she suggests that a particular gene, named RS+, induces the development of speech in the left hemisphere which incidentally increases the chances of greater skill in the right hand, mainly controlled by the left hemisphere. Secondly, McManus proposed the existence of two different genes, one that would directly lead to the development of right-handedness while the other would lead to a 50% chance of right or left handedness. However, all the above-mentioned genetic theories suffer from one major weakness which is that, to date, there has been no success in finding and isolating the genes responsible for right-handedness.

Environmental and socio-cultural factors have also been hypothesized to play a role in the existent bi-as towards right-handedness. Indeed, several studies have reported that there is a larger proportion of right-handed individuals in the older sectors of the population (Beukelaar and Kroonenberg, 1986; Gilbert and Wysocki, 1992). This leads to the hypothesis that a large amount of left-handed individuals might have been forced by social pressure to become right-handed. However, this argument is not very strong as studies by Porac and colleagues have shown that arm preference is not easily changed even when environmental pressure is important (Porac et al., 1986). Indeed, most attempts to change handedness either fail or lead to motor performance that is inferior to that of the original dominant arm (Porac et al., 1990).

Altogether, while it is possible that both genetics and social environment play a role in the definition of handedness and influence the bias observed in the population towards right-handedness, more evidence is required in order to

confirm their impact.

1.1.2 Differences in motor output

One of the simplest ways of studying differences between the two arms is the quantification of performance during the generation of motor tasks. Indeed, asymmetries in performance of the two arms have been observed in a variety of tasks. For instance, Annett et al. (1979) tested right-handed individuals and showed that the amount of time necessary to place pegs in small holes was significantly shorter when they used their dominant right arm. They also reported that participants using their non-dominant arm performed more corrective movements, which caused the increased time required to perform the task. Based on this result it was argued that the non-dominant arm motor output suffered from a greater variability when compared to the dominant arm. Similar conclusions have been drawn from the study of tasks such as line-tracing, aiming, tapping (Kalisch et al., 2006) or during the production of force (Salimpour and Shadmehr, 2014; Salimpour et al., 2015). The lesser variability associated with the control of the dominant arm is often assumed to be the cause of the preference, for human subjects, to select their dominant arm when performing unimanual tasks.

In addition to differences in the variability of motor output, several fundamental differences in movement strategy have also been highlighted in the literature. Sainburg and Kalakanis (2000) studied the inter-segmental coordination patterns of the dominant and non-dominant arm during targeted reaching movements. They reported that the dominant arm had a better control of inter-segmental dynamics than the non-dominant arm. More precisely, they demonstrated that movements performed with the dominant arm were generated by a different pattern of joint torques than movements performed with the non-dominant arm; the movements of the dominant arm were performed through a more efficient intra-limb torque coordination. Subsequent studies also reported a dominant arm advantage for trajectory control (Bagesteiro and Sainburg, 2002; Sainburg, 2002; Wang and Sainburg, 2003). Based on these fundamental differences in the control of the two limbs, Sainburg (2002) proposed the hypothesis of a dynamic-dominance of handedness. Contrary to many other behavioral approaches to handedness, which assume that the non-dominant arm is inferior for most aspects of movement, the dynamic dominance hypothesis proposes the idea that each arm specializes on different aspects of movement. Results supporting this idea were first presented by Bagesteiro and Sainburg (2003) who looked at elbow flexion movements with, on random trials, an artificial increase in the subjects arm weight. They observed that the dominant arm tends to overcompensate the effects of the load leading to overshoots whereas the non-dominant arm effectively compensates the change in

load. This result suggests a specialized role of the non-dominant arm in load compensation. Such a specialization of the left arm was further highlighted in subsequent studies who reported advantages of the non-dominant arm in the transfer of limb position information (Wang and Sainburg, 2003; Bagesteiro and Sainburg, 2005). Further support for this non-dominant arm advantage was found by Yadav and Sainburg (2014a) in which the authors asked subjects to perform reaching movements while being confronted to a curl force field. The results highlighted better performance, i.e. lesser deviation, less jerk, etc., of the non-dominant arm when faced with an unpredictable curl force field and a better performance of the dominant arm when faced with a predictable force field. More recently, a study by Aoki et al. (2016) reported a similar specialization of the two limbs during index finger movements performed on a small touch screen.

To explain the specialized behavior of each limb, Yadav and Sainburg (2014a) hypothesized that differences in motor output across arms originate from asymmetries in the use of predictive and impedance control mechanisms. More precisely, they suggest that the dominant arm relies more on predictive control mechanisms to perform a movement whereas the non-dominant arm relies more on impedance control mechanisms. According to this hypothesis, the greater reliance of the non-dominant arm on impedance control leads to the better performance in load compensation. The authors formalized this hypothesis in a subsequent study (Yadav and Sainburg, 2014b) in which they used a controller mixing predictive and impedance control mechanisms to predict the behavior of the two arms during reaching movements. The controller they developed started movements using predictive control mechanisms and switched to impedance control mechanisms during the latter part of the movement. They observed that differences in behavior across the two arms could be explained by a different switching time between these two mechanisms, with the non-dominant arm controller switching to impedance control earlier than the dominant arm.

1.1.3 Physiological differences related to handedness

Various results suggest the existence of hemispheric differences of brain regions in the control of movement (Haaland and Harrington, 1989a,b, 1994). It is often assumed that control of the upper limbs is lateralized with the left hemisphere playing a more significant role in the control of the right arm and vice-versa. In the studies by Haaland and Harrington, performance during guided reaching movements of healthy individuals and individuals with right or left hemispheric brain damage, due to stroke, was compared. They reported that injuries in the left or right hemisphere lead to different deficits in mo-tor output in the ipsi-lesional arm. Indeed, individuals with left hemispheric damage presented an in-crease in reaction time (Haaland and Harrington, 1989b, 1994) whereas

individuals with right hemispheric damage presented a reduced accuracy in the final target position (Haaland and Harrington, 1989a). However, given the intrinsic variability of brain lesions contradictory results have been reported (Fisk and Goodale, 1988; Haaland and Harrington, 1996).

More recently, a study by Schaefer et al. (2012) suggested that the deficiencies observed in brain lesioned patients were a reflection of specialization of hemispheric brain regions for particular control mechanisms. They showed that individuals with right hemisphere damage had difficulties terminating their movements with their less affected ipsi-lesional arm through a deficit in the timing of online corrections. In addition, they showed that left hemisphere damage was associated with poor intersegmental coordination. Subsequent studies on brain lesioned individuals provided new results supporting this hypothesis (Mani et al., 2013). Mutha and colleagues suggested that such hemispheric specialization were compatible with the specialized role associated with each arm by the dynamic dominance hypothesis (Mutha et al., 2012). This claim was later emphasized by studies that presented other differences between individuals with left and right hemispheric lesions that were compatible with the dynamic dominant hypothesis (Mani et al., 2013; Mutha et al., 2013).

Altogether these results suggest that hemispheric brain regions specialize in different aspects of control, which lead to asymmetrical arm performance. However, it is important to note that the high variability in the characteristics and positions of brain lesions leads to rather inconsistent and hardly reproducible results.

1.1.4 Differences in the use of sensory feedback

It is possible that asymmetries in motor performance across arms arise from differences in the use of sensory feedback. This topic has been largely documented in the literature with most studies focusing on either visual feedback or proprioceptive feedback.

Asymmetries in the use of visual feedback were first revealed by Honda (1982) who showed that, in right-handed individuals, movements of the right hand are more dependent on vision than movements of the left hand. More precisely, he observed that right hand movements are preferentially monitored by gaze during a bimanual movement which leads to better performance from the right arm. Subsequent studies revealed that modifying parameters of visual feedback given to participants impacted the asymmetries in performance across arms. For instance, the size of the target presented to participants will greatly impact the performance of the two arms; the smaller the target the greater the asymmetries in performance between arms (Elliott et al., 1995; Carson et al., 1996; Mieschke et al., 2001). Other studies such as the one by Roy and colleagues modified

the amount of light available to participants when per-forming arm movements and showed enhanced performance of the dominant arm in all light conditions (Roy et al., 1994). In addition, a recent study by (Przybyla et al., 2013) showed that removing visual feed-back improved the relative performance of the non-dominant arm and increased the choice to use this arm for targets near the midline during reaching movements.

Proprioceptive feedback plays an important role in the control of upper-limb movements as it provides the central nervous system (CNS) with information about position and velocity of body segments and muscle tension. The study of asymmetries across limbs in the use of proprioceptive feedback has led to somewhat contrasting results. Indeed, some studies have reported non-dominant arm advantages during position matching tasks (Goble et al., 2006), whereas others have observed no difference across arms in similar position matching tasks (King et al., 2013). Subsequent studies by Goble and Brown reported that asymmetries in the use of proprioceptive feedback during static position matching tasks are task-dependent, and are more prominent when memory or inter-hemispheric transfer is needed (Goble and Brown, 2007). Similarly, during a dynamic target matching task, advantages of the non-dominant arm were reported in the matching of target acceleration in certain conditions (ipsilateral remembered) but not other conditions (Goble and Brown, 2009). Altogether, these results suggest that the non-dominant arm has a slight task-dependent advantage in the use of proprioceptive feedback, but whether such an advantage is a possible source of differences in performance observed during reaching tasks has remained largely unexplored.

1.1.5 Differences in learning across arms

In addition to asymmetries in motor output, several studies have reported asymmetries across arms in the learning of a new motor task. Very recently, a study by McGrath and Kantak (2016) observed important differences in learning between the dominant and the non-dominant hand of right-handed participants during a track tracing task; Right-handed participants improved much more quickly with their dominant arm. They also reported reduced asymmetric learning in left-handed subjects when compared with right-handed subjects. Similar observations were reported by Yadav and Sainburg (2014b) who reported that when performing a reaching task with a predictable force field, the dominant arm adapts its trajectory more rapidly across trials than the non-dominant arm. Interestingly, greater activation in brain regions is observed during non-dominant arm learning when compared with dominant arm learning (Aznárez-Sanado et al., 2013), suggesting a greater complexity in the learning of a motor task with the non-dominant arm. These results suggest advantage of the dominant arm during the learning of a motor task that results in a faster

improvement rate across trials.

Complementing the differences observed in the learning rate of the two arms, studies have observed asymmetries in the transfer of skills learned with one arm to the other arm. For instance, learning a visuomotor rotation task with the dominant arm improved the final position accuracy in subsequent trials performed with the non-dominant arm. In contrast, learning a visuomotor rotation with the non-dominant arm lead to an improvement in the initial direction of subsequent dominant arm movements confronted to the same perturbation (Sainburg and Wang, 2002; Wang and Sainburg, 2003). Similar results were found in the learning of novel inertial dynamics (Wang and Sainburg, 2004). However, in this task Wang and Sainburg (2004) observed that initial learning with the dominant hand leads to improved performance of the non-dominant hand, while initial learning with the non-dominant hand does not lead to significant improvement of performance of the dominant hand. More in line with the results from Sainburg and Wang concerning visuo-motor rotations, recent studies by Carroll and colleagues reported significant transfer of non-dominant arm skill to the dominant arm. They showed that new visuo-motor maps encoded with one limb are immediately available to the opposite limb (Carroll et al., 2014). Moreover, they showed that adaptation to a viscous force field with the non-dominant limb generalizes significantly to the dominant limb (Carroll et al., 2016). Together with Joiner et al. (2013), the studies by Carrol and colleagues reported that improvements after transfer of learning are primarily observed in the early phases of movement. In addition to these results a recent study by Lefumat and colleagues showed that inter-limb transfer of learning from the dominant to the non-dominant arm is determined by variability of motor learning and laterality of arm movements (Lefumat et al., 2015). This result indicates that the larger the asymmetries in performance across arms, the more important the transfer of learning from the dominant arm to the non-dominant arm.

1.1.6 Effect of age on handedness

The effect of aging on handedness has been subject to debate in recent years. Some studies suggest that aging has no effect on hand dominance, whereas other studies suggest that aging leads to a reduced effect of hand dominance. For instance, two recent studies performed with participants spanning from childhood to old age did not observe differences in performance between young and old adults in various tasks such as grasping and the construction of an object (Gonzalez et al., 2014), or connecting boxes and moving the hands through mazes (Gooderham and Bryden, 2014). In contrast to these results, it has been reported that dominant hand performance decreases more significantly with increasing age than non-dominant hand performance (Kalisch et al., 2006).

More precisely, in a series of tasks such as line tracing, tapping or holding a position steady, Kalisch and colleagues observed reduced differences in performance across arms with increasing age. A similar evolution with age was also observed during a bimanual force production task (Salimpour and Shadmehr, 2014; Salimpour et al., 2015). In this study, variability of unimanual force production was measured and used as a predictor of performance during the bimanual task. While young participants presented important differences in unimanual force production variability across arms, no such difference in unimanual force output variability was observed in older participants. Another study also reported a decline in motor learning with age for the dominant hand but not for the non-dominant hand (Cirillo et al., 2010). While contrasting results have been found, altogether these results point towards a reduced asymmetry in performance across arms with increasing age.

1.2 Bimanual coordination

Coordinating the movement of the two limbs to perform a single task poses several new challenges to the CNS. For instance, consider tapping at a regular rhythm with one hand and an accelerated rhythm with the other hand. While doing each separately is very easy, the combined performance results in substantial interference. This indicates that principles of inter-limb coordination are unique and cannot be inferred from the laws of single arm movements.

1.2.1 Temporal and spatial constraints of inter-limb coordination

Analyzing the relative phase between the two limbs has allowed revealing clear temporal preferences during bimanual tasks. During cyclical bimanual movements, it has been shown that in-phase coordination, i.e. mirror symmetrical movements, is the more accurate and stable mode (Kelso, 1984; Carson, 1995; Jirsa et al., 1998) and requires less attention than anti-phase mode (Temprado et al., 1999). When performing anti-phase coordinated movements an increase in movement frequency will ultimately lead to a phase transitions towards mirror symmetrical mode. Moreover, phase patterns that differ from in-phase or anti-phase coordination are more difficult to perform and often require intensive training before being performed successfully. With respect to finger tapping, a distinction is made between simple rhythms in which one rhythm is an integer multiple of the other (such as 1:1, 2:1 or 3:1), and polyrhythms in which this condition is not met (such as 3:2). Polyrhythmic finger tapping is more difficult to perform and shows higher variability (Deutsch, 1983; Treffner and Turvey, 1993; Peper et al., 1995a). Moreover, higher order ratios (such as 5:4) are less

stable than lower-order ratios (3:2, 2:2 or 2:1), often resulting in transitions to lower-order ratios when increasing tapping frequency (Treffner and Turvey, 1993; Peper et al., 1995b).

Spatial constraints can also be easily revealed with simple line drawing tasks. Indeed, when drawing lines of different amplitudes, one with each hand, a tendency for the amplitudes to become similar emerges (Diedrichsen et al., 2001; Swinnen, 2002). It has also been revealed that movement direction constraints coordination. Drawing parallel lines in front of you is easy whereas drawing orthogonal lines is likely to give interference in the directional specification of both limbs (Jirsa et al., 1998). In addition to the preference to move both limbs together towards and away from the body midline in the mediolateral plane (same muscles, different directions), bimanual movements performed in the sagittal plane (same muscles, same directions) are produced with even higher stability. This suggests the existence of two constraints that reinforce each other to improve performance during coordinated movements: the principle of homologous muscle grouping and of direction in extrinsic space (Swinnen et al., 1997, 1998; Lee et al., 2002). It is worth noting that directional constraints are also apparent when arm and leg movements are performed together: Segments movement in the same direction are performed more easily than movements in different direction (Baldissera et al., 1982; Kelso and Jeka, 1992; Serrien and Swinnen, 1997). Therefore, these results suggest that directional coding could be more abstract than strictly referring to muscle homology principles.

Another interesting constraint proper to bimanual coordination arises when the two arms act together to achieve a single objective. Indeed, in this context there is redundancy in the way task success can be achieved, with different coordination patterns leading to successful performance during a task. For instance, steering an automobile can be performed using a single arm or a combined effort of the two arms. When performing such bimanual tasks the brain will consistently appoint one arm as the prime actor (Johansson et al., 2006; Theorin and Johansson, 2010). Rather surprisingly, it has been reported that the choice of the acting hand is flexible and is determined by spatial relationships between hand actions and goal motions (Johansson et al., 2006). More precisely, the hand that experiences the most natural directional relationship between forces generated and desired motion consequences is appointed as prime actor.

1.2.2 Handedness in bimanual coordination

Handedness has been shown to impact the way the arms are coordinated during a bimanual task. Indeed, as mentioned earlier, the control of the dominant arm is often associated with lesser variability in motor output leading to a reduced number of corrections during a unimanual task (Kalisch et al., 2006). The reduced variability in the control of the dominant arm has been shown to impact

the distribution of forces across arms during a bimanual isometric force task (Salimpour and Shadmehr, 2014; Salimpour et al., 2015). More precisely, differences across arms in unimanual variability during isometric force production predicted the distribution of forces across arms during a subsequent bimanual force production task. Moreover, Salimpour and Shadmehr were able to artificially modulate the unimanual variability in force production of the two arms through the use of transcranial direct current stimulation (tDCS). They showed that changes in unimanual force production variability lead to corresponding changes in the distribution of forces during the subsequent isometric bimanual force task.

In addition to these results, an asymmetrical use of the two arms compatible with the idea of a specialized role of each arm suggested by the dynamic dominance hypothesis has been observed during manipulation tasks (Guiard, 1987). For instance, when manipulating various pieces in order to construct an object, the dominant arm is often assigned as prime actor and given an exploratory role while the non-dominant arm is used in a supporting role to stabilize the object being grasped (Stone et al., 2013).

1.2.3 Brain regions associated with bimanual coordination

The supplementary motor area (SMA) has traditionally been associated with the control of bimanual coordination patterns. However, there is mounting evidence to assign the control of bimanual coordination to a network rather than a single locus (Swinnen, 2002). Studies using medical imaging have studied rhythmical tasks involving either bilateral finger tapping (Goerres et al., 1998; Jäncke et al., 2000; Immisch et al., 2001; Nair et al., 2003) or forearm and wrist movement (Toyokura et al., 1999; Tracy et al., 2001). These studies have revealed the activation of a general sensorimotor network that is similar to the one observed during unimanual tasks (Swinnen, 2002), hence suggesting that a specialized "coordination controller" structure does not appear to exist.

To identify coordination related areas, activation levels measured during bimanual coordination tasks have been compared with activation levels during unimanual tasks. This revealed an increased coordination effort from the nervous system that exceeds the sum of single effector demands (Toyokura et al., 1999, 2002; Tracy et al., 2001). More precisely, an increased activation of the primary motor cortex (M1), premotor cortex (PM) and SMA (Toyokura et al., 1999, 2002) as well as the cerebellum were identified (Tracy et al., 2001). Given the distributed nature of cerebral control of inter-limb coordination it is not surprising that patients who suffer from brain lesions or neurodegenerative disorders show deficits in bimanual coordination. Evidence of such deficits has been found in patients with lesions in the cerebellum (HOLMES, 1917; Brown et al., 1993; Serrien and Wiesendanger, 2000), the SMA and/or cingulate cor-

tex (Laplane et al., 1977; Dick et al., 1986; Stephan et al., 1999), the corpus callosum (Serrien et al., 2001a) and in the parietal cortex (Serrien et al., 2001b; Jackson et al., 2000). Lesions to the left hemisphere affect bimanual coordination more significantly than right-hemisphere lesions (Wyke, 1971), which is in agreement with fMRI studies that revealed a greater involvement of the left hemisphere during bimanual coordination (Jäncke et al., 1998).

It is also well known that neuronal interactions exist when bimanual actions are performed (Swinnen, 2002; Rokni et al., 2003; Swinnen and Wenderoth, 2004; Carson, 2005). The functional role of these neuronal interactions remains unclear and they are often considered as interference that must be overcome when performing a bimanual task (Swinnen, 2002). An example of such interference is the above described difficulty to perform polyrithmic tapping with the two arms. However, recently a novel interpretation of the function of these neuronal interactions was proposed by Yokoi and colleagues, who suggested that these neuronal interactions might play a crucial role in the flexible control of bimanual movements (Yokoi et al., 2011). Indeed, they showed that the neural controller of each arm is capable to predict and adapt to mechanical interactions resulting from movement of the opposite arm (Yokoi et al., 2011),they showed that adaptation to a force field by one arm was influenced by changes in movement direction of the opposite arm, with the non-dominant arm being more influenced than the dominant arm. This poorer motor generalization of the non-dominant arm pattern lead the authors to suggest that the primitives of the non-dominant arm respond more sensitively to the kinematics of the opposite arm (Yokoi et al., 2014). However, it is worth noting that there is a confusion about the exact definition of motor primitives and synergies, which have been shown to be task-dependent and not to generalize across various tasks (Todorov and Ghahramani, 2004).

1.2.4 Use of sensory feedback

Another interesting aspect of bimanual tasks is that the nervous system receives task relevant sensory information from the two arms simultaneously. Recent studies have suggested an asymmetric use of the proprioceptive feedback coming from the two arms (Wong et al., 2014). More precisely, while the brain receives information from the two arms, it principally uses proprioceptive feedback from the limb with the best proprioceptive acuity to perform the bimanual movement (Wong et al., 2014). Other studies have reported a more equilibrated use of the proprioceptive information coming from the two arms, such that perturbing proprioceptive feedback influences the temporal aspects of inter-limb coupling, but not the spatial aspects of movement (Verschueren et al., 1999; Steyvers et al., 2001). More precisely, perturbing proprioceptive feedback of one arm during a bimanual circle drawing task, with vibrations being applied to arm

muscles, leads to increased phase lag differences in movement of the two arms but no difference in spatial characteristics of the movement of the unperturbed arm. A subsequent study by Kazennikov and Wiesendanger (2005) confirmed the importance of proprioceptive feedback for the temporal aspects of bimanual movements. In addition to the importance of proprioceptive feedback on the temporal aspects of movement, improved positional sense during bimanual tasks when compared with unimanual tasks has been observed. Indeed, in a task were subjects had to indicate the sensed position of one arm using a laser pointer attached to their head, participants showed a smaller bias during bimanual performance than during unimanual performance (Kuehn et al., 2015). Altogether this suggests that proprioceptive feedback plays a very important role in the coordination of bimanual movements as it impacts the temporal aspects of the movement.

Visual sensory feedback also impacts the temporal aspects of movement during a bimanual task. Indeed, an increased fixation of the non-dominant left-hand during bimanual tasks leads to a reduction in temporal phase lags between the two hands (Pellegrini et al., 2004). Interestingly, during bimanual movements performed by right-handed participants the left-hand target is preferentially fixated by gaze to account for asymmetries in performance across arms (Riek et al., 2003). In line with these results, Srinivasan and Martin (2010) reported that the movement of the non-dominant hand during a bimanual task relies more on visual feedback than the movement of the dominant hand. Indeed, when faced with competing visual demands, left hand guidance required more visual information of the target while right hand control could proceed until the terminal stages of movement with the target in the peripheral field of view.

1.2.5 Learning bimanual motor tasks

When an error occurs during a bimanual task it can be caused by one of the two limbs or a combination of both, and the CNS must decide to which limb to attribute the error to in order to correct for this error. It has been hypothesized that, during a bimanual task, errors are attributed to the most likely source, which is often considered to be the non-dominant arm. Such a behavior has been observed during a bimanual reaching task in which both arms drive a single cursor that is perturbed using a visuo-motor rotation (White and Diedrichsen, 2010). The attribution of the error to the non-dominant arm led to greater adaptation of the behavior of this arm in subsequent trials. Similar results were presented by Reichenbach et al. (2013), who reported that the assignment of the error to the non-dominant arm leads to a greater adaptation of the feedback gains in this arm. The assignment of error to the non-dominant arm was also observed in tasks involving a single cursor driven by the movement of the right arm. Indeed, Kasuga and Nozaki (2011) performed a bimanual task receiving

feedback from a single cursor representing either the position of one hand or the average position of the two arms. They showed that perturbing the movement of a single cursor assigned to the dominant hand lead to an adaptation in the behavior of the two arms suggesting the presence of cross-talk in credit assignment. These results put forth a tendency to attribute error to the non-dominant arm during a bimanual task and, therefore, to adapt the movement of this arm in a more significant way than the movement of the dominant arm in order to correct for task error.

1.3 Optimal control theory in neuroscience

In recent years optimal control theory has emerged as a powerful theoretical background able to capture many phenomena observed in human motor control. Optimal control theory do not assume the separate presence of a feedback and a feedforward controller. The general idea underlying control theory is that a controller generates motor commands based on inverse models and feedback control policies (see Fig. 1.1). These motor commands are sent to the limb and to the forward model for internal processing. Based on this motor command, the forward model computes a prediction that is then combined with sensory feedback to produce an estimate of the current state of the system. The estimate is used as feedback in the control loop (Shadmehr and Krakauer, 2008). It is worth noting that optimal control makes several assumptions on the system itself (which must be linear) as well as on the disturbances that are applied on the system (the distribution of disturbances is assumed to be known). Several improvements adaptations have been integrated to this framework to bring it closer to realistic systems (Todorov, 2005; Li and Todorov, 2007; Crevecoeur et al., 2011).

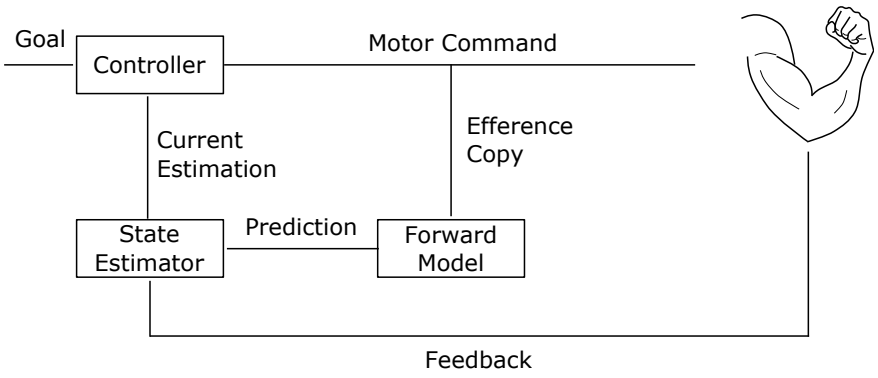

Figure 1.1: Computational model for motor control

The main force of optimal control theory is that it does not enforce partic-

ular trajectories or behavior but uses feedback in an intelligent way in order to correct only for deviations that interfere with task goals (Todorov and Jordan, 2002). From this framework, task-constrained variability, goal-directed corrections, motor synergies, controlled parameters, simplifying rules and discrete coordination modes emerge naturally.

Optimal control theory provides valuable insights into the flexible and task-dependent human motor-control, as it is capable to make accurate quantitative predictions concerning several motor behaviors. For instance, during a reaching movement with a perturbing force applied on the hand, participants modulate their corrective response dependent on the size of the target to reach, which is accurately predicted by optimal control (Nashed et al., 2012). Moreover, another implication of optimal control theory is that reflexes, like voluntary control, support a rich assortment of behaviors (Pruszynski and Scott, 2012).

In the context of bimanual reaching movements, corrective responses to perturbations applied on one hand are modulated dependent on whether the task is performed with a single cursor (at the average position of the two hands) or with two cursors (one for each hand) (Diedrichsen, 2007; Diedrichsen and Dowling, 2009), with such a behavior being accurately predicted by optimal control theory.

Altogether these results highlight the valuable insights optimal control theory provides on human motor control. However, while optimal control theory has been largely used to explore different particularities of human motor control, to the extent of our knowledge it has not yet been used to explore inter-limb differences in motor behavior.

Similarly to optimal control theory, robust control theory has been recently introduced in the neuroscience research field (Ueyama, 2014; Cluff et al., 2015), and provides an interesting theoretical background to understand how the nervous system deals with the uncertainty associated with the internal models used for motor control. For instance, A recent study by Cluff et al. (2015) showed that optimal and robust control framework could capture differences in performance and learning across participants.

1.4 Aim of this work

The overall aim of the work presented in this thesis is to gain greater understanding on the control mechanisms underlying the inter-limb asymmetries in motor output during the production of unimanual and bimanual movements. To do so, we use optimal control as well as robust control theory to explore these asymmetries, and hence bring forth a new hypothesis concerning the origin of

these asymmetries.

Chapter 2 provides information about the mathematical theory underlying optimal control theory and robust control theory, in order to facilitate the use of these tools in the subsequent Chapters.

In Chapter 3 we explore the asymmetries in performance across arms during unimanual movements using optimal and robust control theory. Indeed, while specialized behavior of each arm has been largely reported, the control mechanisms underlying such specialization are not clearly understood. Currently, the main hypothesis to explain differences in performance across arms is that the non-dominant arm relies more heavily on impedance control to perform movements.

Although attractive, this hypothesis implies that participants can modulate the joint mechanical impedance of their limb to modify behavior, presumably through the combined activation of agonist-antagonist pairs of muscles acting on each joint (Hogan, 1985; Burdet et al., 2001). However, the intrinsic impedance of muscles is quite low at spontaneous levels of activation, and the presence of co-contraction mostly impacts the gain of the stretch reflex (Pruszynski et al., 2009; Crevecoeur and Scott, 2014). Furthermore, what is often referred to as the limb stiffness includes the contribution of reflexes and early voluntary responses (up to ~ 300ms, Burdet et al. (2000)), which is known to largely depend on the neural control policy (Scott, 2016). Altogether these observations suggest that inter-limb differences in behavior are due to the use of different control strategies rather than a systematic modulation of the default, or feed-forward muscle activity.

We propose a new hypothesis to explain the differences in behavior that are generally observed across arms. We suggest that differences in the uncertainty associated with internal models of each arm lead to the use of different control strategies. More precisely, we hypothesize that the non-dominant arm has a greater uncertainty associated with its internal model, which leads to the use of a control strategy that is more robust but less flexible, while the dominant arm may have better internal representations, and afford control strategies that are more efficient but also fragile against model errors. We show that control-theoretic solutions obtained by making different assumptions about the nature of the unknown disturbance (i.e. robust or optimal control) can capture this inter-limb difference during learning of a reaching task in the presence of a force field. Moreover, we provide physiological evidence suggesting that better performance during initial exposure to a force field is not related to an increase in muscle activity.

In Chapter 4 we explore how responsibility is shared across limbs during bimanual tasks. To do so, we used optimal control theory to predict the optimal distribution of force across arms, based solely on biomechanical aspects, during

an isometric force production task similar to the one studied by Salimpour and Shadmehr (2014). We compared the predictions of the model to experimental data from right-handed and left-handed individuals to determine the effect of biomechanics and handedness on the behavior of participants. We highlight the fact that handedness has little influence on the distribution of effort across the limbs, and show that biomechanics define a preferential direction of force production for each arm, with the preferential direction of the two arms determining the distribution of effort across arms during the bimanual task. Our results expand the results of Johansson et al. (2006), where it was suggested that the choice of the prime actor between the two arms was driven by spatial relationships between hand action and goal motions, and highlight that biomechanical configuration of the upper-limbs limbs plays a determinant role in this relationship.

In Chapter 5 we summarize the findings of this work, discuss its limitations and provide a series of open questions that remain to be explored using the framework presented in this thesis.

1.5 Publications and communications

Published

- **Barrea A, Cordova Bulens D, Lefevre P, Thonnard J-L**. *Simple and Reliable Method to Estimate the Fingertip Static Coefficient of Friction in Precision Grip*. IEEE Trans Haptics 9: 492–498, 2016.
- **Cordova Bulens D, Crevecoeur F, Thonnard J-L, Lefèvre P**. *Optimal use of limb mechanics distributes control during bimanual tasks*. Journal of Neurophysiology, 2017, DOI: 10.1152/jn.00371.2017.

In preparation

- **Cordova Bulens D, Cluff T, Crevecoeur F, Thonnard J-L, Lefèvre P**. *Differences in the internal representation of the two arms could explain hand dominance*.

Proceedings

- **Barrea A, Cordova Bulens D, Lefèvre P, Thonnard J-L** *A simple and reliable method to measure the fingertip coefficient of friction at different*

levels of grip force, Annual meeting of the Neural Control of Movement society, Amsterdam 2014 (poster).

- **Cordova Bulens D, Crevecoeur F, Thonnard J-L, Lefèvre P** *Differences in the internal representation of the two arms could explain hand dominance*, Annual meeting of the Neural Control of Movement society, Dublin 2017 (poster).
- **Cordova Bulens D, Crevecoeur F, Thonnard J-L, Lefèvre P** *The influence of biomechanical constraints on bimanual coordination*, Annual meeting of the Society for Neuroscience, Chicago 2015 (poster).
- **Cordova Bulens D, Crevecoeur F, Thonnard J-L, Lefèvre P** *Bimanual corrective responses are driven by the biomechanics of the upper limbs*, Annual meeting of the Society for Neuroscience, San Diego 2016 (poster).
- **Cordova Bulens D, Cluff T, Moore R, Crevecoeur F, Thonnard J-L, Lefèvre P** *Differences in the internal representation of the two arms could explain hand dominance*, Annual meeting of the Society for Neuroscience, Washington 2017 (poster).

CHAPTER 2

Mathematical tools

2.1 Introduction

In this chapter we introduce fundamental results obtained in control theory that will be utilized in the subsequent chapters of this thesis. It aims to give a rigorous explanation of the mathematical tools but cannot be exhaustive (see Astrom (1970); Başar and Bernhard (2008); Rawlings and Mayne (2012) for more details). In this chapter we first enounce the general control problem for deterministic systems in continuous time. We enounce and present the necessary and sufficient conditions for the controllability of linear systems. We then introduce the principle underlying optimal control theory and present optimal control algorithms for a class of stochastic systems, which is a theoretical framework largely exploited in neuroscience research. Next we introduce model predictive control (MPC) algorithms, which have the ability to solve problems that include constraints applied on the input or output of the systems and cannot be handles by standard stochastic optimal control. Finally, in order to study the effect of model errors on human motor control, we will introduce minimax control theory, a "robust" control strategy similar to stochastic optimal control algorithms but that does not make any assumption on the disturbances that are applied on the system.

2.2 General control problem

Consider a system with $x(t) \in \mathbb{R}^n$, the vector of state variables, and $u(t) \in \mathbb{R}^m$, the control input at time t. The evolution of the state variables as a function of time through the state of the system and the control variables is defined by:

$$\dot{x} = f(x, u) \tag{2.1}$$

where $f : \mathbb{R}^n \times \mathbb{R}^m \to \mathbb{R}^n$ represents the dynamics of the system.

Given an initial state $x(t_0) = x_0$, the evolution of the state variables as a function of time for a given control input u is given by:

$$x(t) = x_0 + \int_0^t f(x, u)d\tau \tag{2.2}$$

Eq 2.2 is implicit and cannot be solved as is. However, the problem of finding the trajectories of eq. 2.1 can be expressed as finding a function that is a fix point of the application $A(y) = x_0 + \int f(y, u)$. It can be demonstrated that such fix point exists and is unique, provided f is a Lipschitz-continuous.

The general control problem is the following: given an initial condition x_0 and a target set $S \subset \mathbb{R}^n$, find a control function $u(t) : [0, t_f] \to U \subset \mathbb{R}^m$ such that $t_f < \infty, x(t) \in X \subset \mathbb{R}^n, 0 \leq t \leq t_f$, and $x(t_f) \in S$. More intuitively, the control problem is to determine the control input $u(t)$ able to steer the system from the initial state to the objective state in a finite time t_f.

2.2.1 Linear Systems

Consider first the system defined by the state space vector $x(t)$ and initial condition $x(t_0) = x_0$:

$$\dot{x}(t) = Ax(t) \tag{2.3}$$

solving this simple differential equation yields the following result:

$$x(t) = e^{A(t-t_0)}x_0 \tag{2.4}$$

where e^{At} is defined as the exponential matrix which can be computed using its taylor expansion:

$$e^{At} = \sum_{k=0}^{\infty} \frac{t^k A^k}{k!} \tag{2.5}$$

The matrix exponential allows the computation of the general solutions as stated by the following theorem.

Theorem 2.1. *The unique solution of the ordinary differential equation*

$$\dot{x}(t) = Ax(t) + Bu(t) \tag{2.6}$$

with initial condition $x(t_0) = x_0$ *is given by*

$$x(t) = e^{A(t-t_0}x(t_0) + \int_{t_0}^{t} e^{A(t-\tau}Bu(\tau)d\tau \tag{2.7}$$

With eq. 2.7, the system defined by eq. 2.6 is said to be totally controllable if for any initial and final conditions, x_0 and x_f, the system can be driven from its initial state to its final state in a finite time $t_f < \infty$ through some integrable control function $u(t)$ such that:

$$x_f = e^{(t_f-t_0)A}x_0 + \int_{t_0}^{t} e^{A(t-\tau)}Bu(\tau)d\tau \tag{2.8}$$

With eq. 2.8 we can now derive the sufficient and necessary condition for the controllability of linear systems.

Theorem 2.2. *A system defined by eq.2.6 is said to be fully controllable if and only if the matrix* $[BAB...A^(n-1)B]$ *is full rank.*

Given the presence of the exponential e^{At} in the state of the system, it can be easily derived that the system's stability is determined by the eigenvalues of matrix A.

2.3 Introduction to Optimal Control

In order to find the "best possible" controller it is necessary to have a measure of the quality of the controller. Mathematically this can be done by defining a performance index. In this way the "best" possible control signal is found as the result of the minimization (or maximization) of this index. Therefore the principal point of focus when designing a Liner Quadratic Regulator (LQR) is to define the appropriate measure of controller quality.

2.3.1 The general Optimal Control Problem

Let us assume that a system with state vector $x(t) \in \mathbb{R}^n$ and input vector $u(t) \in \mathbb{R}^m$ is described by a general non-linear, time varying state equation:

$$\dot{x}(t) = f(x(t), u(t)). \tag{2.9}$$

Assume also that the initial state of the system is given by $x(t_0) = x_0$. We desire to optimize the control over a given time interval, up to time t_f. The system performance can be described by a performance index, which takes the following general form:

$$J(x,u) = \Phi(x(t_f)) + \int_{t_0}^{t_f} L(x(\tau), u(\tau))d\tau, \tag{2.10}$$

and depends on the state of the system as well as the input of the system at each instant.

2.3.2 Linear Quadratic Gaussian control

In this section we will study the Linear Quadratic Gaussian (LQG) control problem which is based on stochastic dynamic programming. In this context, we will introduce stochastic disturbances into the system and derive the solution of this problem for a discretized system with imperfect measurements of the output of the system. Let our system be defined by:

$$x_{k+1} = Ax_k + Bu_k + \omega k \tag{2.11}$$

$$y_k = Cx_k + \eta_k \tag{2.12}$$

Where matrices A and B define the dynamics of the system and C is the observability matrix which defines the information the controller gets from state feedback. Noise in the system dynamics is introduced through ω_k and η_k which are multivariate Gaussian random variables with zero mean and covariance matrices designated by Ω_ω and Ω_η respectively. The cost per step is defined as:

$$J_k = x_k^T Q_k x_k + u_k^T R u_k, k = 1, ..., N \tag{2.13}$$

Where Q_k is a positive semidefinite matrix and R is a positive definite matrix. N defines the time horizon which is assumed to be finite in this work, but infinite horizon formulations exist in the literature (Astrom, 1970). The goal of optimal control is to minimize the total cost obtained by summing J_k at each step of the path. In the presence of stochastic dynamics, the cost-to-go is defined as the expected cost to accumulate from the present time until the final time. Calling $v_k(x,u)$ the cost-to-go at step k, one can show that this quantity satisfies:

$$v_k(x,u) = \min_{u_k} x_k^T Q_k x_k + u_k^T R u_k + E(v_{k+1}) \tag{2.14}$$

Where the notation $E(.)$ denotes the expected value of the argument.

A fundamental result in stochastic optimal control is that the cost-to-go for the problem defined above is in fact a quadratic function of the states:

Theorem 2.3. *Under the optimal control policy, the cost-to-go has the following form:*

$$v_k = x_k^T S_k x_k + s_k \tag{2.15}$$

where S_k are symmetric positive semidefinite matrices and s_k is a non negative scalar quantity.

Proof. The proof is given by induction of the backward recursion of the cost-to-go. From hypothesis, the claim is true when $k = N$ with $S_N = Q_N$ and $s_N = 0$. Assume the claim is true for $k + 1 < N$. The cost-to-go at time k that must be minimized becomes:

$$v_k = x_k^T Q_k x_k + u_k^T R u_k + E(v_{k+1}|x_k, u_k) \tag{2.16}$$

From the induction hypothesis and the system dynamics, the expected value of v_{k+1} given x_k and u_k, plugged into the above equation gives:

$$\begin{aligned} v_k =& x^T(Q_k + A^T S_{k+1} A)x_k + u_k^T(R + B^T S_{k+1} B)u_k \\ &+ 2x^T A^T S_{k+1} B u_k + tr(S_{k+1}\Omega_\omega) + s_{k+1} \end{aligned} \tag{2.17}$$

it is a quadratic form in u_k which is minimized when u satisfies the following:

$$u_k = -(R + B^T S_{k+1} B)^{-1} B^T S_{k+1} A x_k. \tag{2.18}$$

The matrix being inverted is non-singular from assumptions. We define L_k such that $u_k = -L_k x_k$ in eq 2.17. By inserting eq. 2.17 into eq. 2.18 we have:

$$v_k = x_k^T (Q_k + A^T S_{k+1}(A - BL_k))x_k + s_k, \tag{2.19}$$

where we defined $s_k = s_{k+1} + tr(S_{k+1}\Omega_\omega) > 0$. Using the definition of L_k, by completing the square we have:

$$S_k = Q_k + (A - BL_k)^T S_{k+1}(A - BL_k) + L_k^T R L_k, \tag{2.20}$$

Which is positive semidefinite from assumptions which completes the proof. □

Eq. 2.20 is the algebraic Ricatti equation. For a controller with infinite horizon ($N \to +\infty$), the stationary control law is obtained by dropping index k in eq. 2.20 and solving for S. Now we consider the fact that the controller receives information about the state of the system through y_k. Let us introduce the notation $\hat{x}_k$ which represents the estimated state. From the definition of the feedback output, $y_k = -C\hat{x}_k$ is a multivariate Gaussian random variable with 0 mean and covariance matrix $\Omega_\eta + C\Sigma_{\hat{x}}C^T$ ($\Sigma_{\hat{x}}$ is the covariance matrix of $\hat{x}$). Hence, only the independent term of the last proof is affected by the use of the state estimate instead of the true state:

$$s_k = s_{k+1} + tr(S_{k+1}K_k(\Omega_\eta + C\Sigma_{\hat{x}}C^T)K_k^T). \tag{2.21}$$

Thus the same optimal feedback control policy as in the fully observable case can be used, i.e. when all information is directly available to the controller and is not obtained through y_k, and the optimal feedback gains simply apply to the estimated state rather than the true state. This result is known as the separation principle (Astrom, 1970): under the state dynamics and output feedback as defined in eq. 2.11 and 2.12, the problems of estimation and control are independent and can therefore be solved separately. The estimation error is defined as:

$$e_k = x_k - \hat{x}_k. \tag{2.22}$$

and we can compute the Kalman gains K_k from the dynamics of e_k given in eq. 2.22. The covariance of e_k is a quadratic function of K_k that is minimized over K_k when the following holds:

$$K_k = A\Sigma_{e_k}C^T(C\Sigma_{e_k}C^T + \Omega_\omega)^{-1}, \tag{2.23}$$

where we introduced the error covariance at time step k under the notation Σ_{e_k}. This covariance matrix is updated in a forward recursion from the definition of the Kalman's gains and the error dynamics:

$$\Sigma_(e_{k+1}) = (A - K_kC)\Sigma_{e_k}A^T + \Omega_\omega, \tag{2.24}$$

and the estimated state is given by:

$$\hat{x}_{k+1} = A\hat{x}_k + Bu_k + K_k(y_k - C\hat{x}_k). \tag{2.25}$$

The prior estimate $(A\hat{x}_k + Bu_k)$ is the maximum likelihood estimation of x_{k+1} given $\hat{x}_k$ and u_k. The prior estimate is then corrected by the difference between the expected and actual feedback. This estimation is known as the predictive Kalman filter. In recent years optimal control theory has emerged as a powerful theoretical background able to explain many phenomena observed in voluntary motor control. Indeed, this framework is interesting in the context of human motor control as it does not enforce particular trajectories or behaviors but uses feedback in an intelligent way in order to correct only for deviations that interfere with task goals (Todorov and Jordan, 2002).

2.4 Model Predictive Control

The general design objective of model predictive control is to compute trajectory of a future manipulated variable u to optimize the future behavior of the output of the system y. The optimization is performed within a limited time window by giving plant information at the start of the time window. The general ideas appearing in this type of algorithm are basically:

- Explicit use of a model to predict the process output at future time instants (horizon);
- Calculation of a control sequence minimizing an objective function;
- Receding strategy, so that at each instant the horizon is displaced towards the future, which involves the application of the first control signal of the sequence calculated at each step.

Let us consider the system defined by eq. 2.12 and expand the system to a finite horizon of size N:

$$X = \Phi x_0 + \Gamma U, \tag{2.26}$$

where $X = \begin{bmatrix} x_1 & x_2 & \cdots & x_N \end{bmatrix}^T$, $\Phi = \begin{bmatrix} A & A^2 & \cdots & A^N \end{bmatrix}^T$, $\Gamma = \begin{bmatrix} B & 0 & \cdots & 0 \\ AB & B & \cdots & 0 \\ \vdots & \vdots & \ddots & \vdots \\ A^N B & A^{N-1}B & \cdots & B) \end{bmatrix}$ and $U = \begin{bmatrix} u_0 & u_1 & \cdots & u_N \end{bmatrix}^T$. Also expanding the cost to go function to the finite horizon N gives us the following equation:

$$V = x_0^T Q_0 x_0 + \Omega X + \Phi U, \tag{2.27}$$

Where $\Omega = \begin{bmatrix} Q_1 & 0 & ... & 0 \\ 0 & Q_2 & \cdots & 0 \\ \vdots & \vdots & \ddots & \vdots \\ 0 & 0 & \cdots & Q_N \end{bmatrix}$ and $\Psi = \begin{bmatrix} R & 0 & \cdots & 0 \\ 0 & R & \cdots & 0 \\ \vdots & \vdots & \ddots & \vdots \\ 0 & 0 & \cdots & R \end{bmatrix}$. Using eq. 2.26 to expand eq. 2.27 we obtain the following:

$$V(x_0, U) = x_0^T (Q_0 + \Phi^T \Omega \Phi) x_0 + U^T (\Psi + \Gamma^T \Omega \Gamma) U + 2U^T \Gamma^T \Omega \Phi x_0, \tag{2.28}$$

In order to simplify the notations let us define $G \doteq 2(\Psi + \Gamma^T \Omega \Gamma) > 0$ and $F \doteq 2\Gamma \Omega \Phi$.

Let us now introduce constraints on the input and output of the following form:

$$u_{min} \leq u_{k+j} \leq u_{max}, j = 0, ..., N-1, \tag{2.29}$$

$$y_{min} \leq y_{k+j} \leq y_{max}, j = 0, ..., N, \tag{2.30}$$

Recalling that $y_k = Cx_k$ this is equivalent to:

$$\begin{bmatrix} 0 \\ 0 \\ -C \\ +C \end{bmatrix} x_k + \begin{bmatrix} -I \\ +I \\ 0 \\ 0 \end{bmatrix} u_k \leq \begin{bmatrix} u_{min} \\ +u_{max} \\ -y_{min} \\ +y_{max} \end{bmatrix}, k = 0, ..., N-1, \tag{2.31}$$

These constraints can be rewritten in the following form:

$$M_k x_k + E_k u_k \leq b_k, k = 0, ..., N-1, \tag{2.32}$$

$$M_N x_N \leq b_N. \tag{2.33}$$

by defining $M_k \doteq \begin{bmatrix} 0 & 0 & -C & +C \end{bmatrix}^T$, $E_k \doteq \begin{bmatrix} -I & +I & 0 & 0 \end{bmatrix}^T$ and $b_k \doteq \begin{bmatrix} -umin & +umax & -ymin & +ymax \end{bmatrix}^T$, for $k = 0, ..., N-1$, $M_N \doteq \begin{bmatrix} -C & +C \end{bmatrix}^T$ and $b_N \doteq \begin{bmatrix} -y_{min} & +y_{max} \end{bmatrix}^T$. Taking all the constraints in the finite horizon N into account we obtain the following system:

$$\begin{bmatrix} M_0 \\ 0 \\ \vdots \\ 0 \end{bmatrix} x_0 + \begin{bmatrix} 0 & \cdots & 0 \\ M_1 & \cdots & 0 \\ \vdots & \ddots & \vdots \\ 0 & \cdots & M_N \end{bmatrix} X + \begin{bmatrix} E_0 & \cdots & 0 \\ \vdots & \ddots & \vdots \\ 0 & \cdots & E_{N-1} \\ 0 & \cdots & 0 \end{bmatrix} \begin{bmatrix} u_0 \\ \vdots \\ u_{N-1} \end{bmatrix} \leq \begin{bmatrix} b_0 \\ b_1 \\ \vdots \\ u_N \end{bmatrix}, \tag{2.34}$$

Which by appropriately defining D, M, E and c can be rewritten as follows:

$$Dx_0 + MX + EU \leq c. \tag{2.35}$$

By introducing $X = \Phi x_0 + \Gamma U$ into eq. 2.35 we obtain:

$$\Xi U \leq c + W x_0, \tag{2.36}$$

Where $\Xi = M\Gamma + E$ and $W = -D - M\Phi$. Now our problem can be rewritten as follows:

$$\min_U \frac{1}{2} U^T G U + U^T F x, \tag{2.37}$$

subject to: $\Xi U \leq c + W x_0$, which is by definition a quadratic program (QP).

Definition 2.1. *Given matrices Z and Ξ and vectors c and b, the optimization problem is defined as:*

$$\min_\theta \frac{1}{2} \theta^T Z \theta + c^T \theta$$

subject to: $\Xi\theta \leq b$

Proposition 2.1. *If $Z \geq 0$ in the above quadratic program, then the following properties are verified:*

- *The optimization problem is strictly convex;*
- *A global minimizer can always be found;*
- *The global minimizer is unique.*

In our case we have by definition $G \geq 0$ and therefore the problem we have to solve is strictly convex and has a unique global minimum that can be found.

2.4.1 Minimization with equality constraints

To minimize the objective function subject to equality constraints we consider the so-called Lagrange expression

$$J = \frac{1}{2}\theta^T Z\theta + c^T\theta + \lambda(\Xi\theta - b). \tag{2.38}$$

The value of eq. 2.38 subject to satisfied equality constraints $\Xi\theta = b$ is equal to the original objective function. We now consider J as an objective function in variables θ and λ. To minimize this function we compute the first partial derivative with respect to the vectors θ and λ, and then equate these derivatives to zero:

$$\frac{\partial J}{\partial \theta} = Z\theta + c^T + \Xi^T\lambda = 0, \tag{2.39}$$

$$\frac{\partial J}{\partial \lambda} = Z\theta - b = 0, \tag{2.40}$$

The elements of vector λ are called the Lagrange multipliers.

The minimization of the system defined by eq. 2.39 and 2.40 is given by:

$$\lambda = -(\Xi Z^{-1}\Xi^T)^{-1}(b + \Xi Z^{-1}c^T), \tag{2.41}$$

$$\theta = -Z^{-1}(\Xi^T\lambda + c^T). \tag{2.42}$$

2.4.2 Minimization with Inequality Constraints

When considering inequality constraints, the number of constraints might be larger than the number of decision variables. In such a case, the inequality constraints $\Xi\theta \leq b$ may be composed of active and inactive constraints. A constraint is said to be active if $\Xi_i\theta = b_i$ and inactive if $\Xi_i\theta < b_i$ where Ξ_i and b_i are the ith row of matrix Ξ and the ith element of vector b respectively. We introduce the Kuhn-Tucker conditions which define the active or inactive constraints in terms of Lagrange multipliers.

The necessary conditions for this optimization problem are:

$$\begin{aligned} &Z\theta + c^T + \Xi^T\lambda = 0 \\ &\Xi\theta - b \leq 0 \\ &\lambda^T(\Xi\theta - c^T) = 0 \\ &\lambda \geq 0, \end{aligned} \tag{2.43}$$

where the vector λ contains the Lagrange multipliers. These conditions can be expressed in simpler for in terms of the set of active constraints. Let S_{act} denote the index set of active constraints. Then the necessary conditions become:

$$Z\theta + c^T + \sum_{i \in S_{act}} \lambda_i \Xi_i^T = 0$$

$$\Xi_i \theta - b_i = 0, i \in S_{act}, \tag{2.44}$$

$$\Xi_i \theta - b_i < 0, i \notin S_{act}, \tag{2.45}$$

$$\lambda_i \geq 0, i \in S_{act}, \tag{2.46}$$

$$\lambda_i = 0, i \notin S_{act}, \tag{2.47}$$

eq. 2.44 represents the active constraints while eq. 2.45 represents the set of inactive constraints. For an active constraint, the corresponding Lagrange multiplier is non-negative (eq. 2.46) whereas for an inactive constraint the Lagrange multiplier is zero (eq. 2.47).

If the active set is known than the original problem can be replaced by the corresponding problem having only equality constraints. Therefore the objective of minimizing this function subject to inequality constraints can be replaced by the problem of finding the active set of constraints.

Active set methods

The idea of active set methods is to define at each step a set of constraints, termed the working set, which is to be treated as the active set. The working set is to be chosen to be a subset of the constraints that are actually active at the current point hence making the current point feasible for the working set. At each step, an equality constraint problem is solved. If all Lagrange multipliers $\lambda_i \geq 0$, then the point is a local solution of the original problem. If there exists a $\lambda_i < 0$, then the objective function value can be decreased by relaxing the constraint i. During the course of minimization, it is necessary to monitor the values of all constraints to be sure they are not violated, since all points defined by the algorithm must be feasible. If a new constraint boundary is encountered it is necessary to add this constraint to the working set and then proceed to the re-defined working set.

2.5 Min-max Control

In this section we present the discrete-time minimax controller design problem. Contrary to the LQG controller, which assumes the unmodelled disturbances are

known in distribution, min-max control does not make any assumption about the nature of the external disturbance. Rather, the min-max control makes the assumption that disturbances act as a second control input that opposes the minimization of the cost function. More intuitively, the min-max problem, solved here in the context of game theory, will find a solution to the control problem for a worst-case scenario of the disturbance, meaning that the solution will achieve optimal disturbance attenuation.

Given that minimax controller makes no assumption on the disturbance of the system it is more robust than stochastic optimal control in the presence of unmodelled disturbances. In Chapter 3 we will use the differences between minimax control and LQG control to study differences in performance across arms at initial exposure to new environment dynamics.

Without any loss of generality let us consider the following system:

$$x_{k+1} = A_k x_k + B_k u_k + D_k \omega_k, x_1 = 0, k \in [1, K], \tag{2.48}$$

$$\begin{aligned} J_\gamma(u, \omega) &= x_{K+1}^T Q_f x_{K+1} + \sum_{k=1}^{K} (x_k^T Q_k x_k + u_k^T u_k - \gamma^2 \omega_k^T \omega_k) \\ &= J(\mu, \omega) - \gamma^2 ||\omega_k||^2, \\ &\qquad Q_f \geq 0; Q_k \geq 0, k = 1, 2, ... \end{aligned} \tag{2.49}$$

We also define the following matrices:

$$H_k^T H_k = Q_k, H_k^T G_k = 0, G_k^T G_k = I.$$

While very similar to the LQG problem, we notice that the disturbance is now included in J_γ with the term $-\gamma^2 \omega_k^T \omega_k$. The objective of min-max control is to determine control policies $u = u_[1, K]$ and $\omega = \omega_[1, K]$ that are the solution of:

$$\min_u \max_\omega J_\gamma(u, \omega), \tag{2.50}$$

The procedure to compute the saddle-point solution of this game is first to fix the open-loop policy of signal ω, say $\tilde{\omega}_{[1,K]}$, and minimize $J_\gamma(u, \omega_{[1,K]})$ given by eq. 2.49 with respect to $u = u_{[1,K]}$. From linear quadratic optimal control theory it is well known that the solution to this problem exists and is unique. Now, if we fix the open loop policy of vector u, say $\tilde{u}_{[1,K]}$, and maximize $J_\gamma(\tilde{u}_{[1,K]}, \omega)$ with respect to ω, existence and uniqueness of the solution will depend on the fact that J_γ is strictly concave in ω or not. This requirement can be translated as follows:

Lemma 2.1. *The quadratic function J_γ given by eq. 2.49 is strictly concave in ω for every policy u if and only if*

$$\gamma^2 I - D_k^T S_{k+1} D_k > 0, k \in [1, K], \tag{2.51}$$

Where the sequence s_{k+1}, $k \in [1, K]$, *is generated by the Riccati equation*

$$S_k = Q_k + A_k^T S_{k+1} A_k + A_k^T S_{k+1} D_k (\gamma^2 I - D_k^T S_{k+1} D_k)^{-1} D_k^T S_{k+1} A_k; \quad (2.52)$$

$S_{K+1} = Q_f$.

Under the condition defined by eq. 2.51, the quadratic problem becomes strictly convex-concave and hence it follows that it admits a unique saddle-point which has to be fixed to:

$$u_{[1,K]} = l^1(\omega_{[1,K]}, x_1); \omega_{[1,K]} = l^2(u_{[1,K]}, x_1)$$

. This unique solution is defined by a discrete time Riccati equation.

Theorem 2.4. *For the discrete time linear quadratic zero sum dynamic game, let eq 2.51 be satisfied and* M_k, $k \in [1, K]$, *be a sequence of matrices generated by*

$$M_k = Q_k + A_k^T M_{k+1} \Lambda_k^{-1} A_k; M_{k+1} = Q_f \quad (2.53)$$

Where

$$\Lambda_k = I + (B_k B_k^T - \gamma^{-2} D_k D_k^T) M_{k+1}. \quad (2.54)$$

Then

1. Λ_k, $k \in [1, K]$, *are invertible.*
2. *The game admits a unique saddle-point solution given by*

$$u_k = -B_k^T M_{k+1} \lambda_k^{-1} A_k \hat{x}_k \quad (2.55)$$

$$\omega_k = \gamma^{-2} D_k^T M_{k+1} \Lambda_k^{-1} A_k \hat{x}_k, k \in [1, K] \quad (2.56)$$

   Where $\hat{x}_k$ *is the corresponding state trajectory, generated by*

$$\hat{x}_{k+1} = \Lambda_k^{-1} A_k \hat{x}_k, \hat{x}_0 = x_0. \quad (2.57)$$

3. *The saddle-point value of the game is*

$$J_\gamma^* = J_\gamma(u^*, \omega^*) = x_1^T M_1 x_1. \quad (2.58)$$

4. *If eq. 2.53 is not satisfied, then the upper value becomes unbounded.*

It is worth noting that if the matrix sequence generated by eq. 2.53 and 2.54 is invertible, then eq. 2.53 can be rewritten as:

$$M_k = Q_k + A^T (M_{k+1}^{-1} + B B^T - \gamma^{-2} D D^T)^{-1} A; M_{K+1} = Q_f. \quad (2.59)$$

A sufficient condition for invertibility of M_k, $k \in [1, K]$, is that $\begin{bmatrix} A_k^T & H_k^T \end{bmatrix}^T$ be injective and Q_f be positive definite.

2.5.1 Disturbance attenuation problem

Let us now consider a system with imperfect state measurements:

$$x_{k+1} = Ax_k + Bu_k + D\omega_k, \tag{2.60}$$

$$y_k = Cx_k + E\omega_k. \tag{2.61}$$

With the performance index defined as:

$$J_\gamma(u,\omega) = |x_(K+1)|^2_{Q_f} + ||x||^2_Q + ||u||^2 - \gamma^2||\omega||^2 - \gamma^2|x_1|^2_{Q_0} \tag{2.62}$$

With Q_0 positive definite.

The problem to be solved is then the following:

Problem P_γ. Obtain necessary and sufficient conditions on γ for the upper value of the game $\inf_{\mu\in M}\sup_{\omega\in\Omega} J_\gamma(u,\omega)$ to be finite, and for such a γ find a controller u under which this upper value is achieved. The infimum of all γ's will be denoted γ^*.

The solution to this problem is found by solving the complementary problem of seeking the worst overall disturbance ω compatible with the information available at time τ. Therefore, x_0 and past values of ω should agree with past control and past measurements without any constraint imposed on them leading to a least cost-to-go $v(\tau; x(\tau))$. A detailed solution of this problem can be found in the book by Başar and Bernhard (2008). The solution to this problem requires the introduction of Lagrange multipliers and the use of the following Riccati equation:

$$\Sigma_{k+1} = A(\Sigma_k^{-1} + C^T N_k^{-1} C - \gamma^{-2} Q_k)^{-1} A^T + DD^T, \Sigma_1 = Q_0^{-1} \tag{2.63}$$

The complete solution is given by the following theorem:

Theorem 2.5. *Let the following three conditions hold:*

1. *Eq. 2.61 has a solution over* $[1, K+1]$*, with*

$$M_{k+1}^{-1} - \gamma^{-2} DD^T > 0, \forall k \in [1, K];$$

2. *Eq. 2.65 has a solution over* $[1, K+1]$*, with*

$$\Sigma_k^{-1} + C^T N_k^{-1} C - \gamma^{-2} Q_k > 0, \forall k \in [1, K];$$

3. *The following condition holds:*

$$\forall k, M_k - \gamma^{-2}\Sigma_k^{-1} < 0, \tag{2.64}$$

Under these three conditions, $\gamma \leq \gamma^*$, and an optimal controller is given by eq. 2.61, 2.63 and by:

$$\begin{aligned}\hat{x}_{k+1} = A\hat{x}_k + B\hat{u}_k + A(\Sigma_k^{-1} + C^T N_k C - \gamma^2 Q_k)^{-1} \cdot \\ [\gamma^{-2} Q_k \hat{x}_k + C N_k^T (y_k - C\hat{x}_k)]; x_1 = 0\end{aligned} \tag{2.65}$$

$$\hat{u}_k = -B^T (M_{k+1}^{-1} + BB^T - \gamma^{-2} DD^T)^{-1} A(I - \gamma^{-2}\Sigma_k M_k)^{-1} \hat{x}_k, \tag{2.66}$$

If one of the three conditions is not met, then $\gamma \leq \gamma^*$, i.e. for any smaller γ the problem P_γ has an infinite supremum for any admissible controller u.

2.6 Towards neuroscience

In this chapter we introduced the solution for the optimal feedback control and optimal state estimation for a class of stochastic systems, which constitutes the well-known LQG control framework and makes the assumptions that disturbances that are applied on the system are known in distribution. We also introduced the minimax control framework which is similar to the LQG control framework but makes no assumption on the disturbances applied on the system, hence finding a solution to the control problem for a worst-case scenario of the disturbance. Given the different assumptions made by these two frameworks about the nature of the disturbance, they perform differently when an unexpected error is introduced in the model of the controlled system. We will use this difference to explore the hypothesis that humans use different control strategies with their two arms when first introduced to new environment dynamics. Indeed, as new environment dynamics are not anticipated by participants, it introduces an error in the internal model of the arm used to perform the task. We expect that if different control strategies are used by the two arms, they can be captured by the LQG and the "robust" controllers.

In addition to LQG and minimax control, we introduced MPC control, which is interesting because of its ability to deal with constraints applied on the input, output or state of the system. In chapter 4, we explore the distribution of control across the two arms during a bimanual task. To do so, we will use a model of the upper-limb containing six muscle groups. The relation between muscle force and muscle length or contraction speed is non-linear (Brown et al., 1999), hence in order to linearize the system we modelled muscle tension as a second-order, low-pass response to the control input. However, as muscle force generation is limited to contraction (muscles can only pull on the bones), we introduced constraints on the input of the system. Given the presence of constraints on the input of the system, we could not use LQG control and hence used MPC to control the system.

CHAPTER 3

Differences in the internal representation of the two arms could explain hand dominance

Abstract. Any daily motor task involve the decision of which arm to perform the task with. In general, humans have a natural tendency to use their "dominant arm" which is generally considered more dexterous than the other arm. However, instead of assuming a dominant arm that is better on the whole, recent studies have suggested that each arm may have a specialized role. Indeed, it has been reported that the dominant arm has an advantage in trajectory control, whereas the non-dominant arm has an advantage during load compensation, leading to the hypothesis that predictive and impedance control characterize the behavior of the dominant and non-dominant arms respectively. Considering that the intrinsic mechanical impedance of limb muscles is in fact quite low, we suspected that these differences may be rooted in distinct control strategies rather than on distinct viscoelastic properties. We investigated this issue in a series of experiments in which participants performed reaching movements while being perturbed by a force field. We observed different behaviors across limbs during the adaptation of behavior to a curl-force field, with the dominant arm being more affected by the perturbation than the non-dominant arm. In a control experiment using the same paradigm we show that differences in performance across participants are not a related to differences in the co-contraction

of agonist-antagonist muscle pairs. Finally we show that such differences in behavior can be qualitatively captured in the control strategy without assuming differences in mechanical impedance.

3.1 Introduction

Handedness is a prominent feature of human motor behavior. Indeed, most humans have a natural tendency to use one of their two arms more often, i.e. the dominant arm, when performing a wide range of tasks. The dominant arm is generally assumed to be more dexterous than the other arm. However, recent studies focusing on the asymmetric performances observed across arms revealed an advantage of the dominant arm in the control of limb dynamics (Sainburg and Kalakanis, 2000; Bagesteiro and Sainburg, 2002) and an advantage of the non-dominant arm during tasks that required load compensation (Sainburg, 2002; Bagesteiro and Sainburg, 2003). From these results, Sainburg (2002) suggested a specialized role for each arm, such that differences in performance across arms arise from differences in the use of predictive and impedance control (Yadav and Sainburg, 2014a). More precisely, this hypothesis suggests that both arms are controlled using a mix of predictive and impedance control; asymmetric performances are due to the fact that the dominant arm relies more heavily on predictive control and the non-dominant arm relies more heavily on impedance control (Yadav and Sainburg, 2014b).

Although attractive, this hypothesis implies that participants can modulate the joint mechanical impedance of their limb to modify the behavior, presumably through the combined activation of agonist-antagonist pairs of muscles acting on each joint (Hogan, 1985; Burdet et al., 2001). However, the intrinsic impedance of muscles is quite low at spontaneous levels of activation, and the presence of co-contraction mostly impacts the gain of the stretch reflex (Pruszynski et al., 2009; Crevecoeur and Scott, 2014). Furthermore, what is often referred to as the limb stiffness includes the contribution of reflexes and early voluntary responses (up to ~ 300ms, Burdet et al. (2000)), which is known to largely depend on the neural control policy (Scott, 2016). Thus, it seems that the modulation of the default, or feed-forward muscle activity may not explain the different behaviors observed across limbs. Regarding the role of feedback, Walker and Perreault (2015) reported very small changes in background EMG activity across limbs in a perturbation task. Altogether these observations warrant a careful reexamination of the neurophysiological basis of inter-limb differences during motor control.

Instead of assuming differences in biomechanical impedance, we investigated the possibility that differences in performance across limbs originate from different internal representations and control strategies associated with each arm.

More precisely, we hypothesize that the internal representation of the non-dominant may be less accurate, which promotes the use of a robust strategy in the sense that it is less sensitive to errors in the internal representation of limb and environment dynamics. In contrast, the dominant arm may have better internal representations, and afford control strategies that are more efficient but also fragile against model errors.

To test this, we measured participants' performance as they learned to move a robotic handle in a force field (Experiment 1). We observed differences in accuracy, precision, trajectory and learning rate across arms that reproduce qualitatively previous results (Schabowsky et al., 2007; Yadav and Sainburg, 2014a). Importantly, we show that control solutions obtained by making different assumptions about the nature of the unknown disturbance (i.e. robust or stochastic optimal control) can capture the inter-limb difference observed experimentally. We then report the result of the same experiment performed in an exoskeleton (Experiment 2) in which we did not observe any difference in performance across limbs, nor any systematic variations in EMG activity that could account for the wide range of movement errors following the introduction of the force field. Taken together, our study suggests that inter-limb differences are context-dependent and relate to the neural control policy more than to feed-forward control of limb impedance.

3.2 Materials and methods

3.2.1 Participants

46 right-handed participants performed the task. Two experimental setups detailed in the subsequent sections were used. 26 participants were involved in Experiment 1, and 20 participants were involved in Experiment 2. All participants provided written informed consent before participating in this study. The volunteers had no known neurological disorders and were naïve to the purpose of the experiment. Handedness was assessed using the Edinburgh Inventory (Oldfield, 1971). The experimental procedures were approved by the local ethics committee at the Université catholique de Louvain for Experiment 1, and at the University of Calgary for Experiment 2.

3.2.2 Behavioral task

Participants performed reaching movements to one of three targets positioned 15cm away from the starting position and spaced of $45\circ$ from each other (Fig.

3.1C and D). Participants were provided no visual feedback of their hand position during movement but received visual feedback of the end-point position of their reaching movements. Participants also received feedback of the speed of their movement through the color of the end-point feedback: they were presented with a green end-point feedback when the peak speed was comprised between 50cm/s and 80cm/s, yellow when above and blue when below. This feedback about the peak speed was used to obtain stereotyped movement profiles. At the beginning of each trial participants positioned their hand in a target representing the starting position. After 1s the starting target disappeared and the target to reach was presented. End-point feedback was displayed when participants hand speed fell below 5cm/s for a duration of 100ms. Before the task, participants were trained to perform movements at the desired speed. The behavioral task was divided into two blocks. The first block consisted of 20 unperturbed reaching movements towards each target for a total of 60 trials. This block was used to measure baseline performance of participants during the task.

In the second block, a speed-dependent curl force field was introduced (Fig. 3.1A and B):

$$\begin{pmatrix} F_x \\ F_y \end{pmatrix} = \begin{pmatrix} 0 & -\alpha \\ \alpha & 0 \end{pmatrix} \begin{pmatrix} v_x \\ v_y \end{pmatrix} \tag{3.1}$$

where F_x and F_y represent the forces applied at the end-point in the x and y axes respectively, v_x and v_y represent the speed in the x and y axes and α represents the parameter defining the force intensity. Participants performed 80 reaching movements towards each target for a total of 240 trials.

On each trial the presented target was randomly selected for subjects not to be able to anticipate the position of the target before it was displayed. During the task, a score was presented on the virtual reality display. Participants received a point for each reaching movement performed with a peak speed comprised between 50cm/s and 80cm/s and for which the end-point lied inside the target.

3.2.3 Experiment 1

In Experiment 1 participants performed the experiment holding the handle of a robotic arm (KINARM end-point, BKIN Technologies, Kingston) permitting movements in the horizontal plane. Participants' arm position was not constrained during movement. The robotic arm was able to apply mechanical loads to the participants' hand. Direct vision of participants' limbs were blocked but targets and hand feedback were projected on top of the participants' arm using a TV monitor and a semitransparent mirror. In this experiment the force field was defined by $\alpha = 20$ for the group that performed the task with their

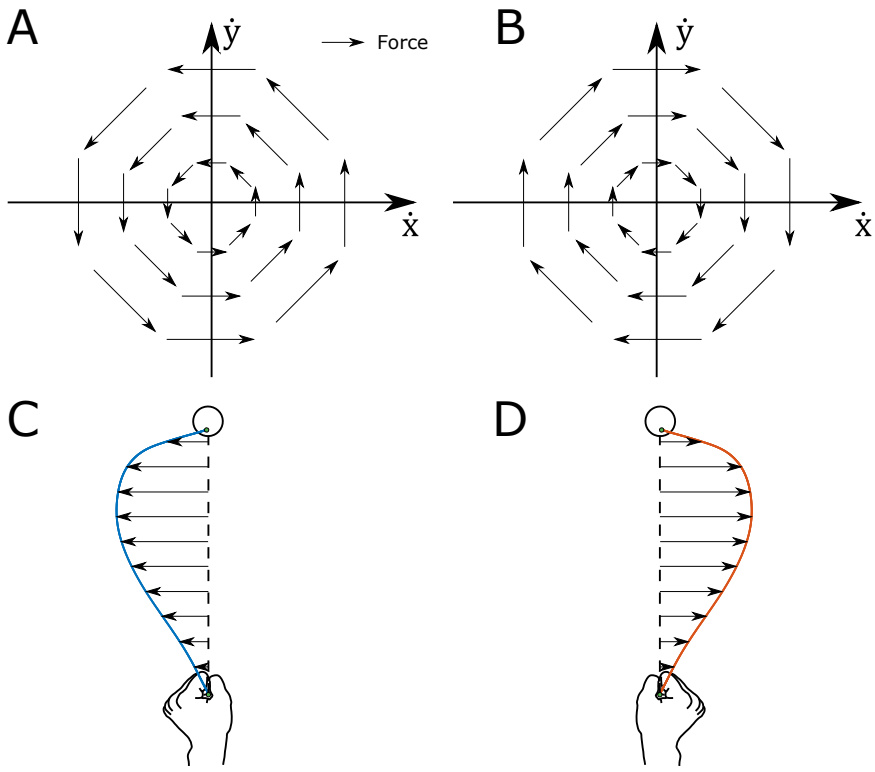

Figure 3.1: Curl field applied on participants' arm and minimum jerk trajectory during perturbed trials. A) Relationship between applied force and movement speed during perturbed trials for participants performing the task with their non-dominant arm. The size of the arrow represents the intensity of the applied force. B) Relationship between applied force and movement speed during perturbed trials for participants performing the task with their dominant arm. C) Minimum jerk trajectory of a reaching movement for the non-dominant arm (black arrows) towards each of the three targets (black disks) tested during the task. Blue arrows represent the forces applied on the hand along the trajectory. D) Minimum jerk trajectory of a reaching movement for the dominant arm (black arrows) towards each of the three targets tested during the task. Orange arrows represent the forces applied on the hand along the trajectory.

non-dominant arm and $\alpha = -20$ for the group that performed the task with their dominant arm, hence presenting mirrored force fields to the two arms (Fig. 3.1A, B, C and D).

3.2.4 Experiment 2

In Experiment 2, participants performed the task in an exoskeleton device that constrained arm position to the horizontal plane (KINARM Exoskeleton, BKIN Technologies, Kingston). Given that the arms are supported in the horizontal plane, muscles active during the reaching task can be easily identified. For this reason, this setup was more favorable for the recording of surface electromyographic signals (EMG). As in Experiment 1, direct vision of participants' limbs were blocked but targets and hand feedback were projected on top of the participants' arm using a TV monitor and a semitransparent mirror. The exoskeleton was able to apply torques to the shoulder and elbow joints. The joint-based force-field was automatically generated so as to produce a perturbation to the hand equivalent to the one in Experiment 1.

3.2.5 Mathematical modeling

The problem was modeled as the translation of a point mass ($m = 1$) in the horizontal plane in the presence of three forces: a viscous force proportional to the velocity with opposite sign, a controlled force (F) and an external force (F_ext). Muscle dynamics were approximated using a first-order linear filter between the controlled force and the control variable. The system is given by the following differential equations:

$$m\dot{p} = -K_v\dot{p} + F + F_ext, \tag{3.2}$$

$$\tau\dot{F} = u - F \tag{3.3}$$

where m is the mass (set to 1 in our model), p represents the 2D coordinate vector of the point-mass, K_v is the viscous constant, F represents the controlled force, F_ext represents the curl force field and u represents the 2D control vector. The dynamics of the system were discretized using an explicit Euler integration scheme in order to introduce noise disturbances and was rewritten in the form of state-space equations:

$$x_{k+1} = (A + \Delta A)x_k + Bu_k + \beta_k, \tag{3.4}$$

where $x_k = \begin{bmatrix} p_x & p_y & \dot{p}_x & \dot{p}_y & F_x & F_y \end{bmatrix}$ represents the state space vector at time k and includes position, velocity and controlled and external forces, A and B are matrices that describe the system dynamics, u is the input vector, and

β_k and ΔA represent disturbances in the system. We will consider two sources of disturbances: the first is the motor noise represented here as β_k, composed of two different terms: an additive term $(N(0, \Omega_\omega))$, with noise being only applied on the input of the system $(\Omega_\omega(5,5) = \Omega_\omega(6,6) = 0.25)$, and a control dependent term capturing signal-dependent noise aligned with the direction of the control vector (Li and Todorov, 2007). The second source of disturbance is the model error (ΔA) that arises upon introduction of the force field: indeed, before participants can learn to move in the force field, they must perform reaching movements in the presence of a model error, which is the impact of the force field that the nervous system cannot anticipate. Hence we can rewrite the system as follows:

$$x_{k+1} = Ax_k + Bu_k + Dw_k, \tag{3.5}$$

with $D = \begin{bmatrix}\Delta A & I\end{bmatrix}$ and $w_k = \begin{bmatrix}x_k & \beta_k\end{bmatrix}$ will include both random and arbitrary disturbances. The model error will play a critical role in the control solution as we show below. The feedback signal at each time step is defined as follows:

$$y_k = Cx_k + \zeta_k, \tag{3.6}$$

where y_k is the feedback vector, $C = I_{6x6}$ is a matrix describing the systems feedback and ζ_k is the sensory noise vector; ζ_k is represented as zero-mean Gaussian white noise with unity covariance $(N(0, \Omega_\zeta))$ with $\Omega_\zeta = diag\begin{pmatrix}0.0001 & 0.0001 & 0.001 & 0.001 & 0.025 & 0.025\end{pmatrix}$ (Ueyama, 2014).

Stochastic Optimal Control

We used a linear quadratic gaussian (LQG) control strategy to represent our stochastic optimal controller. One basic assumption of the LQG controller is that the disturbance vector w_k is zero-mean white Gaussian noise with covariance Ω. Equivalently, this approach assumes that $\Delta A = 0$. For such a controller the cost function is defined as:

$$J(x_k, u_k) = x_k^T Q_k x_k + u_k^T R u_k, \tag{3.7}$$

where Q_k and R are the state and input cost matrices respectively. In our case we defined the state cost function such that the final cost is given by:

$$cost = a_1||p||^2 + a_2||\dot{p}||^2 + a_3||F||^2, \tag{3.8}$$

where $a_1 = 250000$, $a_2 = 1$ and $a_3 = 10^{-6}$. The input cost matrix was defined as $R = I_{6x6}$. The optimal linear state estimator can be derived following standard procedures (Kalman filter, Todorov (2005); Crevecoeur et al. (2011)).

$$\hat{x}_(k+1) = A\hat{x}_k + Bu_k + K_k(y_k - C\hat{x}_k), \tag{3.9}$$

Where $\hat{x}_k$ is the estimated state at time k and K_k is the Kalman filter. In the framework of extended LQG (Todorov, 2005) we iterate a controller of the form of eq. 3.10 and a state estimator in the form of eq. 3.9 until convergence:

$$u_k = -L_k \hat{x}_k. \tag{3.10}$$

Robust feedback controller

Contrary to the LQG design, robust control makes no assumption about the disturbance w_k Başar and Bernhard (2008). Solving this problem requires considering the presence of w_k in the cost function, and the best strategy consists in minimizing the worst impact of this disturbance. This can be achieved in the context of game theory by introducing the following term in the cost function:

$$J(x_k, u_k, w_k) = x_k^T Q_k x_k + u_k^T R u_k - \gamma^2 w_k^T w_k, \tag{3.11}$$

where the disturbance is accounted for as a variable that opposes the minimization of the cost function. Parameter γ defines the impact of the disturbance on the controller Başar and Bernhard (2008) and is minimized numerically to achieve optimal disturbance rejection. As for the LQG design, a theoretical control solution of the form presented in eq. 3.10 can be derived (for more details see Chapter 2 or Başar and Bernhard (2008)). In the context of robust control, state estimation cannot be performed using a Kalman filter because no assumption is made on the distribution of the disturbance, the estimated state is computed as follows:

$$\hat{x}_{k+1} = A\hat{x}_k + Bu_k + G_{1_k}\hat{x}_k + G_{2_k}(y_k - C\hat{x}_k), \tag{3.12}$$

more details on the computation of the different parameters of this equation can be found in Chapter 2 or in Başar and Bernhard (2008). It is worth noting that the derivation of the estimator for the robust controller differs from that of a Kalman filter due to the fact that no hypothesis on the distribution of the disturbance is made however, if such an hypothesis were to be introduced in the derivation of this estimator, it would lead to the same expression as in LQG control. Thus we solve the same problem with the same system and the same cost function, the only difference is the assumption made about the nature of the input disturbance and about the presence of an arbitrary model error.

3.2.6 Data acquisition

Position, velocity and force at the handle of the KINARM end-point, as well as flexion and elbow movement for the KINARM exoskeleton, were sampled at 1kHz. Surface electromyographic recordings were obtained from the brachioradialis (Br), triceps lateral (TLat), pectoralis major (PM), posterior deltoid

(PD), biceps brachii (BB) and triceps long head (TLo) for the participants performing the task in the exoskeleton setup (Experiment 2). EMG signals were sampled at 1kHz.

3.2.7 Data analysis

All signals were aligned on movement onset, which is defined as the moment when hand speed exceeds 5cm/s. All EMG signals were band-pass filtered ($20 - 450$Hz) and full wave rectified. EMG signals were normalized by their mean activity recorded in a separate set of trials where subjects maintained a constant posture against 1Nm torques applied to each joint individually. For each target, EMG signals where averaged across all unperturbed trials and across the 10 first perturbed trials towards each target. End of movement was determined when participant's hand speed fell below 5cm/s for a period of 100ms.

To measure the impact of the force field on participants' behavior we extracted the maximal deviation from the straight line in the direction of the force field (clock wise for the right arm and counter-clock wise for the left arm) for each trial of each participant. To analyze how participants adapted their behavior to the force field, we computed the mean maximal deviation in four sets of 10 trials for all targets pooled together, The first set includes the 10 first trials, the second set includes 10 trials one third into the 240 trials, the third set of trials includes 10 trials two thirds into the 240 trials, and the last set includes the 10 last trials. In order to determine whether participants performing the task with their non-dominant arm deviated less than participants performing the task with their dominant arm at initial exposure to the force field, we performed a rmANOVA with maximal deviation as the dependent variable, set of trials as the within subjects independent variable and body-side (right or left arm) as the between subjects dependent variable. As a post-hoc test we performed independent t-tests on the maximal deviation of each set of trials separately to test for differences across arm.

To analyze control near the end-point of the movement, we looked at the accuracy and precision of participants' movement during the same four sets of trials. We computed the average error and end-point dispersion on each set of trials trials of the second block (curl force field block). The average error was computed as the distance between the mean end-point of participants' movement and the center of the target (Fig. 3.3). To compute the error-dispersion we first computed the covariance matrix of the x and y coordinates of the end-points. From this covariance matrix we computed the 95% confidence ellipse of the end-points and computed the surface of this ellipse (Fig. 3.3). We defined end-point dispersion as the surface of the 95% confidence ellipse. To determine whether participants performing the task with their non-dominant

arm were more accurate and precise than participants performing the task with their dominant arm we performed two rmANOVAs with either average error or end-point dispersion as the dependent variable, set of trials as the within subjects independent variable and body-side (right or left arm) as the between subjects dependent variable. As in the case of maximal deviation, we performed a independent t-tests on each set of trials to test for differences across arms.

As we show below, the inter-limb difference in behavior that we observed in Experiment 1 was not reproduced in Experiment 2. Therefore, in order to determine whether co-contraction can explain differences in performance across participants at initial exposure to the force field, we separated participants based on the maximal deviation measured on the ten first trials perform with the curl force-field active. One group was composed of the 10 participants that had the Smaller Maximal Deviation (SMD) during the ten first trials and the other group was composed of the 10 other participants (Large Maximal Deviation, LMD). The LMD group was composed of 6 participants who performed the task with their dominant arm and 4 who performed the task with their non-dominant arm.

In order to verify whether the activity in the six measured muscles was modulated to counter the force field we computed the mean of the EMG signals in two time windows, from 100ms before movement onset to movement onset and from movement onset to 100ms after movement onset. We performed a repeated measures analysis of variance (rmANOVA) for each time window and for each muscle separately to determine whether target, initial performance, and the introduction of the force field had a significant effect on muscle activation. In this series of rmANOVAs muscle activity was the dependent variable, target and condition (perturbed, unperturbed) were the within subjects variable and group (SMD, LMD) was the between subjects variable.

Finally, to determine whether difference in performance at initial exposure to the force field could be linked to differences in the use of impedance control, we tested for differences in co-contraction between the SMD and LMD groups. To extract the co-contraction level for each pair of muscles, we computed the minimum EMG signal in each muscle pair (Elbow, shoulder and bi-articular muscles) as done in Gribble et al. (2003) (Fig. 3.2). For each participant and each target, we computed the mean co-contraction signal in four time windows, from 200 to 100ms before movement onset (E1), from 100ms before movement onset to movement onset (E2), from movement onset to 100ms after movement onset (E3) and from 100 to 200ms after movement onset (E4), for both baseline and curl force-field trials separately (Fig. 3.2). To test for significant differences in co-contraction level across targets and groups we performed a rmANOVA, for each joint and for each time window separately, with co-contraction level as the dependent variable, target as within subjects independent variables and group as the between subjects variable.

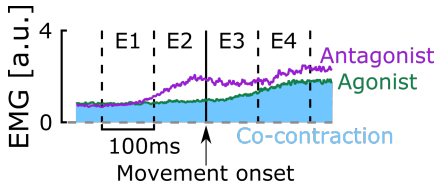

Figure 3.2: Computation of co-contraction for an exemplar agonist-antagonist muscle pair. The purple and green line represent the EMG signals averaged across all trials of all participants for the TLat and Br muscles respectively. The light blue region represents common activation level of the agonist-antagonist muscle pair and is defined as co-contraction in this study. The solid black line represents movement onset. The dashed black lines delimit four 100ms time windows (E1, E2, E3 and E4).

For all rmANOVA, sphericity was verified using Mauchly's test and corrected when necessary. Homoscedasticity was verified using Levene's test (homogeneity of variance).

3.3 Results

3.3.1 Simulation results

We performed simulations using two control strategies with different sensitivities to model error to verify whether differences in performance across arms could be captured in the control strategy, without assuming any difference in the intrinsic mechanical impedance of the limbs. While both controllers are applied on the same problem and share similar cost functions, the robust controller aims at minimizing the worst possible impact of disturbances, in this case the model error, leading to trajectories that are less affected by the introduction of the force field. Indeed trajectories performed by the robust controller deviated less during movement than those performed by the stochastic optimal controller (see inset in Fig. 3.3A). In addition, the robust controller was more accurate (smaller average error) and precise (smaller error dispersion) (see Fig. 3.3A). Speed profiles of the two controllers showed two peaks, one corresponding to the initiation of movement and the other corresponding to the corrective response (see Fig. 3.3A). The second speed peak of the optimal controller was larger than the second peak of the robust controller (see Fig. 3.3A). We think that these simulations are relevant to describe differences in control strategy of the two arms at the introduction of the force field because, as the force field is not anticipated by participants, it introduces an error in the internal model of the corresponding arm at initial exposure to novel dynamics.

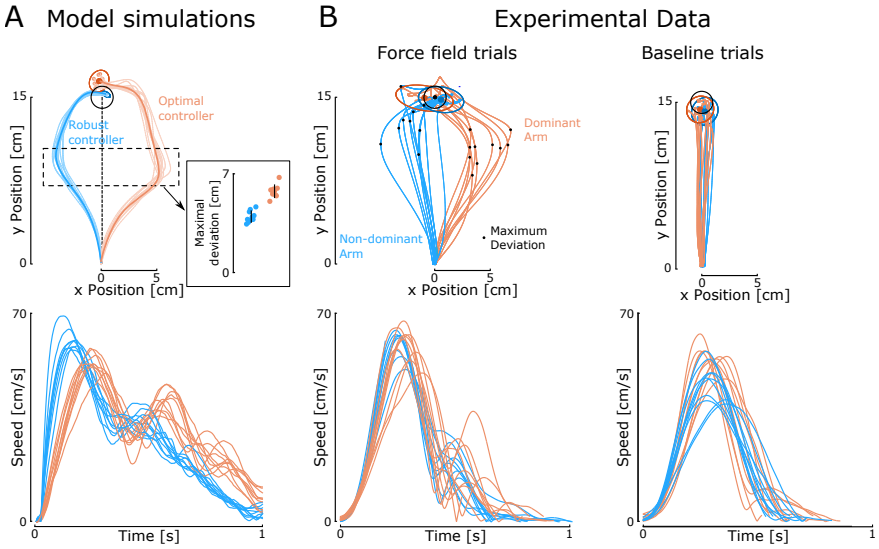

Figure 3.3: Model simulations and initial trials of representative participants. A) Model simulations performed with the stochastic optimal controller (orange lines) and the robust controller (blue lines) with no knowledge of the perturbation. Light blue and orange dots indicate the end-point of the trajectory for the robust and optimal controller respectively. The blue and dark orange dots represent the average end-point across the simulated trials. Blue and orange ellipse represents the 95% confidence ellipse of the 10 simulated trials. Black disk represents the target and the black dot represents the center of the target. The insert presents with more detail the maximum deviation for the optimal and the robust controllers. The bottom panel presents the predicted velocity profiles for the two control strategies B) 10 first trials for two representative participants. Light blue lines represent the trajectories of the movement of the participant performing the task with his non-dominant arm and orange lines represent the trajectories of the participant performing the task with his dominant arm, during baseline and force field trials. Black dots indicate the maximum deviation of each trial for the trials performed while facing a curl force field. The bottom panel presents the measured velocity profiles for the two arms in baseline and force field trials.

3.3.2 Experiment 1

During the baseline block of trials, i.e. without the force field, participants' movements did not deviate significantly form a straight trajectory (see Fig. 3.3B). During the initial trials performed with the curl force field active, trajectories from participants who used their dominant arm consistently deviated more than those of participants who used their non-dominant arm (see Fig. 3.3B and Fig. 3.4A first block of trials), moreover we observed a greater average error and end-point dispersion from participants using their dominant arm (Fig. 3.4B and C), indicating greater accuracy and precision from non-dominant arm participants. Furthermore, as in simulations we observed two peaks in the speed of the movement, with the dominant arm presenting a larger second speed peak (see Fig. 3.3B). These results are in line with those previously reported in the literature (Schabowsky et al., 2007; Yadav and Sainburg, 2014a), and suggest that the non-dominant arm is more robust, and hence less affected, when initially confronted to the unexpected effect of the force field.

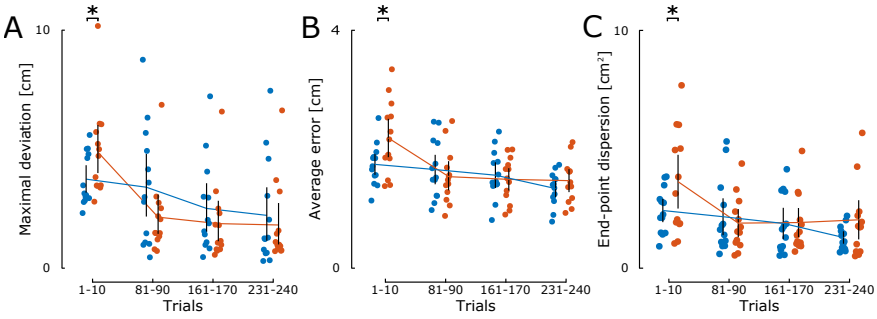

Figure 3.4: Mean maximal deviation, average error and end-point dispersion of participants of Experiment 1. A) Mean maximal deviation in four sets of 10 trials placed at the beginning of the task, after 1/3 of trials, after 2/3 of trials and at the end of the 240 trials for all participants in Experiment 1. Each blue and orange dot represents the average maximal deviation across ten trials of a participant who used his non-dominant arm and dominant arm, respectively. The solid blue and orange lines represent the evolution of the mean maximal deviation across trials. B) Average error for the four sets of trials for all targets pooled together. Blue and orange dots correspond to data from participants who used their non-dominant and dominant arm respectively. C) End-point dispersion for the four sets of 10 trials for all targets pooled together. Colors are defined as in panel B.

We analyzed the maximum deviation of hand-path as a measure of the impact of the force field on the control of movement during the exposure to the perturbation, the evolution of this maximum deviation across trials allowed us to determine the time course of learning of each arm. We performed a rmANOVA with average maximum deviation in four different blocks of ten trials, distributed equally across all trials for all targets pooled together, to test for differences

between the non-dominant and dominant arm (Fig. 3.4A). The rmANOVA revealed a significant main effect of time ($F(3,72)=18.44$, $p<0.001$), indicating that maximum deviation decreased across trials for both arms, no effect of body-side ($F(1,24)=0.23$, $p=0.63$), indicating no difference between non-dominant and dominant arm across the four sets of trials, and a significant interaction time*body-side ($F(3,72)=4.38$, $p=0.007$) indicating that the participants who used their non-dominant arm learned at a different rate than participants who used their dominant arm (Fig. 3.4A). One-sided independent t-tests performed on each block of trials separately revealed a significant effect of body-side on the maximal deviation in the first block of trials ($t(23.24)=-1.83$, $p=0.04$) but not in the other blocks ($p>0.08$) (Fig. 3.4A). Altogether these results indicate that participants performing the task with their non-dominant arm deviated less during the first block of trials, but also learned at a slower rate, than participants using their dominant arm, which lead to similar performance in the subsequent blocks of trials (Fig. 3.4A).

Looking at the control near the end of movement revealed differences across arms that were consistent with the observations done on maximal deviation. We extracted the average error and the end-point dispersion as measures of the accuracy and precision of reaching movements, and performed an rmAnova to test for differences in performance across arms and across sets of trials. The rmANOVA on the average error revealed a significant main effect of time ($F(3,72)=11.51$, $p<0.001$), indicating that average error decreased across trials for both arms, no effect of body-side ($F(1,24)=1.15$, $p=0.29$), indicating no difference between non-dominant and dominant arm across the four sets of trials, and a significant interaction time*body-side ($F(3,72)=2.99$, $p=0.04$) indicating that the participants who used their non-dominant arm learned at a different rate than participants who used their dominant arm (Fig. 3.4B). A one-sided independent t-test on each set of trials revealed a significant effect of body-side on the first set of trials ($t(18.9)=-2.28$, $p=0.02$) and no significant difference for the other three set of trials ($p>0.05$) (Fig. 3.4B).

Concerning end-point dispersion, the rmANOVA revealed a significant main effect of time ($F(3,72)=7.02$, $p<0.001$) and no other significant main effect ($p>0.15$). The independent t-tests revealed a significant effect of body-side on the end-point dispersion for the first set of trials ($t(16.4)=-1.77$, $p=0.047$) but not for the other three sets of trials ($p>0.05$). Altogether the results of these rmANOVAs indicate that the non-dominant arm was more accurate and more precise than the dominant arm at the initial exposure to the curl force-field. Accuracy and precision of the two arms improved across trials with differences across arms were not significant on later trials (Fig. 3.4C).

Altogether results of Experiment 1 show differences in performance across arms that are similar to those observed in the model predictions (Fig. 3.3A and B, 3.4A, B and C). Indeed, participants using their non-dominant arm were less

affected, i.e. more accurate (Fig. 3.4B), more precise (Fig. 3.4C) and deviated less (Fig. 3.4A), by the introduction of the force field than participants using their dominant arm. Hence, this suggests that the non-dominant arm used a more robust control strategy to perform reaching movements in the face of a force field.

Experiment 2

Experiment 2 was initially designed to address whether the differences in behavior observed in Experiment 1 could be related to a systematic increase in the levels of co-contraction in the non-dominant arm, which would suggest that participants may have used a default stiffening of the non-dominant limb instead of distinct control strategies. To address this question, we used the same experimental paradigm as in Experiment 1 in an exoskeleton setup, allowing for a more accurate experimental control of the muscles involved in reaching movements, hence allowing more reliable EMG data collection. In this experiment, we did not observe any difference in maximal deviation, average error or error dispersion between the non-dominant and the dominant (Fig. 3.5A, B and C), despite that we used exactly the same paradigm as in Experiment 1. This surprising observation suggests that differences in behavior across limbs may be task or context-dependent, such that, in our case, the setup used altered participants' behavior.

Looking at the same parameters as in Experiment 1, namely the maximal deviation, end-point error and average error, we performed similar statistical analysis to verify that there were no differences across dominant and non-dominant arm. Concerning maximal deviation, the rmANOVA revealed a significant main effect of Time ($F(3,54)=60.05$, $p<0.001$), no significant effect of body-side ($F(1,18)=1.24$, $p=0.28$) and no interaction effect ($F(3,54)=0.92$, $p=0.43$). The independent t-tests performed on each set of trials revealed a significant difference between the dominant and non-dominant arm for the last set of trials ($t(15.2)=-2.36$, $p=0.01$) but not for the other sets of trials ($p>0.05$). The rmANOVA performed on average error revealed a significant main effect of time ($F(3,54)=11.65$, $p<0.001$), no effect of body-side ($F(1,18)=1.19$, $p=0.28$) and no interaction effect ($F(3,54)=0.45$, $p=0.7$) (Fig. 3.5B). The four independent t-tests performed on each set of trials revealed no significant effect of body-side on any of the 4 sets of trials ($p>0.1$). Similarly for the end-point dispersion, the rmANOVA revealed a significant main effect of time ($F(3,54)=4.43$, $p<0.001$) and no significant effect of body-side ($F(1,18)=0.2$, $p=0.65$) and no interaction effect ($F(3,54)=0.58$, $p=0.6$) (Fig. 3.5C). The four independent t-tests revealed no significant effect of body-side on any set of trials ($p>0.1$). Altogether these results confirm that in Experiment 2 both arms were equally affected by the introduction of the force field and learned at similar rates (Fig. 3.5A, B and C).

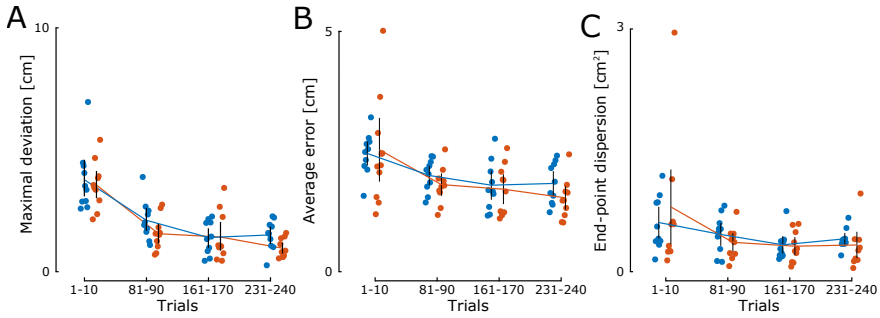

Figure 3.5: Maximal deviation, average error and end-point dispersion for participants who performed the task in Experiment 2. A) Mean maximal deviation in four blocks of 10 trials placed at the beginning of the task, after 1/3 of trials, after 2/3 of trials and at the end of the 240 trials for participants who performed the task in the exoskeleton setup. Blue dots represent data from participants who used their non-dominant arm to perform the task, and orange dots represent data from participants who used their dominant arm to perform the task. The solid black lines represent the mean +/- SD of the data of each group of participants and for each block of trials. The solid blue and orange lines represent the evolution of mean maximum deviation across the four blocks of trials. B) Average error of all participants on the 10 first successful trials for all targets pooled together. Colors are defined as in panel A C) End-point dispersion on the 10 first successful trials for all targets pooled together. Colors are defined as in panel A.

In order to determine whether differences in co-contraction could explain the wide array of performances observed during the experimental task, we formed two groups of participants based on the average maximum deviation on the 10 first successful trials (SMD and LMD) (see Fig. 3.6). Before analyzing co-contraction we analyzed whether the activity in the measured muscles was modulated to account for the introduction of the force field, and whether this activity differed between LMD and SMD groups (Fig. 3.6A). We performed rmANOVAs on muscle activation, for each muscle separately, to test for differences in activation between SMD and LMD groups. Prior to movement onset, this series of rmANOVAs revealed a significant main effect of target for Br, TLat, TLo, PM and PD ($p<0.05$) but not for BB, indicating that muscle activity prior to movement onset is modulated dependent on the target presented to the participant, a significant interaction condition (perturbed vs unperturbed trials) *target for Br, TLo and TLat, indicating that these muscles activity was adjusted differently to the perturbation dependent on the target, and finally a significant interaction group*condition for Br ($F(1,18)=5.05$, $p=0.03$), indicating that the SMD group adapted the activity in this muscle differently to the presence of the perturbation than the LMD group. All other main effects and interactions were not significant. In the 100ms following movement onset a series of rmANOVAs revealed a significant main effect of target for TLo, TLat, PD and PM ($p<0.005$) but not for Br and BB, a significant main effect

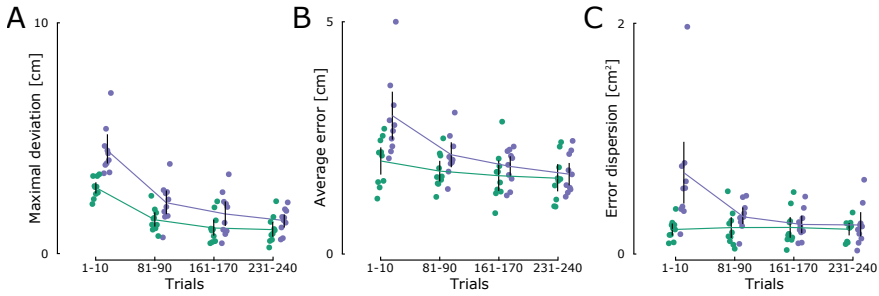

Figure 3.6: Mean maximal deviation, average error and end-point dispersion of participants of Experiment 2 with a large and small maximal deviation at initial exposure to the force-field. A) Maximal deviation in hand trajectory in four block of 10 trials positioned at the beginning, 1/3, 2/3 and at the end of the trials. Purple dots represent data from the 10 participants who had the Larger Maximum Deviation during the 10 first trials. Green dots represent data from the 10 participants who had the Smaller Maximum Deviation during the 10 first trials. The solid purple and green lines represent the evolution of maximum deviation across trials. Solid black lines represent the mean +/- SD of each set of dots. B) Average error of participants performing the task in Experiment 2. Colors are defined as in panel A. C) End-point dispersion for participants who performed the task in Experiment 2. Colors are defined as in panel A.

of condition for Br, BB, TLo and PD ($p<0.03$), and a significant interaction condition*target for BB, TLat, TLo and PD ($p<0.02$). All other effects were not significant. These results suggest that the activation of all muscles except Br and BB is adapted depending on the target direction and that the activation of all muscles except TLat and PM is modulated depending on the presence of the force field (Fig. 3.6A for the central target).

Finally, to examine whether better initial performance (smaller maximum deviation, average error and end-point dispersion) could be related to increased co-contraction, we computed the common activation level across agonist-antagonist muscles pairs for the three measured pairs (Elbow, Shoulder and Bi-articular, see Fig. 3.2). We compared the average co-contraction level in two time windows preceding movement onset (E1 and E2 on Fig. 3.2), and two time windows following movement onset (E3 and E4 on Fig. 3.2), to look for differences between the SMD and LMD groups of participants.

First, focusing on co-contraction levels in the two time interval preceding movement onset, in E1 a rmANOVA revealed a significant main-effect of target in the elbow muscle pair ($F(2,36)=4.035$, $p=0.02$), but not for the shoulder or bi-articular muscle pair, and no other significant main effect or interaction. In E2, the rmANOVAs revealed a significant main effect of target for all three muscle pairs ($p<0.001$), a significant interaction target*condition for the elbow muscle pair only ($F(2,36)=14.66$, $p<0.001$), and a significant interaction

group*condition for the shoulder muscle pair only ($F(1,18)=7.54$, $p=0.01$). These results indicate that, as muscles were activated differently dependent on the target to reach, co-contraction levels also differed across targets. Moreover, only co-contraction in the elbow muscle pair was significantly adapted to account for the introduction of the force field, and the two groups of participants (LMD and SMD) adjusted co-contraction in the shoulder muscle pair differently to the presence of the force field. Finally, given that group (SMD and LMD) had no significant main effect, participants' performance cannot be related to differences in co-contraction during the moments preceding movement onset (Fig. 3.6B for the central target).

If we now analyze co-contraction levels after movement onset, rmANOVAs performed on average co-contraction in E3 revealed a significant main effect of target for the elbow ($F(2,36)=7.75$, $p=0.001$) and the bi-articular muscle pair ($F(2,36)=5.65$, $p=0.007$), a significant main effect of condition for the shoulder muscle pair ($F(1,18)=4.42$, $p=0.049$), but not for the elbow and bi-articular muscle pairs, with all other main effects being not significant. The analysis also revealed a significant interaction group*condition for the shoulder muscle pair ($F(1,18)=4.48$, $p=0.048$) and a significant interaction group*target for the bi-articular muscle pair ($F(2,36)=4.1$, $p=0.02$), all other interaction were not significant. In E4, the rmANOVA revealed a significant main effect of condition for both the elbow ($F(1,18)=5.78$, $p=0.027$) and bi-articular ($F(1,18)=5.70$, $p=0.028$) muscle pairs, and no other significant main effect or interaction effect ($p>0.05$). Altogether these results point out that co-contraction after movement onset was modulated in the elbow and bi-articular muscle-pairs dependent on the target, and to account for the presence of the force field. The fact that group had no significant effect in the two time windows indicates that co-contraction levels were similar between LMD and SMD participants, hence suggesting participants less affected during initial exposure to the force field did not use a default stiffening of their arm to achieve such better performance, but rather that they used a distinct control strategy than participants more affected by the introduction of the force field (Fig. 3.6B for the central target).

Given that results in Experiment 2 did not reproduce results of Experiment 1 we performed a bootstrap two sample t-test on data of Experiment 1 to verify the significance of the effect (Kushary et al., 1997). 10000 repetitions revealed that 75% of tests were significant and that only 6% of the determined t-statistics were more extreme than the one computed with the base groups participants, hence suggesting the effect observed in Experiment 1 was really significant and was not due to chance.

Results of Experiment 2 suggest that differences in performance across participants cannot be linked to differences in co-contraction of agonist-antagonist muscle pairs (Fig. 3.5D, E and F and 3.6B). Moreover, the different behavior observed between the results of Experiment 1 and Experiment 2 suggest that

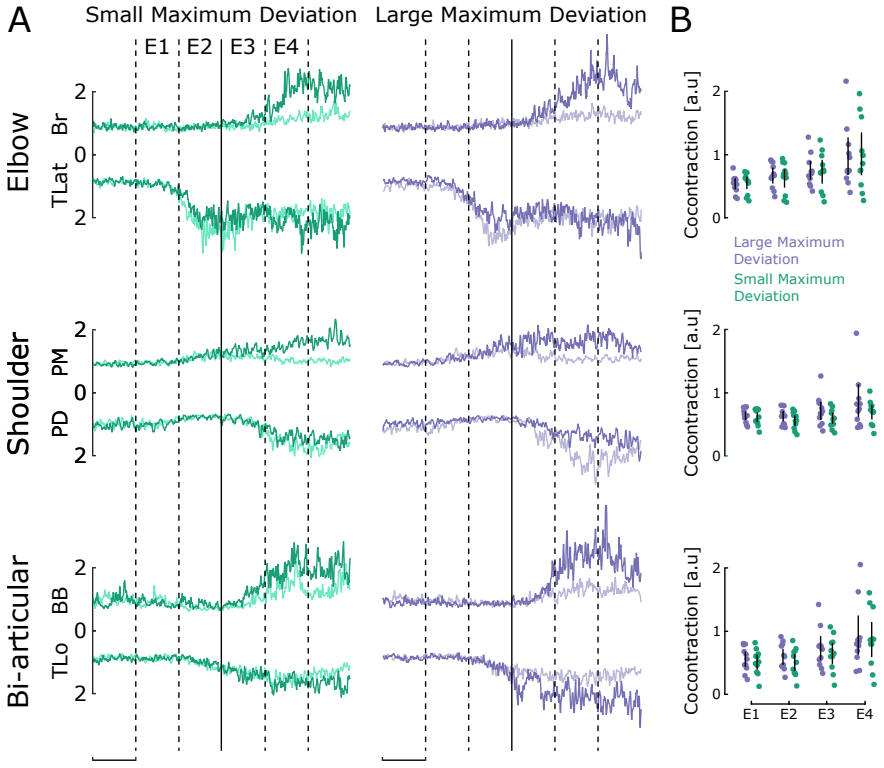

Figure 3.7: EMG signals and co-contraction averaged across all subjects for the central target and the three muscle pairs for baseline and force-field trials. A) EMG signals for the elbow, shoulder and bi-articular muscle pairs averaged across 10 trials and across all subjects for the central target. The solid dark green and dark purple lines represent the averaged EMG signal during the 10 first force-field trials for participants with a small and large initial deviation respectively. The light green and light purple solid lines represent data from baseline trials for participants with a small and large initial deviation respectively. The solid vertical black line indicates movement onset. The dashed black lines delimit four 100ms time windows: E1, E2, E3 and E4. B) Mean co-contraction in each time window for each subject and for the central target. Green and purple dots represent data from participant with a small and a large initial deviation respectively. Solid black lines represent the mean and SD of each group of dots.

inter-limb differences in performance are context-dependent.

3.4 Discussion

We investigated whether asymmetries in performance across arms during motor learning could be explained by the use of distinct control strategies rather than by a greater use of impedance control by the non-dominant arm. More precisely, we tested the hypothesis that the non-dominant arm is controlled using a strategy that is more robust than the dominant arm, in the sense that it is less sensitive to errors in the internal representation of dynamics. We modeled this hypothesis using two different controllers and illustrated, on a simple example, that the impact of the force field on end-point accuracy, precision and on the maximal deviation could be partially mitigated by the use of the robust controller, which explicitly considers the presence of model error (Fig. 3.3A).

To test this hypothesis, we investigated motor learning across dominant and non-dominant arms in two experiments performed with distinct experimental apparatus. First, we reproduced asymmetries in performance across arms previously reported in the literature (Schabowsky et al., 2007; Yadav and Sainburg, 2014a) in an end-point setup (Experiment 1, see Fig. 3.4A, B and C). In order to address whether co-contraction could account for these results, we performed the same experiment in an exoskeleton (Experiment 2), and, surprisingly did not observe differences in performance between the dominant and non-dominant arm in this setup (Fig. 3.5A, B and C). This null result suggests that differences in behavior across limbs are context-dependent and reflect how participants interact with the robotic device. However, by splitting participants of Experiment 2 into two groups based on their performance during initial exposure to the force field, we found no systematic link between differences in performance and co-contraction (Fig. 3.5D, E, F and 3.6B).

Previous studies hypothesized that differences in performance across arms could be explained by a greater reliance of the non-dominant arm on impedance control (Schabowsky et al., 2007; Yadav and Sainburg, 2014a,b). However, it has been reported that the intrinsic impedance of muscles is quite low at spontaneous levels of activation, and that a substantial and voluntary co-contraction does not elicit any clear change in the limb intrinsic properties, but rather only impacted the gain of the stretch reflex (Crevecoeur and Scott, 2014). The absence of differences in co-contraction observed in Experiment 2 across the groups with large and small maximum deviation during initial trials (Fig. 3.6A and B), along with the very limited impact of co-contraction and the low impedance at spontaneous background EMG, questions the possibility that participants used a default strategy based on a modulation of the limb impedance to mitigate the impact of the force field.

Instead, we hypothesize here that differences in performance across arms arise from differences in the uncertainty associated with the internal models of each arm. We suggest that the controller of the non-dominant arm considers explicitly the presence of model errors, likely because the internal representation of dynamics for this arm is less accurate. As a consequence, hand paths are less perturbed when exposed to the force field for participants using their non-dominant arm (Fig. 3.4A, B and C). Consistent with our hypothesis, studies have suggested that control of the non-dominant arm is associated with higher variability (Adam et al., 1998; Kalisch et al., 2006; Salimpour and Shadmehr, 2014), which might be a reflection of greater uncertainty in the internal models, however model errors were not considered in these studies.

We observed that movements performed with the non-dominant arm in Experiment 1 were less affected when initially exposed to the force field. So why is the dominant arm more perturbed if it is generally more skilled? In control theory, there is always a trade-off between robustness and efficiency. Indeed, greater robustness to model error comes at the cost of reduced efficiency, and vice versa. Such a trade-off is reflected in the results of Experiment 1, where the control strategy of the dominant arm is more sensitive to the introduction of the force field, leading to greater initial deviation, but is also more adaptive, leading to greater improvement across trials (Fig. 3.4A). Similar observations can be made between participants with small and large maximum deviation during the initial trials in Experiment 2 (Fig. 3.5D). Such an hypothesis was introduced by (Cluff et al., 2015) who reported that such a trade-off could capture differences in learning across participants. Consistent with these observations, Albert and Shadmehr (2016) showed that a smaller error experienced during initial trials leads to a smaller improvement in the following trials, without explaining the source of the initial error. Moreover, asymmetries in learning rate between the two arms in track-tracing tasks have been reported in the literature (McGrath and Kantak, 2016). Altogether, these results suggests the existence of a trade-off between sensitivity to model error and the ability to learn, with robustness being an advantage when the force field is first introduced but also reflecting reduced learning abilities. From this perspective, the sensitivity to model errors and the performance during learning reflect inter-limb differences in the internal models of reach dynamics.

The difference in adaptiveness of control strategies might also impact the transfer of learned motor skills from one arm to the other, with the arm more able to adapt its model during learning maybe being more able to transfer motor skill to the other arm. Contrasting results have been shown in the literature concerning this topic, with some studies reporting asymmetric transfer of features learned during a reaching task between the two arms (Wang and Sainburg, 2004, 2006), while others reported no differences in transfer across arms (Stockinger et al., 2015). However, it has been reported that skill transfer from the dominant arm to the non-dominant arm depends on the level of hand-

edness (Lefumat et al., 2015), with participants presenting greater asymmetries in dexterity across arms also presenting the most significant transfer. Hence, these results suggest that greater adaptiveness of internal models might be related to greater skill transfer but that, similarly to asymmetries in performance across arms, asymmetries in transfer of motor skill might be task-dependent and be present mainly when use of different control strategies is elicited.

We did not observe differences in behavior across arms in Experiment 2, suggesting that asymmetries in arm performance are context-dependent, but how could the change in experimental setup lead to such different results? It the framework we propose, it is conceivable that manipulating the handle of a robotic arm, which leads to different inertial properties, and having to control a greater number of degrees of freedom requires better internal models, or greater compensation for potential model errors, which in principle is clearly favorable to the expression of a robust control strategy. Moreover, it has been shown that the nervous system was able to switch between different feedback control policies dependent on the task being performed (White and Diedrichsen, 2013). In Experiment 1 forces were applied on the hand, whereas torques were applied on upper-limb joints in Experiment 2, and It was previously shown that different types of dynamical perturbations applied to the arm lead to distinct time course of learning (Lackner and DiZio (2005) but Davidson et al. (2005)). Moreover, while learning reaching movements with a tool in hand leads to the formation of a model of the tool as well as to a change in the formation of the internal model of participant's arm (Kluzik et al., 2008), which might impact the behavior of participants. Another difference between the two experimental setups was the constraints imposed on arm position; with the unconstrained position of the arms in Experiment 1 being associated with the control of a greater number of degrees of freedom (DOF) when compared to Experiment 2. Constraining the position of the arm to the horizontal plane has been shown to impact movement trajectory during reaching movements (Desmurget et al., 1997), with unconstrained reaching movements being more curved than constrained reaching movements. Furthermore, differences in motor adaptation and rehabilitation have been reported between 2D and 3D reaching movements (Scharver et al., 2005; Lledó et al., 2016) and, very recently, Schaffer and Sainburg (2017) observed differences in performance across arms during a 3D reaching task that were dissimilar from previous findings observed during 2D reaching tasks. Altogether these results suggests that the greater number of degrees of freedom controlled in experiment 1, as well as the application of the force field on the hand, might favor the expression of a more robust control strategy due to greater complexity of controlling such tasks.

In conclusion, we observed context-dependent differences in performance across arms that could not be related to differences in co-contraction. Of course this evidence is not definitive because we could not address co-contraction during Experiment 1 reliably (muscles active during the task less easily identifiable

due to more DOF), whereas we did not observe inter-limb differences in Experiment 2. The context-dependency of asymmetries in arm behavior as well as the role of co-contraction in such asymmetries should be further explored in future studies. In this work we suggest an alternative interpretation of inter-limb differences based on distinct control strategies, which are directly linked to the quality of internal models of each limb. This hypothesis captures distinct sensitivities to model errors upon the introduction of a force field without assuming differences in body size or mechanical impedance, and suggests a meaningful link between control and learning as a trade-off between efficiency and robustness that is rooted in neural representation of movement dynamics.

CHAPTER 4

Optimal use of limb mechanics distributes control during bimanual tasks

Abstract. Bimanual tasks involve the coordination of both arms, which often offers redundancy in the ways a task can be completed. The distribution of control across limbs is often considered from the perspective of handedness. In this context, although there are differences across dominant and non-dominant arms during reaching control (Sainburg, 2002), previous studies have shown that the brain tends to favor the dominant arm when performing bimanual tasks (Salimpour and Shadmehr, 2014). However, biomechanical factors known to influence planning and control in unimanual tasks may also generate limb asymmetries in force generation, but their influence on bimanual control has remained unexplored. We investigated this issue in a series of experiments in which participants were instructed to generate a 20-N force with both arms, with or without perturbation of the target force during the trial. We modelled the task in the framework of optimal feedback control of a two-link model with six human-like muscles groups. The biomechanical model predicted a differential contribution of each arm dependent on the orientation of the target force and joint configuration that was qualitatively matched by the participants' behavior, regardless of handedness. Responses to visual perturbations were strongly influenced by the perturbation direction, such that online corrections

also reflected an optimal use of limb biomechanics. These results show that the nervous system takes biomechanical constraints into account when optimizing the distribution of forces generated across limbs during both movement planning and feedback control of a bimanual task.

4.1 Introduction

Generally, healthy people are able to perform a wide variety of tasks that require the coordination of several actuators. For instance, steering an automobile involves a coordinated effort of two arms, but the effort produced can be distributed across the arms in a variety of ways. During the performance of bimanual tasks, the central nervous system must deal with redundancy and share control across limbs. An important factor to consider in this sharing is the asymmetry across flexor and extensor muscles (Kawakami et al., 1994), which may favor an anisotropic contribution of each arm during bimanual actions.

To date, the main source of limb-use asymmetry that has been considered is hand dominance. Previous studies have shown that the CNS favors the dominant hand during bimanual tasks (Swinnen et al., 1996; Salimpour and Shadmehr, 2014; Salimpour et al., 2015). Generally, this tendency is attributed to the lesser variability that is associated with controlling the dominant arm (Kalisch et al., 2006), which may, in principle, impact how the brain coordinates the two arms in bimanual tasks (O'Sullivan et al., 2009). Compatible with this hypothesis, Salimpour and Shadmehr (2014) reported that the dominant arm showed less variability during unimanual force production and suggested that this limb contributed more during a bimanual force-production task.

Beyond handedness, the possibility that biomechanical properties influence how we distribute control across our limbs has remained largely unexplored. However, in the context of unimanual tasks, it is clear that the CNS monitors biomechanical constraints arising during movements and adjusts subsequent motor decisions or trajectories accordingly (Sabes et al., 1998; Cos et al., 2011, 2012, 2013). It has been established that the CNS accounts for torque interactions at the shoulder and elbow joints during planning and control of reaching movements (Hollerbach and Flash, 1982; Gribble and Ostry, 1999; Dounskaia et al., 2011, 2014; Wang et al., 2012). Other parameters such as expected effort and success affect the arm choice when performing reaching movements (Schweighofer et al., 2015). Given the strong influence of biomechanics on unimanual control, we hypothesized that biomechanical factors should also play an important role in bimanual control.

To test this hypothesis, we adopted an isometric force production paradigm for two limbs (Salimpour and Shadmehr, 2014) and modified it for variance of

the orientation of target forces and joint configurations to asses how biomechanical factors influence the contribution of each arm to overall force generation during both motor planning and online corrective responses. We developed an optimized control model of two human-inspired two-jointed arms with which to predict optimal cooperation of the arms across three different joint configurations. We tested how well the model could predict the way right- and left-handed human participants distribute force across their arms. The model accounts for optimization of weighting of each limb during both unperturbed movements and responses to perturbations with visual feedback and was used to predict the influence of biomechanics on the force distribution across arms. We predicted that the arms' joint configuration would be shown to have a strong influence on the participants' adjustments to the distribution of forces produced across the limbs.

4.2 Materials and methods

4.2.1 Participants

Ten healthy right-handed participants (6 females, average Oldfield score 95, 9th right decile) and ten healthy left-handed participants (5 females, average Oldfield score -88.5, 7th left decile) participated in Experiment 1. Twelve right-handed participants (4 females, average Oldfield score 90, 7th right decile) participated in Experiment 2. The average age of participants was 27 years old. All participants provided written informed consent before participating in this study. The volunteers had no known neurological disorders and were naïve to the purpose of the experiment. Handedness was assessed using the Edinburgh Inventory (Oldfield, 1971). The experimental procedures were approved by the local ethics committee at the *Université catholique de Louvain*.

4.2.2 Behavioral task

Two different experiments were performed using the same general paradigm. Participants held the handles of two robotic arms (KINARM, BKIN Technologies, Kingston), one in each hand (Fig. 4.1A). Each handle was equipped with a force sensor (Mini-40 F/T sensors, ATI Industrial Automation, NC, USA). The forces measured by the transducers were mapped onto cursor position on a virtual reality display. Direct vision of the limbs and of the robotic handles was blocked. In this device, we must account for a delay of ~ 60ms between the computation of an event by the real time computer and the display of such an event on the screen. The robotic arms counteracted the forces applied by

the subject with a very stiff force field ($K = 2000$ N/m, $B = 50$ Ns/m). This force field limited movement of the robotic and participants' arms to negligible movements (isometric task). The position of the cursor (radius, 0.5cm), which was denoted by the two-dimensional vector $\vec{z}$, was proportional to the sum of the force vectors ($\vec{f}_L$) and ($\vec{f}_R$) produced by the left and right arm, respectively (see Fig. 4.1A):

$$\vec{z} = b(\vec{f}_L + \vec{f}_R) + \vec{z}_0 \tag{4.1}$$

In eq. 4.1, ($\vec{z}_0$) is the center of the workspace, corresponding to the initial location of the cursor with no forces being applied to the handles. The scaling factor b was set to 0.5cm/N. At the beginning of each trial, a reference target (radius 1 cm) was displayed at the center of the workspace. After 1s, the reference target vanished and a goal target appeared in one of 16 possible positions equally spaced around a circle with a 10-cm radius, centered on the reference target site (see Fig. 4.1C). The goal of the task was to produce a total force of 20 N in the direction of the target. Participants were instructed to reach the target within 800 ms, and then to maintain the cursor at the target site for 1 s. Participants were instructed to perform the task using both arms at the same time. Trials in which the ratio of forces produced by the two arms exceeded 10:1 were considered to be unimanual trials and omitted (5.75% of all trials were omitted; participant trial omission range, $0\tilde{}27\%$). Participants' arms were supported against gravity in the horizontal plane by slings, arm joint configurations were described in terms of elbow and shoulder joint angles (θ_1 and θ_2, respectively, in Fig. 4.1B).

In experiment 1, three different joint configurations were tested in three configuration-specified blocks (Fig. 4.2A). Joint angles were measured by a goniometer at the start of each block; the means and standard deviations of the measured joint angles for each configuration are reported in Table 4.1. In each configuration, the 16 possible targets were presented in a random order with each target being presented 10 times, resulting in 160 trials per configuration and a total of 480 trials for each subject.

In experiment 2, the subjects performed the task with their arms constrained to configuration 3 (Fig. 4.2A) with eight possible targets (Fig. 4.1C, red circles). In 80% of the trials, the cursor relocated perpendicular relative to the target direction midway through the movement (Fig. 4.1D). The relocated cursor appeared 3 cm or 5 cm, clockwise (CW) or counterclockwise (CCW), from the cursor's last location. We employed an orthonormal definition of location relative to initial reach direction such that cursor relocations in the CW and CCW direction were termed negative and positive cursor jumps, respectively. The presentation of these four possible cursor jump amplitudes (-5 cm, -3 cm, $+3$ cm, and $+5$ cm) and the unperturbed condition (0cm, 20% of trials) was random in order, but balanced in quantity for each subject. To reach the target, subjects had to adapt the forces they were applying to correct for the cursor's

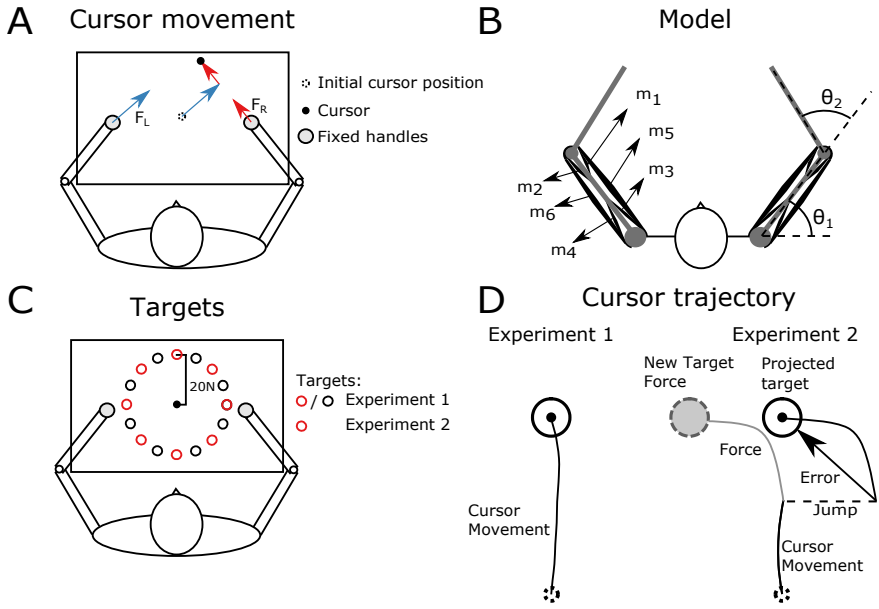

Figure 4.1: Human-inspired model and experimental procedure performed on the KINARM robot. A) Each subject sat in front of a screen holding two robotic arm handles. Movements were countered by a very stiff force field ($k = 2000$N/m, $B = 50$Ns/m). Participants are asked to push on both handles to reach a total force of 20N in the horizontal plane. A cursor (black dot) indicated the total force being produced. The sum of forces produced by both arms was mapped onto the cursor position (black dot) on the virtual reality display. B) Two human-inspired upper-limbs actuated by six muscle groups (numbered 1–6) corresponding to the mono- and bi-articular muscles at each joint. Both limbs work in the horizontal plane. The joint configuration was defined by the joint angles θ_1 and θ_2. C) The possible targets (black and red circles) were positioned on a 10cm radius circle and evenly spaced. Targets represented by black and red circles were used in experiment 1 and only the targets represented by red targets were used in experiment 2. D) Cursor trajectory (solid black line) from the initial cursor position to the target center in experiments 1 and 2. The force produced by the subject is presented as a gray line. In experiment 2, the cursor jumped midway through the movement. The target projected onto the screen was presented as a black circle. The new target force after the cursor jump is presented as a dashed gray disk.

shift in location which allowed us to study whether biomechanics has an influence on corrective online responses or not. More precisely, if online corrections use the same weighting as during the planning phase then we should observe no change in the force distribution across limbs following a cursor jump, leading to the same force distribution across arms as during unperturbed trials. In contrast, if CNS considers biomechanical factors during movement, then the response to a cursor jump should reflect the weighting associated with the new target force (Fig. 4.1D). Subjects performed 10 trials with each cursor jump possibility for each of eight target locations (Fig. 4.2C, red circles), yielding a total of 400 trials (10 trials * 5 jump/unperturbed options * 8 locations).

4.2.3 Data analysis

We computed the mean value of force produced by each arm during the 200–400ms time period after the target was reached and then projected the computed force amplitude along the corresponding target direction. An elliptical fit was performed on the computed forces for all targets and for each arm of all participants. The elliptical fit was performed by direct least square fitting (Fitzgibbon et al., 1999). A measure of the directionality of the fit was obtained from the ratio of the ellipse axes. A measure of the dominant direction of force production of each arm was obtained from the angle formed by the main axis of the ellipse and the x-axis of the horizontal plane. The surface of the fitted ellipse was used as a measure of the global contribution of each arm for each configuration, wherein the force produced by each arm was averaged across all target directions.

Experiment 1

To detect significant changes in the preferential direction of force production, we conducted a repeated-measures analysis of variance (rmANOVA) with main-axis orientation as the dependent variable, joint configuration and arm as within-subject independent variables, and handedness as a between-subjects independent variable. To detect significant axis orientation differences across configurations, we conducted a rmANOVA with axis ratio as the dependent variable and arm and joint configuration as within-subject variables, and handedness as a between-subjects variable. To compare the relative contributions of each arm during task performance, we conducted a rmANOVA with the total contribution of each arm as a dependent variable, arm- and joint-configuration as within-subject factors, and handedness as a between-subjects factor. For all tests, sphericity was verified with Mauchly's test.

Experiment 2

We computed the average force produced by the left arm and the right arm across all unperturbed trials. These average forces were used as baseline measures for the corresponding left and right arm forces. The forces measured during the cursor-jump perturbed trials were compared to these baseline forces to reveal course-corrective force changes induced by each perturbation. For each trial, we computed the difference between the force produced by the right arm and the left arm from 10ms prior to cursor jump to 500ms after the cursor jump.

To test whether the forces produced at target reach differed in relation to cursor jump amplitude, we conducted a rmANOVA with the forces produced by the two arms at target reach as the dependent variable and with body-side and cursor jump amplitude as within-group independent variables for each target. Sphericity was verified with Mauchly's test. To determine the instant at which the corrective force adjustments started to differ across cursor jump amplitudes, we conducted a rmANOVA with the derivative of the force difference as the dependent variable and cursor jump amplitude as the within group variable on every 10ms window after the cursor jump. To determine whether the force distribution across arms during rapid online corrections is optimized based on biomechanics we extrapolated predictions of the force each arm would produce along the direction of the target force after cursor jump (see Fig. 4.1D) for each jump amplitude and target from the elliptical fits of the forces obtained during unperturbed trials. Correlational analysis was performed between the predicted and measured forces of the perturbed trials.

Joint configuration	Shoulder angle (θ_1) [$\circ$]	Elbow angle (θ_2) [$\circ$]
1	$23.86 + -5.94$	$88.53 + -5.08$
2	$16.53 + -3.95$	$76.51 + -5.7$
3	$21.28 + -5.59$	$51.59 + -11.26$

Table 4.1: Mean joint angles ($+-$standard deviations) for all participants. Values reflect averages of all participants pooled together in the three configurations of experiment 1.

4.2.4 Mathematical modeling

Biomechanical and physiological model

We used a two-segment upper-limb model as described in detail previously (Li and Todorov, 2007). In this model, each limb is actuated by six muscle groups representing mono-articular flexors (m_1 and m_3) and extensors (m_2 and m_4)

at the shoulder and elbow joints, respectively, plus a bi-articular flexor (m_5) and extensor (m_6) spanning both joints (see Fig. 4.1B). Limb configuration was defined by the two joint angles θ_1 (ventral shoulder flexion) and θ_2 (elbow flexion), with the joint coordinates being mirrored across the two limbs (Fig. 4.1B). The mechanical model was coupled with a linear, first-order model of muscle tension as a function of neural command. Both arms were modeled identically.

The relationship between end-point force F and joint torque τ is given by:

$$\tau = J(\theta)^T F, \tag{4.2}$$

where $J(\theta)$ is the Jacobian of the system.

$$J(\theta) = \begin{bmatrix} L_1 \sin(\theta_1) - L_2 \sin(\theta_1 + \theta_2) & -L_2 \sin(\theta_1 + \theta_2) \\ L_1 \cos(\theta_1) + L_2 \sin(\theta_1 + \theta_2) & L_2 \cos(\theta_1 + \theta_2) \end{bmatrix}. \tag{4.3}$$

The joint torques are produced by the contraction of the various muscle groups actuating the limb. The torque produced by the contraction of a given muscle group depends on the moment arm (i.e., the distance between the joint's center of rotation and the line of action of the muscle group):

$$\tau = M(\theta)T, \tag{4.4}$$

In eq. 4.4 $T = \begin{bmatrix} T_1 & T_2 & ... & T_6 \end{bmatrix}^T$ represents muscle group contraction force and $M(\theta)$ is the moment arm (with $M_1 = \begin{bmatrix} 4.5 & -2 & 0 & 0 & 4.5 & -2.5 \\ 0 & 0 & 3.2 & -4.5 & 2.3 & -4 \end{bmatrix}$, $M_2 = \begin{bmatrix} 4.2 & -2 & 0 & 0 & 4.2 & -2.5 \\ 0 & 0 & 3.1 & -4.5 & 2.1 & -4 \end{bmatrix}$ and $M_3 = \begin{bmatrix} 3.3 & -2 & 0 & 0 & 3.3 & -2.5 \\ 0 & 0 & 3.15 & -4.5 & 2.2 & -4 \end{bmatrix}$ for configuration 1,2 and 3 respectively; see (Li and Todorov, 2007) for detailed definition of the values of M). Any change in joint configuration (θ) modifies the Jacobian and the moment arm, impacting, in turn, the relationship between muscle contraction and end-point force.

The tension of each muscle group depends upon its corresponding activation level, length, and velocity (Brown et al., 1999). Because we considered the behavioral task to be isometric and because we focused on forces produced at target reach we neglected changes in muscle length arising from muscle contraction and the effect of contraction velocity. We modeled muscle tension as a second-order, low-pass response to the control input u for the sake of simplicity:

$$t_{musc} T_i = k_i a_i - T_i, \tag{4.5}$$

$$t_{act}a_i = u_i - a_i, \tag{4.6}$$

In eq. 4.5 and 4.6, the index i corresponds to the number of the different muscle groups (Fig. 4.1D), such that T_i is the tension of the corresponding group i, a_i is the activation level, u_i is the control input, t_{musc} is the muscle group activation time (set to 90ms), and t_{act} (set to 50ms, as in Li and Todorov (2007)) is the activation dynamics time, k_i is the activation gain of the corresponding muscle group i ($k_1 = 0.87$, $k_2 = 0.67$, $k_3 = 1.06$, $k_4 = 0.58$, $k_5 = 0.24$, $k_6 = 0.48$). Changing activation dynamics (t_act and t_musc) had no impact on the results. Although these two parameters influenced the force rise time in accordance with the control input change, they did not affect the steady-state forces reached. k_i is the activation gain of the corresponding muscle group i ($k_1 = 0.87$, $k_2 = 0.67$, $k_3 = 1.06$, $k_4 = 0.58$, $k_5 = 0.24$, $k_6 = 0.48$) and represents the relative strengths of the corresponding muscle group, with a greater activation gain leading to a greater contraction force for a given neural input. The activation gains were estimated from measurements of cross-sectional areas of human cadaver muscles (Crevecoeur and Scott, 2014). It is worth noting that activation gains were greater for the flexor muscles for the elbow and shoulder muscle pairs ($k_1 > k_2$ and $k_3 > k_4$) but not for the bi-articular muscle pair ($k_5 < k_6$).

All simulations were based on arms of identical dimensions and strength positioned symmetrically relative to the body midline (Fig. 4.1B). Indeed, the forces produced in this task are far from maximum voluntary contraction forces. Variability was also considered identical across arms in simulations. To verify this hypothesis we computed the 95% confidence ellipse of the forces produced by each arm across trials and performed a rmANOVA with this measure. This rmANOVA revealed no significant main effect of body-side ($F(1, 18) = 2.89$, $p = 0.1$), handedness ($F(1, 18) = 0.08$, $p = 0.78$) or target ($F(15, 270) = 1.67$, $p = 0.2$) and no significant interaction effect ($p > 0.16$). Joint angles (θ) were the only parameters modified across simulations, which impacted the Jacobian matrix (J(θ) in Eq. 4.3) and the moment arms ($M(\theta)$ in Eq. 4.4, Li and Todorov (2007). Therefore, the biomechanical factors influencing the predicted force distribution across arms are the asymmetries in strength across flexors and extensors muscle groups in each arm, the relation between joint torques and end-point force ($J(\theta)$) and the moment arm of each muscle group ($M(\theta)$ both of which vary with joint configuration).

Optimal control problem

Because the task requires holding the cursor at the target for 1s, which involves continuous feedback monitoring to compensate for motor noise, the nominally isometric task becomes effectively a dynamic task. Hence, the question of whether a static solution of a global minimization problem can characterize

dynamic control faithfully is nontrivial. Thus, we considered a dynamic control model for the sake of generality.

We employ an optimal feedback control model with a positivity constraint on the neural input, $u = \begin{bmatrix} u_1 & u_2 & ... & u_{12} \end{bmatrix}^T > 0$. The positivity constraint is necessary to avoid negative control input (and tension) for any muscle group and was applied to represent the physiological property of muscle force generation being limited to contraction (muscles can only pull on the bones). The state-space representation of the system dynamics in discrete time is defined as

$$x_{t+1} = Ax_t + Bu_t + \omega_t, \tag{4.7}$$

where $x_t = [\ x\ y\ F_x^R\ F_x^L\ F_y^R\ F_y^L\ T_1^L \cdots T_6^L\ T_1^R \cdots T_6^R\ a_1^L \cdots a_6^L\ a_1^R \cdots a_6^R\ x^*\ y^*]$ represents the state of the system at time step t and contains endpoint force, muscle tension, and muscle activation values respectively. The variable u_t represents the neural input at time t, with $\omega_t \sim N(0, \Omega_\omega)$ defining the random Gaussian noise. The covariance of the state noise $\Omega_\omega(19:30, 19:30) = I_1 2 \times 12$ with I being the identity matrix and $\Omega_\omega(i,j) = 0$ otherwise. With the noise covariance matrix defined in this way, random noise is applied only to the control command. The matrices A and B are defined using the equations detailed above. For simplicity, this model does not include signal-dependent noise, thereby exploiting the separation principle and enabling easy computation of the optimal control and estimation in a closed loop, as is needed to handle the positivity constraint on the muscles. Nevertheless, all aspects of the simulations are expected to generalize with the presence of signal-dependent noise.

The available information about the state of the system is given by:

$$y_t = Cx_t + \eta_t, \tag{4.8}$$

where y represents the output of the system, $C = I_3 0$ represent the feedback matrix and $\eta \sim N(0, \Omega_\eta)$ defines the random Gaussian noise applied to the feedback. The covariance of the feedback noise is $\Omega_\eta = \begin{bmatrix} 10^{-3} & 0_{30\times 2} \\ 0_{2\times 30} & 10^{-10} I_2 \end{bmatrix}$.

Following computation of the optimal input, we used Kalman filtering to get an unbiased estimate of the state vector that minimizes estimation variance as shown in eq. 4.9

$$\hat{x}_{t+1} = A\hat{x}_t + Bu_t + K_t(y_t - C\hat{x}_t) \tag{4.9}$$

wherein $\hat{x}$ represents the estimated state of the system and K_t represents the Kalman filter gain.

To compute the optimal neural input u, we minimized the cost function given by

$$V_t = \sum_{i=0}^{N} x(t+i|\hat{x}(t))^T Q x(t+i|\hat{x}(t)) + u(t+i)^T R u(t+i), \qquad (4.10)$$

In eq. 4.10, matrices Q and R define the state and input costs, respectively. The matrix Q penalizes output error and forces differences across the arms. The matrix R penalizes high neural inputs to prevent excessive muscle activation. In our model $R = 10^{-7} I_{12}$. Changing this value did not influence the static end-point forces produced by the two arms in the model, but rather affected the time necessary to reach these end-point forces. The finite horizon N is the predictive horizon that allows us to handle the positivity constraints on the vector u. An analytical solution of the unconstrained problem is generated for each time step. If the analytically computed control input u violates any constraint ($u_i < 0$ for some i), quadratic programming is used to find a numerical solution that does not violate the constraint. The quadratic programming algorithm computes a numerical solution for the time window defined by N. Because the noise that may perturb the system during the time window N is unpredictable, we use a receding horizon policy, take the first element of the computed control vector, and restart the process at the next time step.

Developing the first part of eq. 4.10 gives the following expression:

$$x^T Q x = w_1(x-x^*)^2 + w_2(y-y^*)^2 + w_3(F_x^L - F_x^R)^2 + w_4(F_y^L - F_y^R)^2, \quad (4.11)$$

where x and y represent the coordinates of the cursor location, x^* and y^* represent the target coordinates, and the F_x^L,F_y^L,F_x^R and F_y^R variables represent the x and y forces of the left and right arm, relative to each coordinate axis, respectively. Force differences across the two arms were penalized to account for the fact that participants were instructed to use both arms while carrying out the behavioral task (w_3 and w_4 in eq. 4.11). In our model, $w_1 = w_2 = 1000$ and $w_3 = w_4 = 10^{-3}$. The large difference between w_1 and w_2 versus w_3 and w_4 can be explained, in large part, by the factor b ($= 0.05$), which is introduced between the forces produced by the two arms and the cursor position. These parameters were adjusted to limit inter-limb force differences while allowing us to still observe asymmetries in static forces produced by each limb.

The expression of muscle tension in the model was simplified and modeled as a second-order, low-pass response to the control input u, making the system linear. The input u had to be constrained to prevent negative muscle tension in the model. This positivity constraint required using the model predictive control (MPC; Camacho and Bordons (2007); Rawlings and Mayne (2012)) framework because standard stochastic optimal control models (LQG see Astrom (1970) for details) do not deal directly with bounded solution spaces. However, MPC is similar to the standard model type in principle, with the only difference being

that MPC uses quadratic programming to derive a numerical solution to the control problem that meets a positivity constraint.

4.3 Results

4.3.1 Optimal weighting of the left and right arms in isometric force production

In Experiment 1, participants were free to modulate the amount of force produced by each arm while generating a total force of 20 N. Model simulations performed using the average joint angles presented in Table 1 predicted that the force produced by each arm would vary depending upon the direction of the target force in a manner that exploits this redundancy (Fig. 4.2B). Each arm was predicted to have a preferential direction in which it would produce a larger force (Fig. 4.2B), and this direction changed with joint configuration. In the simulations, control was distributed across the two arms based on their respective preferential directions. Therefore, changing joint configuration in the model impacted the force distribution across the limbs in the simulations. For instance, the left arm produced larger forces in the up-right direction in configuration 1, but produced larger forces in the up-left and down-right directions in configuration 3. In the model, three factors explain these differences in preferential direction of force production across configurations. Firstly, the Jacobian of the system and the moment arm of each muscle group which are both dependent on the joint configuration are the two factors having the greatest impact on the preferential direction of force production. Secondly, differences in strength across the various muscle groups, with flexor muscles being stronger than extensor muscles, also impact the force distribution across arms. The two extreme configurations, 1 and 3 on Fig. 4.2, were selected because the preferential directions of the two arms were inverted between these two configurations. Configuration 2 was chosen as an intermediate configuration.

The experimental data from right- and left-handed participants followed the same pattern as the model simulations (Fig. 4.2C and D). The preferential direction of each arm changed progressively across configurations in a way that is similar to the changes observed in model simulations. The preferential direction of the two arms determined the force distribution across limbs. More precisely, the main-axis orientation of the model simulations are good predictions of the main-axis orientation observed in the experimental data for configurations 1 and 3, but not for configuration 2 (Fig. 4.2B, C and D). A rmANOVA revealed no main effect ($p > 0.2$ in all cases) of handedness ($F(1, 18) = 1.425$), body-side (left vs. right arm, $F(1, 18) = 3.202$), or joint configuration ($F(2, 36) = 1.42$) on the preferential direction of force production. There was a significant

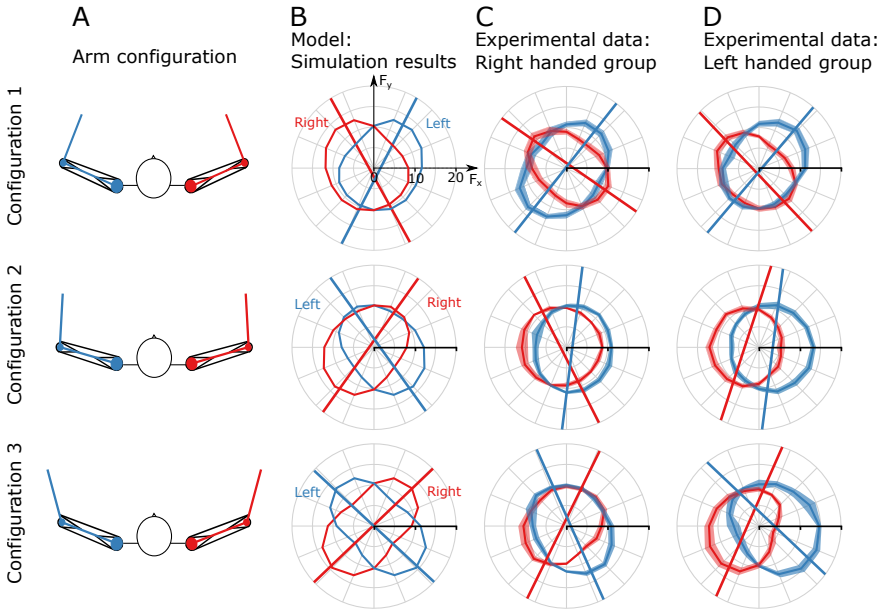

Figure 4.2: Arm configuration, model predictions, and mean experimental results for right- and left-handed participants. A) The three joint configurations tested in model simulations and experiments. B) In the simulations, the force produced by each arm was projected along the direction of the target and plotted in the target's direction. Solid grid lines show target directions and force levels. Simulation results are plotted in red for the right arm and in blue for the left arm. The main axis orientation of an elliptical fit performed on simulation data is presented as a solid blue or red line. C) Mean and standard error of the mean (SEM) of the experimental results of all right-handed participants pooled together. The forces are displayed in a manner identical to the simulation results. The solid lines represent the mean main-axis orientations of the arms of all right-handed participants pooled together. D) Mean and SEM of the experimental results of all left-handed participants pooled together. The lines represent the pooled mean main-axis orientations as in panel C.

interaction between joint-configuration and body-side ($F(2, 36) = 40.79, p < 0.001$), but no other significant interactions ($p > 0.1$), indicating that joint configuration affected the main-axis orientation differently across the subjects' two arms. More precisely, the influence of joint configuration on the main-axis orientation of the left arm was the inverse of its influence on the main-axis orientation of the right arm (Fig. 4.2B–D and Fig. 4.3D). Bonferroni post hoc tests revealed that main-axis orientation differed significantly across joint configurations for both arms ($p < 0.05$ in all cases). Moreover, the main-axis orientations of the left and right arm differed significantly from each other in configurations 1 and 3 ($p < 0.001$ in both cases) but not in configuration 2.

To understand how the preferential direction of force production of the two

arms transitions between configuration 1 and configuration 3, we varied the simulated elbow angles of the model continuously from 35° to 110°, we also varied the shoulder angles linearly across the values measured for configurations 1, 2 and 3 (see Table 1). We measured the preferential direction of force production and the overall contribution of each arm using an elliptical fit (see methods). The directional preference of each arm was measured as the orientation of the main axis of the fitted ellipses. Data from the simulations (Fig. 4.3A) and from an exemplar participant (Fig. 4.3B) in configuration 1 are shown in Fig. 3, note the elliptical fit performed as well as the main axis of the ellipse. Simulations across elbow angles showed a progressive transition of the preferential direction of force production of the two arms relative to the elbow angle (Fig. 4.3C). In simulations, the preferential directions of the two arms reversed at the same elbow angle of 86°. More precisely, when the elbow angle reached 86°, the preferential direction of the left arm changed from lying in the down-left to up-right direction towards lying in the up-left to down-right direction and vice versa for the right arm. Experimental results of all participants pooled together showed similar behavior except that the transition angle was $\sim 76^\circ$, corresponding to a smaller elbow angle close to configuration 2 (Fig. 4.3D). The gradual transition observed in the simulations (Fig. 4.3C) is also observed in our experimental observations (Fig. 4.3D), however a general shift towards larger elbow angles is observed in simulations when compared to experimental data. It is possible that no significant difference in preferential direction was observed in configuration 2 in our experiment because the elbow angle in configuration 2 ($76.51 + -5.70^\circ$) is closer to the reversal point of experimental results than the elbow angle of configuration 1 ($88.53 + -5.08^\circ$).

The axis ratio of the fitted ellipse showed a maximum at the switching point in both the simulation and experimental results (Fig. 4.3E and F). At the switching point, the elliptical fits were almost circular, rendering the extraction of the main axis orientation very sensitive to variability in the data. A rmANOVA revealed a significant main effect of joint configuration ($F(2, 36) = 4.535$, $p = 0.0175$), but not of body-side ($F(1, 18) = 2.02$, $p = 0.173$) or handedness ($F(1, 18) = 0.519$, $p = 0.48$), on axis ratio and no significant interactions ($p > 0.1$). A post-hoc analysis with adjusted paired t-tests (Fig. 4.3F) revealed that the axis ratio of configuration 2 differed significantly from that of configuration 1 for both arms ($p < 0.001$), as well as from that of configuration 3 for the right arm ($p = 0.027$), but not the left arm ($p = 0.09$). The axis ratio did not differ between configurations 1 and 3 for either arm.

Altogether the model qualitatively predicted the transitions in main axis orientation across configurations (Fig. 4.3C-D), as well as the increase followed by a decrease in the axis ratio (Fig. 4.3E-F). The model quantitatively predicted main axis orientation of configurations 1 and 3 (Fig. 4.4A-C).

The measured main-axis orientations in configurations 1 ($136.6 + -21.1^\circ$ for

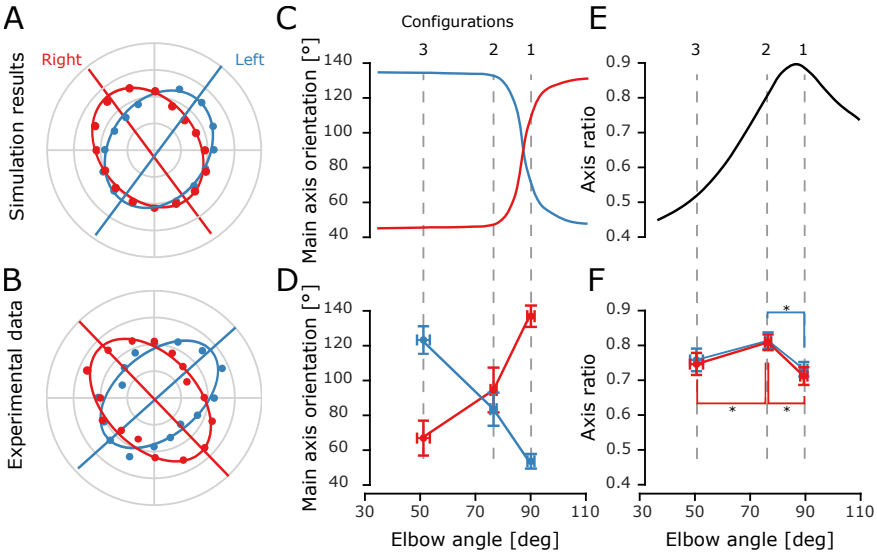

Figure 4.3: Main-axis orientation and axis ratio for simulations at various elbow angles and for experimental data. A) Simulation data for the left (blue dots) and right arm (red dots) in configuration 1. The elliptical fit performed on these data is presented as a solid line ellipse. The main axis orientation of the fitted ellipses are presented as solid lines. B) Exemplar participant data for the left and right arm (blue and right disks, respectively). The elliptical fit is presented as a solid line ellipse. The main axis orientation of the ellipse is presented as a solid line. C) Main-axis orientation of the left (blue line) and right arm (red line) of the simulations for elbow angles ranging from 35° to 110°. Shoulder angles were linearly interpolated between the angles presented in Table 1 in order to match the experimental joint configurations as closely as possible. The dashed gray lines indicate the elbow angles measured during the experiment for configurations 1, 2, and 3. D) Main-axis orientation for the left (blue line) and right arm (red line) of all participants pooled together for the three tested configurations. E) Axis ratio for the two arms in the simulations (black line). Both arms had an identical axis ratio. F) Axis ratio for the left and right arm of all participants pooled together for the three configurations.

the right arm and $53.15 + -13.96^\circ$ for the left arm) and 3 ($66.85 + -39.54^\circ$ for the right arm and $123.08 + -29.2^\circ$ for the left arm) were, on average, close to the axis orientations predicted by our model simulations (123.7° and 56.2° for the right and left arm in configuration 1 and 44.52° and 135.8° for the right and left arm in configuration 3, Fig. 4.4A and C). In configuration 2, the measured main-axis orientations ($94.42 + -53.24^\circ$ for the right arm and $83.41 + -37.87^\circ$ for the left arm) were found to be highly variable due to the proximity of this configuration to the elbow angle of reversal (Fig. 4.3C). In addition, the near-circularity of the elliptical fits reduced the reliability of our ellipse orientation estimates (Configuration 2, Fig. 4.4B). The elliptical fits for configurations 1 and 3 had smaller axis ratios than those of configuration

2, enabling less variable main axis estimates. No differences emerged between left- and right-handed participants in any of the three configurations. In terms of main axis orientation the model explained 29% of the variability of the data across the three configurations and 63% when considering only the two extreme configurations (1 and 3).

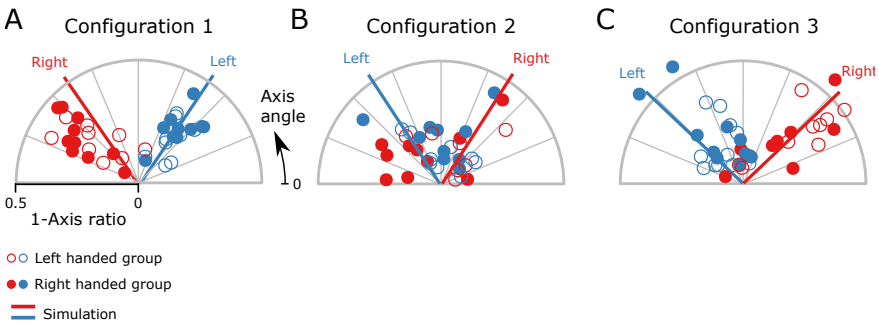

Figure 4.4: Radial plot of 1 - axis ratio and main-axis orientation for all right-handed and left-handed participants in the three experimental configurations. The radius of the plot represents 1-axis ratio and the phase represents the main-axis orientation of the ellipses fitted on participant data. The right- and left-arm data of all participants are presented in red and blue, respectively. The right-handed participants' data are presented as disks and the left-handed participants' data are presented as circles. The main-axis orientation of simulation predictions are presented as solid lines.

Finally, while simulations predicted the progressive change of main-axis orientations across configurations, differences can be observed between simulations and experimental data. As in the model the two arms are modeled identically, the force produced by the two arms in simulations are symmetrical relative to the vertical midline whereas asymmetries can be observed between the right and left arm in experimental data (Fig. 4.2). This suggests that factors other than biomechanics influence participants' behavior. Differences between model simulations and experimental data are not systematic across experimental groups, however similar asymmetries can be observed in both right- and left-handed participants. For instance, we determined the total amount of force generated by each arm based on the surface areas of the fitted ellipses for each arm of each subject. We found that the left arm produced, on average, slightly more force (56% and 53% of the total force for left-handed and right-handed participants, respectively) than the right arm (44% and 47%, respectively). A rmANOVA revealed no main effects of handedness ($F(1,18) = 0.207$, $p = 0.61$), bodyside ($F(1,18) = 4.18$, $p = 0.056$), or joint configuration ($F(2,36) = 0.613$, $p = 0.55$) on fitted ellipse surface area, and no significant interactions (all $p > 0.2$). The fact that both right- and left-handed groups showed similar asymmetries across arms suggests that these differences are not due to handedness.

4.3.2 Effect of biomechanics on corrective bimanual responses

In Experiment 2, the cursor jumped perpendicularly to the target direction at the midpoint of the movement requiring participants to perform corrective force adjustments to direct the cursor towards the target. These corrective force adjustments produced in response to cursor jumps differed dependent on the direction of the target (Fig. 4.5C, D, G and H). For example, the motor response of the right arm was larger when moving the cursor towards the lower target than towards the higher target (Fig. 4.5G and C, inset respectively). The end-point forces produced during unperturbed trials were similar to Experiment 1 in configuration 3, thus reproducing the Experiment 1 results in a distinct group of participants (see Fig. 4.6A and Fig. 4.2C-D). As predicted by the model simulation, the main differences in force produced by the two arms in configuration 3 were seen for the down-right and down-left targets. If motor corrections take biomechanical factors into account, then lateral jumps should evoke online adjustments of the weighing of each arm on the total force production that differ according to the location of the target and to the amplitude of the cursor-jump. For instance, perturbations when moving the cursor towards a straight downward target should elicit distinct corrections dependent on the direction of the cursor jump, with a greater contribution of the right or left arm when the cursor jumps clockwise (CW) or counter clockwise (CCW) respectively (Fig. 4.6A, B and C).

Analysis of the average end-point forces produced in perturbed trials towards the center-down target revealed adjustments consistent with the biomechanically optimal distribution of forces (Fig. 4.6A and B). More precisely, for the center-down target, motor corrections to CCW or CW jumps elicited differential use of the arms that paralleled the differences observed at baseline (Fig. 4.6B).

A series of rmANOVAs was performed for each target on the forces produced by each arm. For the up-right and up-left (diagonal direction) targets, as well as the far-right and far-left targets (along the x-axis), there was a main effect of perturbation (individual tests across target $F(4, 48) > 7$, $p < 0.05$), no effect of body-side ($F(1, 12) < 1.8$, $p > 0.05$), and no interaction ($F(4, 48) < 2.3$, $p > 0.1$). A significant effect of perturbation shows that for these targets the cursor jump amplitude and direction impacts the end-point forces produced by the two arms. For the down-left and down target, we found a main effect of perturbation ($F(4, 48) = 36.5$, $p < 0.001$ and $F(4, 48) = 7.4$, $p < 0.001$ respectively), no effect of body-side ($F(1, 12) = 1.8$, $p = 0.184$ and $F(1, 12) = 7.4$, $p = 0.077$ respectively), and a significant interaction ($F(4, 48) = 9.8$, $p < 0.001$ and $F(4, 48) = 49.6$, $p < 0.001$ respectively). For the down-right target, we found main effects of perturbation ($F(4, 48) = 12.6$, $p < 0.001$), body-side ($F(1, 12) = 7.5$, $p = 0.017$) and a significant interaction ($F(4, 48) = 1.8$, $p = 0.133$). More intuitively, a significant interaction effect means that force

adjustments of the dominant arm changed across cursor jump amplitudes in a different way than the force adjustments of the non-dominant arm (Fig. 4.6B).

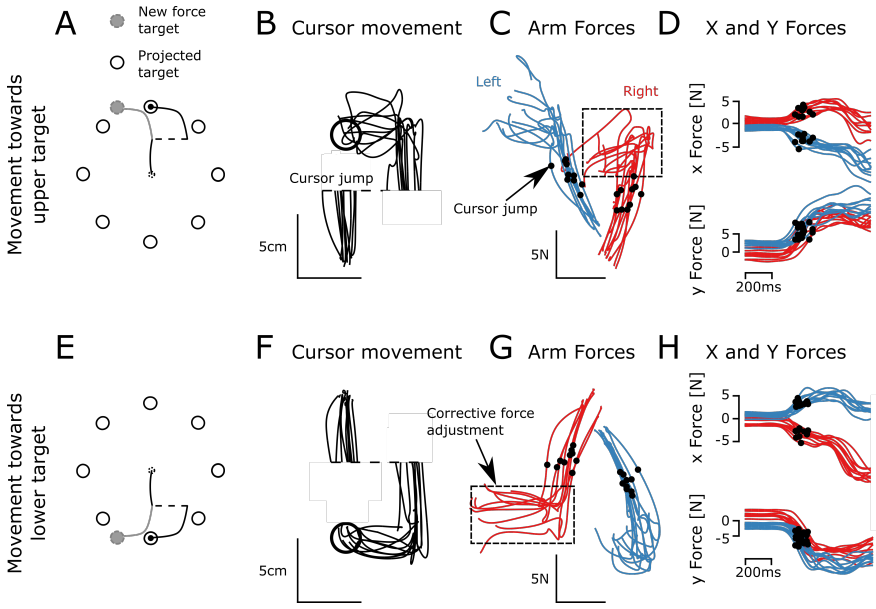

Figure 4.5: Cursor trajectory and arm forces for the top (A–D) and bottom (E–H) targets in exemplar subjects. A, E) Theoretical cursor trajectories of the presented trials for the top (A) and bottom (E) targets. B, F) Cursor trajectory of 10 trials for the top (B) and bottom (F) targets with a 5cm rightward cursor jump. C, G) Corrective force responses (dashed box) of the right (red) and left (blue) arms over 10 trials after cursor jumps (black dots). D, H) Time evolution of the x and y forces of the arms for 10 top-target (D) and 10 bottom-target (H) trials.

For each perturbation amplitude, we measured the forces produced by the right and left arms from 200ms before to 500 ms after the cursor jump. For all targets, corrective responses of the dominant arm started, on average, 160ms after the cursor jump (Fig. 4.6C) while corrections of the non-dominant arm started on average 60ms later, though the adjustments differed with respect to the target direction (reported above). Hence, after 160 ms the weight attributed to the dominant arm on the total force production is modulated online dependent on the cursor jump amplitude (Fig. 4.6C). To determine the moment at which the force of each arm started to diverge across jump amplitudes, we computed the derivative of the forces measured for the right and left arm. With this derivative as the dependent variable, we performed a rmANOVA on each 10ms window starting from the moment of the jump. For the center-down target, we observed a main effect of jump amplitude ($F(4, 48) = 3.617$, $p < 0.05$) starting from $\sim$ 160ms after the jump (all earlier windows, $p > 0.05$) for the right arm, whereas we observed a main effect

of jump amplitude ($F(4, 48) = 5.76, p < 0.001$) starting from $\sim 220ms$ after the jump. This correction latency was later than expected in light of previous reports on online corrections during reaching (Dimitriou et al., 2013). Notwithstanding, similar correction times (~ 150ms) were observed with a unimanual version of the task (data not shown). The difference of 60ms in correction latency between the two arms was surprising as, to our knowledge, such difference has not been reported in the literature. It is worth noting that while the net response of the arms scales with direction and amplitude of the cursor jump, the difference in the response produced by each arm is precisely indicative of the influence of biomechanics in the corrective response, with adjustments differing dependent on target direction in a way that is consistent with the force distribution predicted by joint configuration (Fig. 4.6A). For instance, for the upper target no change in force for the two arms should arise from a left or right-ward cursor jump (Fig. 4.6A), which is what we observed in the time evolution of the perturbed trials towards this target (data not shown).

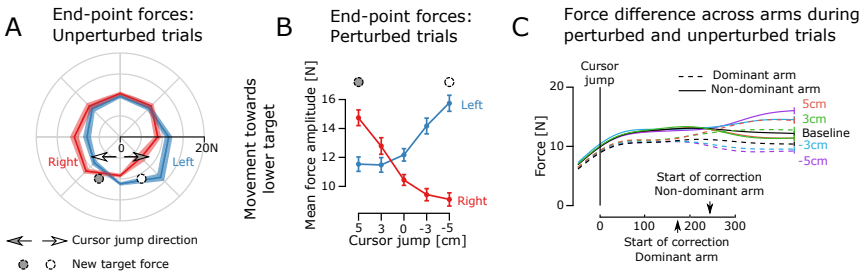

Figure 4.6: Analysis of corrective responses for all cursor jump amplitudes for the bottom target (positioned at $270°$). A) Mean +− SEM of forces produced at target reach for unperturbed trials of all targets. The forces produced by the right (red) and left (blue) arm are projected along the direction of the respective target and plotted in the targets direction. Solid grid lines show the target directions and force levels. Cursor jump directions are indicated by white and gray arrows. The actual endpoint forces that must be produced following a cursor jump are presented as white and gray dashed-circle targets (colors match corresponding jumps). B) Mean +− SEM of forces produced from 200ms after target reach to 400ms after target reach by the left and right arm for the bottom target with all cursor jump amplitudes. C) Time evolution of the force produced by the right (dominant) arm (dashed line) and the left (Non dominant) arm (solid line) for all perturbed and unperturbed trials towards the bottom target. The SEM for each perturbation amplitude is shown at the end of each line. Perturbation amplitudes are color-coded: red, 5cm; green, 3cm; black, unperturbed; light blue, -3cm; and purple, -5cm.

The force distribution across arms observed after cursor jumps was very similar to the force distribution observed during unperturbed trials for the corresponding direction (Fig. 4.7A and D) suggesting that biomechanics impacted the corrective force responses. To further compare the end-point forces of unperturbed and perturbed trials, we fitted an ellipse on the end-point forces

measured during unperturbed trials. Based on this elliptical fit we predicted the forces that should be produced in the direction of the new target forces after cursor jump. We compared the predicted force difference between right and left arm to the forces measured during perturbed trials and observed that the correlations between predicted and measured forces for each cursor jump amplitude were very strong ($R^2 > 0.80$ and $p < 0.001$; Fig. 4.7B, C, E and F), confirming that biomechanical factors were integrated into online corrective force adjustments. We performed the same analysis with model simulations and observed correlations very similar to those observed in experimental data (Fig 4.7B, C, E, F).

4.4 Discussion

We investigated the impact of biomechanical constraints on how the brain weights each arm in the context of bimanual control. More precisely, we studied the impact of asymmetries in the strength across muscle groups of the upper-limbs and the effect of the moment arm of each limb joint and of each muscle group which varied with joint configuration. Our main finding was that the orientation of the axes at which each limb produces more force (ellipse orientation) and how much force production varies across the targets (axis ratio) varied progressively and systematically across joint configurations, independent of handedness, in a way that was predicted by simulations of the optimal control model, in which differences in force across flexor and extensor muscle groups and the moment arm of each upper-limb joint as well as of each muscle group were the only source of mechanical anisotropy. Moreover, following cursor jumps the forces produced by participants were adjusted online optimally with respect to the biomechanical configuration of their arms. The presently observed match between the optimal control model and participants' behavior supports the hypothesis that biomechanics shape neural control solutions during bimanual tasks.

With respect to laterality, there are several known asymmetries between the dominant and non-dominant arm during unimanual movements (see Goble and Brown (2008) for review). For instance, Sainburg and Kalakanis (2000) reported a laterality difference in the control of limb dynamics during reaching. Shabbott and Sainburg (2008) further explored this difference in response to cursor jumps during unimanual reaching movements and found that the right and left arm showed similar timing and amplitude of corrective movements but showed differences in movement trajectories. Mutha et al. (2013) suggested that, when learning to reach in a force field, the dominant hand is better at optimizing task dynamics whereas the non-dominant hand is better at stabilizing around the target.

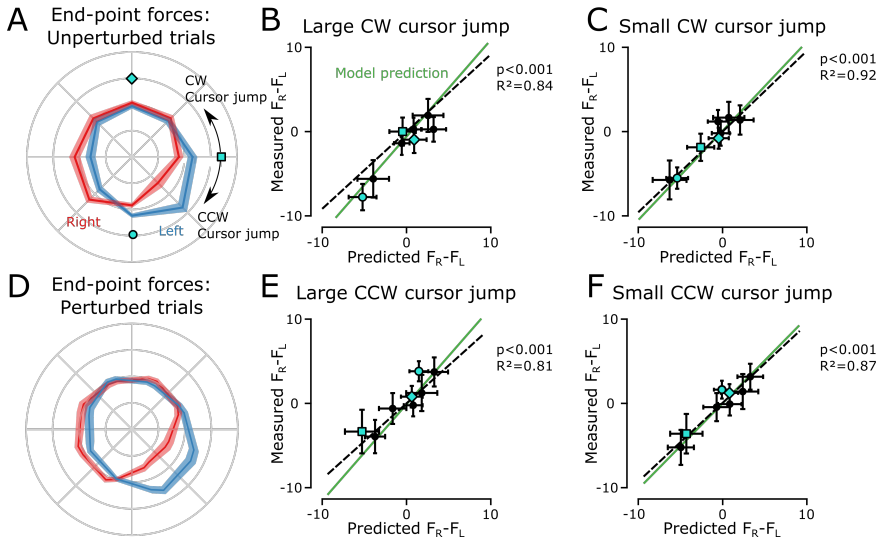

Figure 4.7: Comparison between forces produced during baseline trials and perturbed trials (A and D) and comparison between forces predicted from baseline trials versus measured forces in all perturbed (B, C, E andF) trials. A, D) Means +− SEMs of forces produced at target reach in unperturbed (A) and perturbed (D) trials for all targets. The forces produced by the right (red) and left (blue) arm are projected along the direction of the respective target and plotted in the targets direction. Solid grid lines show the different target directions and force levels. The light blue circle, square, and diamond represent the corresponding targets in all panels of the plot. The two arrows indicate CCW and CW corrections. B, E) Means +− SEMs of measured versus predicted force differences between the right and the left arms for each target in all perturbed trials with -5 cm (B) or 5 cm (E) cursor jumps, which correspond to a large CW (B) or CCW (E) cursor jumps forces. The predicted force differences were extracted from the ellipses fitted on the forces measured for each arm of each subject during unperturbed trials. A dashed black line represents the unity line. The solid green line represents the predictions of model simulations. The light blue square, circle, and diamond correspond to the targets presented in panel A. C, F) Means +− SEMs of measured versus predicted force differences between the right and the left arms for each target in all perturbed trials with -3 cm (C) or 3 cm (F) cursor jumps, which correspond to a small CW (C) or CCW (F) cursor jumps. The solid green line represents the predictions of model simulations. The light blue square, circle and diamond correspond to the targets presented in panel A. Statistical values are shown to the right of all graphs.

Handedness has also been shown to influence bimanual coordination. Control of the dominant arm, relative to the non-dominant arm, has been associated with a smaller variability (Kalisch et al., 2006), and thus better motor control, for which variability and effort are determinant factors (Todorov and Jordan, 2002). In a task similar to the one presented here, Salimpour and Shadmehr (2014) reported a smaller variability in force production for the dominant arm, which led to a greater contribution of this arm during bimanual task performance. White and Diedrichsen (2010) reported that the left hand of right-handed participants corrected more following unexpected visuomotor rotations, but also adapted more in the next trial, suggesting that the CNS may assign error-coping to the non-dominant (and less skilled) arm. Altogether, these findings indicate that cerebral lateralization impacts control across a wide range of contexts.

Surprisingly, our experimental observations from right-handed and left-handed participants in Experiment 1 were identical in terms of overall contribution and preferential direction of force production. These results are in line with those presented by Johansson et al. (2006), where it was suggested that the choice of the prime actor between the two arms during a bimanual task was driven by spatial relationships between hand action and goal motions. Furthermore, in Experiment 2, we found no effect of handedness on the corrective responses for any of the participants precluding our planned analysis of how lateralization of control interacts with optimization related to limb biomechanics. Given that two prior studies that employed the same paradigm found influences of handedness on the inter-arm distribution of force (Salimpour and Shadmehr, 2014; Salimpour et al., 2015), the circumstances under which handedness may influence bimanual control should be examined. Regarding the question of why we did not find an influence of handedness, it is possible that our explicit instruction to use both arms influenced the way the task was performed. Alternatively, constraining the arms' position may have prevented an influence of handedness. If so, these factors may be hierarchically considered during bimanual manipulations. Indeed, it is conceivable that, if the physics of the task is not experimentally imposed (by constraining the configuration), then participants may adopt a configuration in which the mechanical anisotropies play a secondary role and exploit hand dominance to a greater extent.

Importantly, we found that rapid adjustments following cursor jumps, which alter target-bound forces, were also influenced by the optimal weighting of each limb as predicted by the model (Fig. 4.7). That is, the perturbation-compelled force adjustments were generated in a way that integrated optimal limb use. The presently observed motor response to reaching the end-point was delayed by ~ 160ms for the right arm and ~ 220ms for the left arm, which, in light of previous work, seems fairly long. Electromyographic responses to cursor jumps have been detected with delays of 100 ms (Dimitriou et al., 2013; Cluff et al., 2015) and around 120–150ms after reaching the movement end-

point in unimanual reaching tasks (Saunders and Knill, 2003, 2004; Franklin and Wolpert, 2008; Dimitriou et al., 2013) . However, our observation of similar response latencies in a unimanual mode of the task suggests that the mapping of force production to cursor motion in this paradigm may require more internal processing than standard reaching tasks. Functional similarity between motor planning and feedback control appears to be a hallmark of sensorimotor coordination (see Crevecoeur and Scott (2014); Scott et al. (2015) for review) in the sense that corrective responses exhibit flexibility similar to that of unperturbed movements. Our data suggest that neural resources that optimize control distribution across limbs may be shared between movement planning and movement execution during bimanual tasks.

Handedness did play a role in the corrective response of each arm, as we observed differences in corrective latency between the dominant and non-dominant arm of ~ 60ms. The lag from the non-dominant arm likely arises from differences in the uncertainty of the internal model associated with each arm. Indeed, as suggested in Chapter 3, differences in the internal model of the two arms likely lead to the use of distinct control strategies during unimanual movement, and this difference might impact the time required by the nervous system to determine the optimal correction to be performed by each arm. Moreover, the delay between the corrective responses of the two arms supports the idea of Mutha et al. (2013), which suggests that the dominant hand is better at optimizing task dynamics whereas the non-dominant hand is better at stabilizing movement.

In our task, three biomechanical parameters influence the force distribution across arms, the relation between joint torques and end-point force ($J(\theta)$ in the model), the moment arm of each muscle group ($M(\theta)$) and the asymmetries in force between the flexor and extensors muscle groups. Previous studies have shown that biomechanical parameters such as the inertial resistance of the arm (Gordon et al., 1994) or the metabolic energy required for movement production (Shadmehr et al., 2016) define preferential direction of reaching movements. Factors such as the inertial resistance of the arm have no impact during isometric tasks as no movement is involved which suggests that some biomechanical factors underlying preferential directions of movement or force production are specific to the type of task being performed. However, despite different biomechanical factors influencing isometric and dynamical tasks, it has been shown that neurons in the primary motor cortex fire preferentially for elbow flexion combined with shoulder extension or elbow extension combined with shoulder flexion, arrangements that are optimized for limb biomechanics in both isometric and dynamical tasks (Scott et al., 2001; Lillicrap and Scott, 2013; Heming et al., 2016). Intuitively, the preferential directions that we observed in configurations 1 and 3 correspond with this behavior. Indeed, for each configuration, the directions of largest force production of each arm in our simulations corresponded to these combined flexor-extensor arrangements

(data not shown). Hence, the distribution of preferential firing directions of motor cortex neurons, shaped by limb physics, may be an easy and effective way to optimize control solutions during both isometric and dynamical tasks. An interesting challenge for future work will be to investigate the neural basis of optimal sharing of effort across limbs.

In conclusion, we demonstrated a consistent influence of limb physics on the planning and control of bimanual tasks by imposing the direction of force targets. Given the influence of expected motor costs on decisions about how to move (Cisek, 2012; Wolpert and Landy, 2012) (Cisek 2012; Wolpert and Landy 2012), or which target to acquire, our results may also explain possible planning biases during bimanual control. Insofar as a representation of mechanical effort is available during motor planning, we would expect it to impact solution selection. Indeed, for bimanual motor behaviors, our brain may choose a favorable joint configuration as well as a movement plan that is favorable to our limb physics. If so, movement control in general, from planning through execution, may factor in both movement value and biomechanical costs. We expect that prospective studies investigate these question in detail.

Addendum

It would be interesting to use the two distinct control strategies presented in Chapter 3 to explore the differences in behavior across limbs in the task observed here. Indeed, as suggested above, the difference in the delay of the corrective response of the two arms could arise from differences in the uncertainty associated with the internal model of each two arms. More precisely, the delayed corrective response of the non-dominant arm is likely due to greater uncertainty of the internal model associated with this arm, which could lead to increased computation time, or to the decision by the nervous system to delay the correction of the non-dominant arm in favor of the corrective response of the opposite arm. However, the robust control strategy presented in Chapter 2 and used in Chapter 3 cannot be applied to the model used in this chapter easily, as it does not allow to handle constraints on the input of the system directly. Adapting the robust control strategy to the model used in Chapter 4 is not straightforward, and future studies should explore control strategies that allow the use of a robust control strategy and to account for constraints applied on the input of the system.

CHAPTER 5

Conclusion and open questions

5.1 Main Contributions

This thesis inserts itself in the general topic of handedness and bimanual coordination. Our work was driven by fundamental questions about the control strategies underlying asymmetries in motor behavior that can be observed across arms during the performance of a motor task.

Here we present a new hypothesis about the inter-limb differences in performance across arms. We suggest that inter-limb differences in performance arise from the use of distinct control strategies rather than an increased stiffness of the non-dominant arm. More precisely, we propose the idea that the non-dominant arm uses a control strategy that is more robust but less flexible, while the dominant arm dis-plays higher sensitivity to model error but is more adaptive. We further suggest that such control strategies are directly linked to the level of uncertainty of internal models associated with each arm. We show that this hypothesis captures distinct sensitivities to model errors upon the introduction of a force field without assuming differences in body size or mechanical impedance, and suggest a meaningful link between control and learning as a trade-off between efficiency and robustness that is rooted in neural representation of movement dynamics.

Here we also provide physiological evidence showing that better performance

at initial exposure to a force field is not related to increased co-contraction, hence further indicating that differences in performance are due to the use of different control strategies. Indeed, currently, the main hypothesis concerning the asymmetries in performance across arms is that differences in the use of predictive and impedance control mechanisms drive motor output asymmetries (Yadav and Sainburg, 2014a,b), with the non-dominant arm relying more on impedance control mechanisms, and the dominant arm relying more on predictive mechanisms to perform movements. This hypothesis implies that participants can modulate the joint mechanical impedance of their limb to modify the behavior, presumably through the combined activation of agonist-antagonist pairs of muscles acting on each joint (Hogan, 1985; Burdet et al., 2001). Hence the evidence we provide suggests that the better performance of the non-dominant arm when initially confronted to the force field are not related to a greater use of impedance control.

By testing participants in different experimental setups (end-point and exoskeleton), we showed that inter-limb asymmetries in performance are context-dependent, with inter-limb differences observed in the end-point setup but not in the exoskeleton setup. While surprising, this result reinforces the hypothesis that differences in performance across arms are not due to intrinsic differences in limb impedance, but rather to the use distinct control strategies. We suggest that the complexity of the task will affect the control strategy used by the two arms, with a more complex task, i.e. greater number of DOF to control and handling of a robotic arm, favoring the use of more "robust" control strategies.

Finally, by analyzing how both arms coordinate their effort in order to achieve success during a bimanual force task, we showed that the biomechanical configuration of the limbs determined a preferential direction of force production for each limb, the preferential direction of each arm determined the distribution of forces across arms, with the arm having its preferential direction best aligned with the tar-get generally producing more force. Moreover, we reported that handedness has little effect on the force distribution across arms during an isometric bimanual force production task, which was somewhat surprising as an impact of handedness had been observed previously in a similar paradigm (Salimpour and Shadmehr, 2014). Our results are in line with the results of Johansson et al. (2006), who reported, through the analysis of the timing of movement, that one hand is assigned the role of prime executor and that the choice is made dependent on the spatial relationship between effort and target, and show that biomechanics play a fundamental role in the relationship between effort and target.

5.2 Limitations of optimal and robust control

Optimal control is a framework that has been regularly used to study human motor control as it does not enforce particular trajectories or behavior but uses feedback in an intelligent way in order to correct only for deviations that interfere with task goals (Todorov and Jordan, 2002). From this framework task-constrained variability, goal-directed corrections, motor synergies, controlled parameters, simplifying rules and discrete coordination modes emerge naturally. Robust control presents similar advantages to optimal control but has only recently been introduced in the neuroscience domain (Ueyama, 2014). While these frameworks provide very insightful information about human motor control systems they also suffer from several limitations.

Firstly, LQ controllers as well as the minimax controllers presented in Chapter 2 are designed to control systems with linear dynamics. In the context of motor control, the assumption that system dynamics are linear is not conceivable if one considers realistic models for the dynamics of muscular contraction and the geometry of the musculo-skeletal system. Ways of working around this limitation have been presented in the literature for LQ optimal controllers (Li and Todorov, 2007). However, these workarounds differ from optimal feedback control in several ways: The solution is based on a feed-forward solution of the deterministic case, i.e. without noise. Indeed the state feedback control policy is computed by linearizing the system around this optimal, unperturbed path, and this control strategy assumes that state feedback is able to correct for deviations from this optimal trajectory. Therefore, the benefits of optimal feedback control are really present when it is applied to linear systems. Similar concerns can be raised about the robust controller presented in this work. Adaptations to non-linear systems exist in control theory for min-max controllers, but they have yet to be adapted to deal with the particularities of human motor control systems.

Another important aspect of human sensorimotor control is the integration of feedback information in the control of movement. Significant transmission delays exist in the human nervous systems, with information about events occurring on the periphery only reaching the central nervous system with a delay of ~ 30ms, with similar delays existing for the transmission of motor commands (Scott, 2016). Moreover, this sensorimotor delays differ depending on the sensory modality. Most models used to explain motor behavior ignore this sensory and motor delays, even though such delays are devastating in the control of fast movements or corrective responses (Crevecoeur and Scott, 2014). The controllers presented in this work are not able to deal with sensory feedback delays or motor delays in their current form. A method to introduce such delays in linear models such as those used in this work was introduced by Crevecoeur et al. (2011). This method is interesting and offers a wide array of possibilities to explore the effect of delays in the feedback loop. However, it is also rigid in

the sense that feedback delays are fixed and are assumed to be known by the system. In real biological systems it is likely that such delays are unknown or uncertain.

5.3 Open questions

5.3.1 Context-dependent asymmetries in performance across arms

In Chapter 3 we used a single experimental paradigm in two different experimental setups (end-point and exoskeleton Kinarm) and observed very different results in these two setups. In the end-point setup we observed differences in performance across arms at the introduction of the force field, whereas in the exoskeleton setup we did not observe any difference in performance across arms, hence suggesting that asymmetries in performance across arms are context-dependent. We suggest that it is conceivable that manipulating the handle of a robotic arm and having to control a greater number of degrees of freedom requires better internal models, or greater compensation for potential model errors, which likely favors the expression of a robust control strategy. While previous studies have observed that parameters such as target size impact the size of asymmetries in behavior across arms (Elliott et al., 1995; Carson et al., 1996), the influence of the point of application of the perturbation or of the number of DOF to control on inter-limb differences has remained largely unexplored. Performing experiments with control of these parameters should allow identifying the impact of such parameters on the control strategy used by the two arms, which would be interesting as it would bring greater understanding to the flexibility of human motor control strategies.

Another possible way to tackle this problem would be to develop more complex upper-limb models able to account for the different number of degrees of freedom to be controlled during the task. It is likely that such models would introduce non-linearities and would require the adaptation of the two control frameworks used in Chapter 3. However, using adapted versions of the two controllers presented in this work on such models would give us theoretical predictions of the effect of task complexity on these two control strategies, and hence would allow us verifying whether the results observed in Chapter 3 can be theoretically predicted.

In this thesis we tested differences in performance across arms using different groups of participants. In a recent study Cluff et al. (2015) showed that differences in learning existed across participants, which could be also related to a tradeoff between robustness and adaptiveness of movement. Hence analyzing

the performance of the two arms of a single participant will limit limit the influence of inter-participant variability. To do so, the task should be designed as to limit transfer of learning from one arm to the other, with the use of washout trials. Analyzing the results of this task would allow clarifying the differences in control and performance across the two arms ans should be performed in the future.

5.3.2 Learning asymmetries

The results presented in Chapter 3 showed that participants that were highly sensitive to the introduction of the force field rapidly adapted their behavior across trials, whereas participants who were less sensitive also showed less adaptation. Consistent with these observations, Albert and Shadmehr (2016) showed that smaller error experienced during initial trials leads to a smaller improvement in the following trials, without explaining the source of the initial error. Moreover, asymmetries in learning rate between the two arms in track-tracing tasks have been reported in the literature (McGrath and Kantak, 2016). We suggest that these differences in learning rate arise from the existence of a tradeoff between sensitivity to model error and the ability to learn, with robustness being an advantage when the force field is first introduced but also reflecting reduced learning abilities.

We believe that the theoretical framework of robust and optimal control as presented in this work can be an interesting tool to reconcile motor control theory with motor learning theory, where two different learning mechanisms have been regularly highlighted: error-based learning, which allows rapid improvement during the first trials of a motor task, and model-free learning, which allows retention of the motor skill (Huang et al., 2011; Orban de Xivry and Lefèvre, 2015). Parameters such as perturbation schedule (introducing the perturbation gradually or abruptly) have been shown to impact the learning rate as well as the retention of motor skill (Orban de Xivry et al., 2011). Given the above-described considerations, it is likely that error-based learning is impacted by the robustness of the control strategy that is used. Hence studying the effect of perturbation schedule using the two controllers used in Chapter 3 and comparing its predictions to behavioral data could provide interesting insight into learning mechanisms.

The difference in adaptiveness of control strategies might also impact the transfer of learned motor skills from one arm to the other, with the arm more able to adapt its model during learning possibly being more able to transfer motor skill to the other arm. Contrasting results have been reported concerning transfer of motor skill across arms. Certain studies have reported asymmetrical transfer of motor skill across arms (Wang and Sainburg, 2003, 2006), while others have observed no differences in the transfer of motor skill (Stockinger

et al., 2015). Interestingly, it has been reported that the higher the lateralization of arm movement, i.e. the bigger the asymmetries in the use of the two arms, the greater the transfer of motor skill from the dominant to the non-dominant arm (Lefumat et al., 2015). Studying the transfer of motor skills across arms using the theoretical framework presented in Chapter 3 could provide interesting insight on the computational mechanisms underlying transfer of motor skill. To this end we acquired data from participants performing the task with one arm and then with the other but this dataset has yet to be analyzed.

5.3.3 Bimanual coordination

Contrasting results have arisen concerning how efforts are distributed across arms during a bimanual task. Indeed, some studies have suggested that handedness plays a significant role in the assignment of control between the two arms (Salimpour and Shadmehr, 2014; Salimpour et al., 2015) while others have suggested that the prime role is given to the arm with the best spatial relationship between effort and target (Johansson et al., 2006). The results presented in Chapter 4 are in line with results from Johansson and colleagues, and suggest that biomechanical factors play a significant role on the distribution of control across arms. Given the influence of expected motor costs on decisions about how to move (Cisek, 2012; Wolpert and Landy, 2012), or which target to acquire, our results may also explain possible planning biases during bimanual control. If a representation of mechanical effort is available during motor planning, we would expect it to impact solution selection. Indeed, for bimanual motor behaviors, our brain may choose a favorable joint configuration as well as a movement plan that is favorable to our limb physics. If so, movement control in general, from planning through execution, may factor in both movement value and biomechanical costs. We expect that prospective studies investigate this question in detail.

In Chapter 4 we observed a difference in the delay of corrective responses of the dominant arm and the non-dominant arm, with the dominant arm starting to correct for a cursor jump ~ 60ms earlier than the non-dominant arm. This delay is in line with the hypothesis that each arm has a specialized behavior (Mutha et al., 2013), which suggests that the non-dominant arm is better at task stabilization and the dominant arm is better at trajectory control. The difference in timing of corrective responses across arms could arise from differences in uncertainty of internal models associated with the dominant and non-dominant arm. Indeed, as we suggested in Chapter 3, the internal model of the non-dominant arm is likely related to greater uncertainty than the internal model of the dominant arm. A more uncertain internal model likely leads to increased computation time of motor commands, leading to a delayed motor response. Using the robust and optimal controllers presented in Chapter 2 provide an

interesting theoretical framework to explore the difference in corrective response time of each arm during bimanual tasks. This should be explored in great depth in future studies as it could provide great insight into the differences in control of the two arms.

Another interesting challenge for future work will be to investigate the neural basis of optimal sharing of effort across limbs. Indeed, it has been shown that neurons in the primary motor cortex fire preferentially for elbow flexion combined with shoulder extension or elbow extension combined with shoulder flexion, arrangements that are optimized for limb biomechanics in both isometric and dynamical tasks (Scott et al., 2001; Lillicrap and Scott, 2013; Heming et al., 2016). Intuitively, the preferential directions that we observed in configurations 1 and 3 of Chapter 4 correspond with this behavior. Hence, the distribution of preferential firing directions of motor cortex neurons, shaped by limb physics, may be an easy and effective way to optimize control solutions during both isometric and dynamical tasks, and deserves to be explored in future studies.

5.3.4 Dexterous manipulation

Humans have the remarkable capacity to manipulate small objects with great dexterity. Dexterous manipulation has been largely studied using precision grip (i.e., when holding an object between the thumb and index finger). In this context, contact forces at the fingertip-object interface are typically decomposed into two components: the force normal to the object's surface and directly controlled by the subject (normal force, NF), and the force tangential to the object's surface and resulting from the object's weight and inertial forces (tangential force, TF) (Johansson and Westling, 1984). To ensure a stable grasp of the object under predictable conditions, the central nervous system continuously scales and synchronizes NF to the varying TF (Flanagan and Wing, 1993, 1995). In order to achieve such a synchronicity between NF and TF the nervous system must be able to predict changes in TF, and likely does so using internal models of the arm and the object. Hence, if differences in the uncertainty associated with the internal model of the two arms exist, it is conceivable that differences in grip force adjustments could be observed across arms and deserves to be explored in future studies.

5.4 Potential application for upper-limb prostheses

The specialized behavior of the two arms due to the use of distinct control strategies could impact the development of prosthetic arms. Given that each

arm has a specialized behavior, it could be interesting for arm prostheses to have different design depending on whether they are to be used with the dominant or the non-dominant arm. For instance, given that the non-dominant arm is better at stabilizing when confronted to perturbations, one could imagine a prosthesis that does not aim at reproducing the complexity of the human upper-limb but is specially designed for movement stabilization. Indeed, this idea would lead to simpler, and hence less expensive, devices which would provide the main functionality expected from the limb they aim to replace.

5.5 Concluding words

In this work we provided new insight on the control strategies underlying the specialized behavior of the two arms. The fact that one arm uses a control strategy that is more robust but less efficient than the other could appear surprising at first. Indeed, what would be the disadvantage of having two efficiently controlled arms? Analyzing the way humans interact with their environment allows answering this question. Indeed, the specialized behavior of the two arms is perfectly adapted to the manipulation of objects in our environments, with simple tasks such as opening a bottle benefiting from having one arm that is more robustly controlled, and stabilizes the bottle, while the other arm turns the lid of the bottle. Even more fascinating is the ability of human's nervous system to adapt the control strategy that is used dependent on the requirements of the task being performed. These considerations show to which extent human control strategies are perfectly adapted to our environment and are unbeatable, and hence should continue to be thoroughly studied.

Bibliography

Nicolas Schweighofer, Yupeng Xiao, Sujin Kim, Toshinori Yoshioka, James Gordon, and Rieko Osu. Effort, success, and nonuse determine arm choice. *Journal of Neurophysiology*, 114(1):551–559, jul 2015. ISSN 0022-3077. doi: 10.1152/jn.00593.2014. URL http://www.ncbi.nlm.nih.gov/pubmed/25948869http://jn.physiology.org/lookup/doi/10.1152/jn.00593.2014.

Ignasi Cos, N. Belanger, and Paul Cisek. The influence of predicted arm biomechanics on decision making. *Journal of Neurophysiology*, 105(6):3022–3033, jun 2011. ISSN 0022-3077. doi: 10.1152/jn.00975.2010. URL http://jn.physiology.org/cgi/doi/10.1152/jn.00975.2010.

Robert L Sainburg. Evidence for a dynamic-dominance hypothesis of handedness. *Experimental brain research*, 142(2):241–58, jan 2002. ISSN 0014-4819. doi: 10.1007/s00221-001-0913-8. URL http://www.ncbi.nlm.nih.gov/pubmed/11807578.

Giorgio Vallortigara and Lesley J Rogers. Survival with an asymmetrical brain: advantages and disadvantages of cerebral lateralization. *The Behavioral and brain sciences*, 28(4):575–89; discussion 589–633, 2005. ISSN 0140-525X. doi: 10.1017/S0140525X05000105. URL http://www.ncbi.nlm.nih.gov/pubmed/16209828.

RC Oldfield. The assessment and analysis of handedness: The Edinburgh inventory. *Neuropsychologia*, 9(1):97–113, mar 1971. ISSN 00283932. doi: 10.1016/0028-3932(71)90067-4. URL http://www.sciencedirect.com/science/article/pii/0028393271900674http://linkinghub.elsevier.com/retrieve/pii/0028393271900674.

a. N. Gilbert and C. J. Wysocki. Hand preference and age in the United States. *Neuropsychologia*, 30(7):601–608, 1992. ISSN 00283932. doi: 10.1016/0028-3932(92)90065-T.

Marian Annett. Genetic and nongenetic influences on handedness. *Behavior Genetics*, 8(3):227–249, may 1978. ISSN 0001-8244. doi: 10.1007/BF01072826. URL http://link.springer.com/10.1007/BF01072826.

Marian Annett. The genetics of handedness. *Trends in Neurosciences*, 4(C): 256–258, 1981. ISSN 01662236. doi: 10.1016/0166-2236(81)90080-1.

Marian Annett. Handedness and Cerebral Dominance: The Right Shift. *Journal of Neuropsychiatry: Neuropsychiatric Practice and Opinion*, 10(4):459–469, 1998. ISSN 0895-0172 (Print). doi: 10.1176/jnp.10.4.459.

I. C. McManus. Handedness, language dominance and aphasia: a genetic model. *Psychological Medicine. Monograph Supplement*, 8(February 2002):3, jan 1985. ISSN 0264-1801. doi: 10.1017/S0264180100001879. URL http://www.journals.cambridge.org/abstract{_}S0264180100001879.

Leen J. Beukelaar and Pieter M. Kroonenberg. Changes over time in the relationship between hand preference and writing hand among left-handers. *Neuropsychologia*, 24(2):301–303, 1986. ISSN 00283932. doi: 10.1016/0028-3932(86)90066-7.

Clare Porac, Stanley Coren, and Alan Searleman. Environmental factors in hand preference formation: Evidence from attempts to switch the preferred hand. *Behavior Genetics*, 16(2):251–261, mar 1986. ISSN 0001-8244. doi: 10.1007/BF01070800. URL http://www.ncbi.nlm.nih.gov/pubmed/3718414http://link.springer.com/10.1007/BF01070800.

Clare Porac, Laura Rees, and Terri Buller. Switching Hands: A Place for Left Hand Use in a Right Hand World. *Advances in Psychology*, 67(C):259–290, 1990. ISSN 01664115. doi: 10.1016/S0166-4115(08)61250-9.

J. Annett, Marian Annett, P. T. W. Hudson, and Ann Turner. The control of movement in the preferred and non-preferred hands. *Quarterly Journal of Experimental Psychology*, 31(4):641–652, 1979. ISSN 0033-555X. doi: 10.1080/14640747908400755. URL http://www.tandfonline.com/doi/abs/10.1080/14640747908400755.

Tobias Kalisch, Claudia Wilimzig, Nadine Kleibel, Martin Tegenthoff, and Hubert R Dinse. Age-related attenuation of dominant hand superiority. *PloS one*, 1(1):e90, dec 2006. ISSN 1932-6203. doi: 10.1371/journal.pone.0000090. URL http://www.pubmedcentral.nih.gov/articlerender.fcgi?artid=1762407{&}tool=pmcentrez{&}rendertype=abstracthttp://dx.plos.org/10.1371/journal.pone.0000090http://www.ncbi.nlm.nih.gov/pubmed/17183722http://www.pubmedcentral.nih.gov/articlerender.fcgi?artid=PMC1.

Yousef Salimpour and Reza Shadmehr. Motor costs and the coordination of the two arms. *The Journal of neuroscience : the*

official journal of the Society for Neuroscience, 34(5):1806–18, jan 2014. ISSN 1529-2401. doi: 10.1523/JNEUROSCI.3095-13.2014. URL http://www.pubmedcentral.nih.gov/articlerender.fcgi?artid=3905146{&}tool=pmcentrez{&}rendertype=abstract.

Yousef Salimpour, Zoltan K Mari, and Reza Shadmehr. Altering Effort Costs in Parkinson's Disease with Noninvasive Cortical Stimulation. *The Journal of neuroscience : the official journal of the Society for Neuroscience*, 35(35): 12287–302, 2015. ISSN 1529-2401. doi: 10.1523/JNEUROSCI.1827-15.2015. URL http://www.ncbi.nlm.nih.gov/pubmed/26338339.

R L Sainburg and D Kalakanis. Differences in control of limb dynamics during dominant and nondominant arm reaching. *Journal of neurophysiology*, 83 (5):2661–2675, 2000. ISSN 0022-3077.

Leia B Bagesteiro and Robert L Sainburg. Handedness: dominant arm advantages in control of limb dynamics. *Journal of neurophysiology*, 88(5): 2408–2421, 2002. ISSN 0022-3077. doi: 10.1152/jn.00901.2001.

Jinsung Wang and Robert L. Sainburg. Mechanisms underlying interlimb transfer of visuomotor rotations. *Experimental brain research*, 149(4):520–6, apr 2003. ISSN 0014-4819. doi: 10.1007/s00221-003-1392-x. URL http://link.springer.com/10.1007/s00221-006-0543-2http://www.ncbi.nlm.nih.gov/pubmed/12677333http://www.pubmedcentral.nih.gov/articlerender.fcgi?artid=PMC3697093.

Leia B Bagesteiro and Robert L Sainburg. Nondominant arm advantages in load compensation during rapid elbow joint movements. *Journal of neurophysiology*, 90(3):1503–13, sep 2003. ISSN 0022-3077. doi: 10.1152/jn.00189.2003. URL http://jn.physiology.org/cgi/doi/10.1152/jn.00189.2003http://www.ncbi.nlm.nih.gov/pubmed/12736237.

Leia B. Bagesteiro and Robert L. Sainburg. Interlimb transfer of load compensation during rapid elbow joint movements. *Experimental Brain Research*, 161 (2):155–165, feb 2005. ISSN 0014-4819. doi: 10.1007/s00221-004-2055-2. URL http://www.ncbi.nlm.nih.gov/pubmed/12736237http://jn.physiology.org/cgi/doi/10.1152/jn.00189.2003http://link.springer.com/10.1007/s00221-004-2055-2.

V Yadav and R L Sainburg. Handedness can be explained by a serial hybrid control scheme. *Neuroscience*, 278:385–96, oct 2014a. ISSN 1873-7544. doi: 10.1016/j.neuroscience.2014.08.026. URL http://dx.doi.org/10.1016/j.neuroscience.2014.08.026.

Tomoko Aoki, Gil Rivlis, and Marc H. Schieber. Handedness and index finger movements performed on a small touchscreen. *Journal of Neurophysiology*, 115(2):858–867, 2016. ISSN 0022-3077. doi: 10.1152/jn.00256.2015. URL http://jn.physiology.org/lookup/doi/10.1152/jn.00256.2015.

Vivek Yadav and Robert L Sainburg. Limb dominance results from asymmetries in predictive and impedance control mechanisms. *PloS one*, 9 (4):e93892, jan 2014b. ISSN 1932-6203. doi: 10.1371/journal.pone.0093892. URL http://www.pubmedcentral.nih.gov/articlerender.fcgi?artid=3973649{&}tool=pmcentrez{&}rendertype=abstract.

Kathleen York Haaland and Deborah L. Harrington. Hemispheric control of the initial and corrective components of aiming movements. *Neuropsychologia*, 27(7):961–969, 1989a. ISSN 00283932. doi: 10.1016/0028-3932(89)90071-7.

Kathleen York Haaland and Deborah Harrington. The role of the hemispheres in closed loop movements. *Brain and Cognition*, 9(2):158–180, 1989b. ISSN 10902147. doi: 10.1016/0278-2626(89)90027-4.

K.Y. Haaland and D.L. Harrington. Limb-Sequencing Deficits After Left but not Right Hemisphere Damage. *Brain and Cognition*, 24(1):104–122, jan 1994. ISSN 02782626. doi: 10.1006/brcg.1994.1006. URL http://linkinghub.elsevier.com/retrieve/pii/S0278262684710062.

J. D. Fisk and M. A. Goodale. The effects of unilateral brain damage on visually guided reaching: hemispheric differences in the nature of the deficit. *Experimental Brain Research*, 72(2):425–435, 1988. ISSN 00144819. doi: 10.1007/BF00250264.

Kathleen Y. Haaland and Deborah L. Harrington. Hemispheric asymmetry of movement. *Current Opinion in Neurobiology*, 6(6):796–800, 1996. ISSN 09594388. doi: 10.1016/S0959-4388(96)80030-4.

S. Y. Schaefer, P. K. Mutha, K. Y. Haaland, and R. L. Sainburg. Hemispheric Specialization for Movement Control Produces Dissociable Differences in Online Corrections after Stroke. *Cerebral Cortex*, 22(6):1407–1419, jun 2012. ISSN 1047-3211. doi: 10.1093/cercor/bhr237. URL http://www.cercor.oxfordjournals.org/cgi/doi/10.1093/cercor/bhr237https://academic.oup.com/cercor/article-lookup/doi/10.1093/cercor/bhr237.

Saandeep Mani, Pratik K. Mutha, Andrzej Przybyla, Kathleen Y. Haaland, David C. Good, and Robert L. Sainburg. Contralesional motor deficits after unilateral stroke reflect hemisphere-specific control mechanisms. *Brain*, 136(4):1288–1303, apr 2013. ISSN 1460-2156. doi: 10.1093/brain/aws283. URL https://academic.oup.com/brain/article-lookup/doi/10.1093/brain/aws283.

Pratik K Mutha, Kathleen Y Haaland, and Robert L Sainburg. The effects of brain lateralization on motor control and adaptation. *Journal of motor behavior*, 44(6):455–69, jan 2012. ISSN 1940-1027. doi: 10.1080/00222895.2012.

747482. URL http://www.pubmedcentral.nih.gov/articlerender.fcgi?artid=3549328{&}tool=pmcentrez{&}rendertype=abstract.

Pratik K Mutha, Kathleen Y Haaland, and Robert L Sainburg. Rethinking motor lateralization: specialized but complementary mechanisms for motor control of each arm. *PloS one*, 8(3):e58582, jan 2013. ISSN 1932-6203. doi: 10.1371/journal.pone.0058582. URL http://www.pubmedcentral.nih.gov/articlerender.fcgi?artid=3589347{&}tool=pmcentrez{&}rendertype=abstract.

Hitoshi Honda. Rightward superiority of eye movements in a bimanual aiming task. *The Quarterly Journal of Experimental Psychology*, 34(4):499–513, 1982. ISSN 0272-4987. doi: 10.1080/14640748208400833. URL http://www.tandfonline.com/doi/abs/10.1080/14640748208400833.

Digby Elliott, James Lyons, Romeo Chua, David Goodman, and Richard G. Carson. The Influence of Target Perturbation on Manual Aiming Asymmetries in Right-Handers. *Cortex*, 31(4):685–697, 1995. ISSN 00109452. doi: 10.1016/S0010-9452(13)80020-2. URL http://www.sciencedirect.com/science/article/pii/S0010945213800202.

Richard G. Carson, Winston D. Byblow, Bruce Abernethy, and Jeffery J. Summers. The contribution of inherent and incidental constraints to intentional switching between patterns of bimanual coordination. *Human Movement Science*, 15(4):565–589, aug 1996. ISSN 01679457. doi: 10.1016/0167-9457(96)00028-0. URL http://linkinghub.elsevier.com/retrieve/pii/0167945796000280.

P E Mieschke, D Elliott, W F Helsen, R G Carson, and J a Coull. Manual asymmetries in the preparation and control of goal-directed movements. *Brain and cognition*, 45(1):129–140, 2001. ISSN 02782626. doi: 10.1006/brcg.2000.1262.

E A Roy, L Kalbfleisch, and D Elliott. Kinematic analyses of manual asymmetries in visual aiming movements., 1994. ISSN 0278-2626. URL http://www.sciencedirect.com/science/article/pii/S0278262684710177.

A. Przybyla, C. J. Coelho, S. Akpinar, S. Kirazci, and R. L. Sainburg. Sensorimotor performance asymmetries predict hand selection. *Neuroscience*, 228:349–360, 2013. ISSN 03064522. doi: 10.1016/j.neuroscience.2012.10.046. URL http://dx.doi.org/10.1016/j.neuroscience.2012.10.046.

Daniel J Goble, Colleen a Lewis, and Susan H Brown. Upper limb asymmetries in the utilization of proprioceptive feedback. *Experimental brain research*, 168(1-2):307–11, jan 2006. ISSN 0014-4819. doi: 10.1007/s00221-005-0280-y. URL http://www.ncbi.nlm.nih.gov/pubmed/16311728.

Jacqlyn King, Elizabeth Harding, and Andrew Karduna. The shoulder and elbow joints and right and left sides demonstrate similar joint position sense. *Journal of motor behavior*, 45(6):479–86, 2013. ISSN 1940-1027. doi: 10.1080/00222895.2013.832136. URL http://www.ncbi.nlm.nih.gov/pubmed/24079516.

Daniel J. Goble and Susan H. Brown. Task-dependent asymmetries in the utilization of proprioceptive feedback for goal-directed movement. *Experimental Brain Research*, 180:693–704, 2007. ISSN 00144819. doi: 10.1007/s00221-007-0890-7.

Daniel J. Goble and Susan H. Brown. Dynamic proprioceptive target matching behavior in the upper limb: Effects of speed, task difficulty and arm/hemisphere asymmetries. *Behavioural Brain Research*, 200(1):7–14, 2009. ISSN 01664328. doi: 10.1016/j.bbr.2008.11.034.

Robert L. McGrath and Shailesh S. Kantak. Reduced asymmetry in motor skill learning in left-handed compared to right-handed individuals. *Human Movement Science*, 45:130–141, 2016. ISSN 18727646. doi: 10.1016/j.humov.2015.11.012. URL http://dx.doi.org/10.1016/j.humov.2015.11.012.

Maite Aznárez-Sanado, Maria A. Fernández-Seara, Francis R. Loayza, and Maria A. Pastor. Functional asymmetries in early learning during right, left, and bimanual performance in right-handed subjects. *Journal of Magnetic Resonance Imaging*, 37(3):619–631, 2013. ISSN 10531807. doi: 10.1002/jmri.23841.

Robert L. Sainburg and Jinsung Wang. Interlimb transfer of visuomotor rotations: Independence of direction and final position information. *Experimental Brain Research*, 145:437–447, 2002. ISSN 00144819. doi: 10.1007/s00221-002-1140-7.

Jinsung Wang and Robert L Sainburg. Interlimb transfer of novel inertial dynamics is asymmetrical. *Journal of neurophysiology*, 92(1):349–360, 2004. ISSN 0022-3077. doi: 10.1152/jn.00960.2003.

Timothy J Carroll, Eugene Poh, and Aymar de Rugy. New visuomotor maps are immediately available to the opposite limb. *Journal of neurophysiology*, 111(11):2232–43, 2014. ISSN 1522-1598. doi: 10.1152/jn.00042.2014. URL http://www.ncbi.nlm.nih.gov/pubmed/24598522.

T. J. Carroll, A. de Rugy, I. S. Howard, J. N. Ingram, and D. Wolpert. Enhanced cross-limb transfer of force field learning for dynamics that are identical in extrinsic and joint-based coordinates for both limbs. *Journal of Neurophysiology*, 115(1):445–456, 2016. ISSN 0022-3077. doi: 10.1152/jn.00485.2015. URL http://jn.physiology.org/cgi/doi/10.1152/jn.00485.2015.

Wilsaan M Joiner, Jordan B Brayanov, and Maurice A Smith. The training schedule affects the stability, not the magnitude, of the interlimb transfer of learned dynamics. *Journal of neurophysiology*, 110(4):984–98, aug 2013. ISSN 1522-1598. doi: 10.1152/jn.01072.2012. URL http://jn.physiology.org/content/110/4/984.longhttp://www.ncbi.nlm.nih.gov/pubmed/23719204http://www.pubmedcentral.nih.gov/articlerender.fcgi?artid=PMC4422351.

Hannah Zélia Lefumat, Jean-Louis Vercher, R Christopher Miall, Jonathan Cole, Frank Buloup, Lionel Bringoux, Christophe Bourdin, and Fabrice R Sarlegna. To transfer or not to transfer? Kinematics and laterality quotient predict interlimb transfer of motor learning. *Journal of neurophysiology*, 114(5): jn.00749.2015, 2015. ISSN 1522-1598. doi: 10.1152/jn.00749.2015. URL http://jn.physiology.org/content/114/5/2764.abstract.

Claudia L.R. Gonzalez, Jason W. Flindall, and Kayla D. Stone. Hand preference across the lifespan: Effects of end-goal, task nature, and object location. *Frontiers in Psychology*, 5(OCT):1–9, 2014. ISSN 16641078. doi: 10.3389/fpsyg.2014.01579.

Spencer E. Gooderham and Pamela J. Bryden. Does your dominant hand become less dominant with time? The effects of aging and task complexity on hand selection. *Developmental Psychobiology*, 56(3):537–546, 2014. ISSN 00121630. doi: 10.1002/dev.21123.

John Cirillo, Nigel C. Rogasch, and John G. Semmler. Hemispheric differences in use-dependent corticomotor plasticity in young and old adults. *Experimental Brain Research*, 205(1):57–68, 2010. ISSN 00144819. doi: 10.1007/s00221-010-2332-1.

J. A. Kelso. Phase transitions and critical behavior in human bimanual coordination. *The American journal of physiology*, 246(6 Pt 2):R1000–4, jun 1984. ISSN 0002-9513. URL http://ajpregu.physiology.org/content/246/6/R1000.short{%}5Cnhttp://www.ncbi.nlm.nih.gov/entrez/query.fcgi?cmd=Retrieve{&}db=PubMed{&}dopt=Citation{&}list{_}uids=6742155http://www.ncbi.nlm.nih.gov/pubmed/6742155.

Richard G. Carson. The dynamics of isometric bimanual coordination. *Experimental brain research*, 105(3):465–76, 1995. ISSN 0014-4819. doi: 10.1007/BF00233046. URL http://www.ncbi.nlm.nih.gov/pubmed/7498400.

V. K. Jirsa, A. Fuchs, and J. A. S. Kelso. Connecting Cortical and Behavioral Dynamics: Bimanual Coordination. *Neural Computation*, 10(8):2019–2045, nov 1998. ISSN 0899-7667. doi: 10.1162/089976698300016954. URL http://linkinghub.elsevier.com/retrieve/pii/S0925231200002216http://www.ncbi.nlm.nih.gov/pubmed/5571122http://www.mitpressjournals.org/doi/10.1162/089976698300016954.

Jean-Jacques Temprado, Pier-Giorgio Zanone, Audrey Monno, and Michel Laurent. Attentional load associated with performing and stabilizing preferred bimanual patterns. *Journal of Experimental Psychology: Human Perception and Performance*, 25(6):1579–1594, 1999. ISSN 0096-1523. doi: 10.1037/0096-1523.25.6.1579.

Diana Deutsch. The generation of two isochronous sequences in parallel. *Perception & psychophysics*, 34(4):331–337, 1983. ISSN 0031-5117. doi: 10.3758/BF03203045.

Paul J. Treffner and M. T. Turvey. Resonance constraints on rhythmic movement. *Journal of Experimental Psychology: Human Perception and Performance*, 19(6):1221–1237, 1993. ISSN 0096-1523. doi: 10.1037/0096-1523.19.6.1221.

C.E. Peper, Peter J Beek, and Piet C W van Wieringen. Multifrequency coordination in bimanual tapping: Asymmetrical coupling and signs of supercriticality., 1995a. ISSN 0096-1523. URL http://doi.apa.org/getdoi.cfm?doi=10.1037/0096-1523.21.5.1117.

C. E. Peper, Peter J. Beek, and Piet C W van Wieringen. Frequency-induced phase transitions in bimanual tapping. *Biological Cybernetics*, 73(4):301–309, sep 1995b. ISSN 0340-1200. doi: 10.1007/BF00199466. URL http://link.springer.com/10.1007/BF00199466.

J Diedrichsen, E Hazeltine, S Kennerley, and R B Ivry. Moving to directly cued locations abolishes spatial interference during bimanual actions. *Psychological Science*, 12(6):493–498, 2001. ISSN 0956-7976. doi: 10.1111/1467-9280.00391. URL http://www.ncbi.nlm.nih.gov/pubmed/11760137.

Stephan P. Swinnen. Intermanual Coordination: From Behavioural Principles To Neural-Network Interactions. *Nature Reviews Neuroscience*, 3(5):348–359, 2002. ISSN 1471-003X. doi: 10.1038/nrn807. URL http://www.nature.com/doifinder/10.1038/nrn807.

Stephan P. Swinnen, Kris Jardin, Ruud Meulenbroek, Natalia Dounskaia, and Myriam Hofkens-Van Den Brandt. Egocentric and Allocentric Constraints in the Expression of Patterns of Interlimb Coordination. *Journal of Cognitive Neuroscience*, 9:348–377, 1997. ISSN 0898-929X. doi: 10.1162/jocn.1997.9.3.348.

Stephan P. Swinnen, Kris Jardin, Sabine Verschueren, Ruud Meulenbroek, Liz Franz, N. Dounskaia, and C.B Walter. Exploring interlimb constraints during bimanual graphic performance: effects of muscle grouping and direction. *Behavioural Brain Research*, 90(1):79–87, jan 1998. ISSN 01664328. doi: 10.1016/S0166-4328(97)00083-1. URL http://linkinghub.elsevier.com/retrieve/pii/S0166432897000831.

Timothy D. Lee, Quincy J. Almeida, and Romeo Chua. Spatial constraints in bimanual coordination: Influences of effector orientation. *Experimental Brain Research*, 146(2):205–212, 2002. ISSN 00144819. doi: 10.1007/s00221-002-1179-5.

Fausto Baldissera, Paolo Cavallari, and Pietro Civaschi. Preferential coupling between voluntary movements of ipsilateral limbs. *Neuroscience Letters*, 34 (1):95–100, 1982. ISSN 03043940. doi: 10.1016/0304-3940(82)90098-2.

J A S Kelso and J J Jeka. Symmetry breaking dynamics of human multilimb coordination. *Journal of experimental psychology. Human perception and performance*, 18(3):645–68, 1992. ISSN 0096-1523. doi: 10.1037/0096-1523.18.3.645. URL `http://www.ncbi.nlm.nih.gov/pubmed/1500867`.

D J Serrien and S P Swinnen. Coordination constraints induced by effector combination under isofrequency and multifrequency conditions. *Journal of Experimental Psychology-Human Perception and Performance*, 23(5):1493–1510, 1997. ISSN 0096-1523. doi: http://dx.doi.org/10.1037/0096-1523.23.5.1493.

Roland S Johansson, Anna Theorin, Göran Westling, Mikael Andersson, Yukari Ohki, and Lars Nyberg. How a lateralized brain supports symmetrical bimanual tasks. *PLoS biology*, 4(6):e158, jun 2006. ISSN 1545-7885. doi: 10.1371/journal.pbio.0040158. URL `http://www.pubmedcentral.nih.gov/articlerender.fcgi?artid=1457013{&}tool=pmcentrez{&}rendertype=abstract`.

Anna Theorin and Roland S Johansson. Selection of prime actor in humans during bimanual object manipulation. *The Journal of neuroscience : the official journal of the Society for Neuroscience*, 30(31):10448–10459, 2010. ISSN 0270-6474. doi: 10.1523/JNEUROSCI.1624-10.2010.

Yves Guiard. Asymmetric division of labor in human skilled bimanual action: the kinematic chain as a model. *Journal of motor behavior*, 19(4):486–517, 1987. ISSN 0022-2895. doi: 10.1080/00222895.1987.10735426.

Kayla D. Stone, Devon C. Bryant, and Claudia L R Gonzalez. Hand use for grasping in a bimanual task: evidence for different roles? *Experimental brain research*, 224(3):455–67, feb 2013. ISSN 1432-1106. doi: 10.1007/s00221-012-3325-z. URL `http://www.ncbi.nlm.nih.gov/pubmed/23161156`.

G W Goerres, M Samuel, I H Jenkins, and D J Brooks. Cerebral control of unimanual and bimanual movements: an H215O PET study. *Neuroreport.*, 9(16):3631–3638, 1998. ISSN 0959-4965; 0959-4965. doi: Doi10.1097/00001756-199811160-00014. URL `http://www.ncbi.nlm.nih.gov/pubmed/9858371`.

L Jäncke, M. Peters, M. Himmelbach, T Nösselt, J. Shah, and H. Steinmetz. fMRI study of bimanual coordination. *Neuropsychologia*, 38(2):164–74, 2000. ISSN 0028-3932. doi: 10.1016/S0028-3932(99)00062-7. URL `http://www.ncbi.nlm.nih.gov/pubmed/10660227`.

I Immisch, D Waldvogel, P van Gelderen, and M Hallett. The role of the medial wall and its anatomical variations for bimanual antiphase and inphase movements. *Neuroimage*, 14(3):674–684, 2001. ISSN 1053-8119. doi: DOI10.1006/nimg.2001.0856.

Dinesh G. Nair, Kari L. Purcott, Armin Fuchs, Fred Steinberg, and J. A Scott Kelso. Cortical and cerebellar activity of the human brain during imagined and executed unimanual and bimanual action sequences: A functional MRI study. *Cognitive Brain Research*, 15(3):250–260, 2003. ISSN 09266410. doi: 10.1016/S0926-6410(02)00197-0.

M Toyokura, I Muro, T Komiya, and M Obara. Relation of bimanual coordination to activation in the sensorimotor cortex and supplementary motor area: Analysis using functional magnetic resonance imaging. *Brain Research Bulletin*, 48(2):211–217, 1999. ISSN 03619230. doi: Doi10.1016/S0361-9230(98)00165-8.

J I Tracy, S S Faro, F B Mohammed, A B Pinus, S M Madi, and J W Laskas. Cerebellar mediation of the complexity of bimanual compared to unimanual movements. *Neurology*, 57(10):1862–1869, 2001. ISSN 0028-3878. doi: âĂŃ10.âĂŃ1212/âĂŃWNL.âĂŃ57.âĂŃ10.âĂŃ1862.

Minoru Toyokura, Isao Muro, Taizo Komiya, and Makoto Obara. Activation of pre-supplementary motor area (SMA) and SMA proper during unimanual and bimanual complex sequences: an analysis using functional magnetic resonance imaging. *Journal of Neuroimaging.*, 12(2):172–178, 2002. ISSN 1051-2284. doi: 10.1111/j.1552-6569.2002.tb00116.x.

GORDON HOLMES. THE SYMPTOMS OF ACUTE CEREBELLAR INJURIES DUE TO GUNSHOT INJURIES. *Brain*, 40(4):461–535, 1917. ISSN 0006-8950. doi: 10.1093/brain/40.4.461. URL `https://academic.oup.com/brain/article-lookup/doi/10.1093/brain/40.4.461`.

R G Brown, M Jahanshahi, and C D Marsden. The execution of bimanual movements in patients with Parkinson's, Huntington's and cerebellar disease. *Journal of Neurology, Neurosurgery & Psychiatry*, 56(3):295–297, 1993. ISSN 0022-3050. doi: 10.1136/jnnp.56.3.295. URL `http://jnnp.bmj.com/content/56/3/295.short`.

Deborah J. Serrien and Mario Wiesendanger. Temporal control of a bimanual task in patients with cerebellar dysfunction. *Neuropsychologia*, 38(5):558–565, 2000. ISSN 00283932. doi: 10.1016/S0028-3932(99)00116-5.

D. Laplane, J. Talairach, V. Meininger, J. Bancaud, and J. M. Orgogozo. Clinical consequences of corticectomies involving the supplementary motor area in man. *Journal of the Neurological Sciences*, 34(3):301–314, 1977. ISSN 0022510X. doi: 10.1016/0022-510X(77)90148-4.

J. P.R. Dick, R. Benecke, J. C. Rothwell, B. L. Day, and C. D. Marsden. Simple and complex movements in a patient with infarction of the right supplementary motor area. *Movement Disorders*, 1(4):255–266, 1986. ISSN 15318257. doi: 10.1002/mds.870010405.

K. M. Stephan, F. Binkofski, S. Posse, R. J. Seitz, and H. J. Freund. Cerebral midline structures in bimanual coordination. *Experimental Brain Research*, 128(1-2):243–249, 1999. ISSN 00144819. doi: 10.1007/s002210050844.

D J Serrien, a C Nirkko, and M Wiesendanger. Role of the corpus callosum in bimanual coordination: a comparison of patients with congenital and acquired callosal damage. *The European journal of neuroscience*, 14(11):1897–905, dec 2001a. ISSN 0953-816X. URL http://www.ncbi.nlm.nih.gov/entrez/query.fcgi?cmd=Retrieve{&}db=PubMed{&}dopt=Citation{&}list{_}uids=11860484http://www.ncbi.nlm.nih.gov/pubmed/11860484.

Deborah J. Serrien, Arto C. Nirkko, K O Lövblad, and Mario Wiesendanger. Damage to the parietal lobe impairs bimanual coordination. *Neuroreport*, 12(12):2721–2724, 2001b. ISSN 0959-4965. doi: 10.1097/00001756-200108280-00026. URL http://content.wkhealth.com/linkback/openurl?sid=WKPTLP:landingpage{&}an=00001756-200108280-00026.

G M Jackson, S R Jackson, M Husain, M Harvey, T Kramer, and L Dow. The coordination of bimanual prehension movements in a centrally deafferented patient. *Brain : a journal of neurology*, 123 (Pt 2:380–393, 2000. ISSN 0006-8950. doi: 10.1093/brain/123.2.380.

Maria Wyke. The effects of brain lesions on the performance of bilateral arm movements. *Neuropsychologia*, 9(1):33–42, 1971. ISSN 00283932. doi: 10.1016/0028-3932(71)90059-5. URL http://dx.doi.org/10.1016/S0010-9452(71)80022-9.

L. Jäncke, M. Peters, G. Schlaug, S. Posse, H. Steinmetz, and H. W. Müller-Gärtner. Differential magnetic resonance signal change in human sensorimotor cortex to finger movements of different rate of the dominant and subdominant hand. *Cognitive Brain Research*, 6(4):279–284, 1998. ISSN 09266410. doi: 10.1016/S0926-6410(98)00003-2.

Uri Rokni, Orna Steinberg, Eilon Vaadia, and Haim Sompolinsky. Cortical representation of bimanual movements. *The Journal of neuroscience : the official*

journal of the Society for Neuroscience, 23(37):11577–86, dec 2003. ISSN 1529-2401. URL http://www.ncbi.nlm.nih.gov/pubmed/14684860.

Stephan P. Swinnen and Nicole Wenderoth. Two hands, one brain: cognitive neuroscience of bimanual skill. *Trends in Cognitive Sciences*, 8(1):18–25, jan 2004. ISSN 13646613. doi: 10.1016/j.tics.2003.10.017. URL http://linkinghub.elsevier.com/retrieve/pii/S1364661303002961.

R. G. Carson. Neural pathways mediating bilateral interactions between the upper limbs. *Brain Research Reviews*, 49(3):641–662, 2005. ISSN 01650173. doi: 10.1016/j.brainresrev.2005.03.005.

a. Yokoi, M. Hirashima, and D. Nozaki. Gain Field Encoding of the Kinematics of Both Arms in the Internal Model Enables Flexible Bimanual Action. *Journal of Neuroscience*, 31(47):17058–17068, 2011. ISSN 0270-6474. doi: 10.1523/JNEUROSCI.2982-11.2011. URL http://www.u-tokyo.ac.jp/public/public01{_}231123{_}02{_}j.html.

a. Yokoi, M. Hirashima, and D. Nozaki. Lateralized Sensitivity of Motor Memories to the Kinematics of the Opposite Arm Reveals Functional Specialization during Bimanual Actions. *Journal of Neuroscience*, 34(27):9141–9151, jul 2014. ISSN 0270-6474. doi: 10.1523/JNEUROSCI.2694-13.2014. URL http://www.jneurosci.org/cgi/doi/10.1523/JNEUROSCI.2694-13.2014.

E. Todorov and Z. Ghahramani. Analysis of the synergies underlying complex hand manipulation. In *The 26th Annual International Conference of the IEEE Engineering in Medicine and Biology Society*, volume 4, pages 4637–4640. IEEE, 2004. ISBN 0-7803-8439-3. doi: 10.1109/IEMBS.2004.1404285. URL http://ieeexplore.ieee.org/document/1404285/.

Jeremy D Wong, Elizabeth T Wilson, Dinant a Kistemaker, and Paul L Gribble. Bimanual proprioception: are two hands better than one? *Journal of neurophysiology*, 111(6):1362–8, mar 2014. ISSN 1522-1598. doi: 10.1152/jn.00537.2013. URL http://www.pubmedcentral.nih.gov/articlerender.fcgi?artid=4250236{&}tool=pmcentrez{&}rendertype=abstract.

S. M. P. Verschueren, Stephan P. Swinnen, Paul J. Cordo, and Natalia V. Dounskaia. Proprioceptive control of multijoint movement: bimanual circle drawing. *Experimental Brain Research*, 127(2):182–192, jul 1999. ISSN 0014-4819. doi: 10.1007/s002210050788. URL http://link.springer.com/article/10.1007/s002210050788http://link.springer.com/10.1007/s002210050788.

Maarten Steyvers, Sabine Verschueren, Oron Levin, Mourad Ouamer, and Stephan Swinnen. Proprioceptive control of cyclical bimanual forearm movements across different movement frequencies as revealed by means of tendon

vibration. *Experimental Brain Research*, 140(3):326–334, oct 2001. ISSN 00144819. doi: 10.1007/s002210100819. URL http://link.springer.com/10.1007/s002210100819.

Oleg V. Kazennikov and Mario Wiesendanger. Goal synchronization of bimanual skills depends on proprioception. *Neuroscience Letters*, 388(3):153–156, 2005. ISSN 03043940. doi: 10.1016/j.neulet.2005.06.040.

Esther Kuehn, Jack De Havas, Emilie Silkoset, Hiroaki Gomi, and Patrick Haggard. On the bimanual integration of proprioceptive information. *Experimental brain research*, 233(4):1273–88, apr 2015. ISSN 1432-1106. doi: 10.1007/s00221-015-4205-0. URL http://www.ncbi.nlm.nih.gov/pubmed/25618007.

A. M. Pellegrini, E. C. Andrade, and L. A. Teixeira. Attending to the non-preferred hand improves bimanual coordination in children. *Human movement science*, 23(3-4):447–60, oct 2004. ISSN 0167-9457. doi: 10.1016/j.humov.2004.08.017. URL http://www.ncbi.nlm.nih.gov/pubmed/15541528.

S. Riek, J. R. Tresilian, M. Mon-Williams, V. L. Coppard, and R. G. Carson. Bimanual aiming and overt attention: one law for two hands. *Experimental brain research*, 153(1):59–75, nov 2003. ISSN 0014-4819. doi: 10.1007/s00221-003-1581-7. URL http://www.ncbi.nlm.nih.gov/pubmed/12923603.

Divya Srinivasan and Bernard J Martin. Eye-hand coordination of symmetric bimanual reaching tasks: temporal aspects. *Experimental brain research. Experimentelle Hirnforschung. Expérimentation cérébrale*, 203(2):391–405, jun 2010. ISSN 1432-1106. doi: 10.1007/s00221-010-2241-3. URL http://www.ncbi.nlm.nih.gov/pubmed/20431875.

Olivier White and Jörn Diedrichsen. Responsibility assignment in redundant systems. *Current biology : CB*, 20(14):1290–5, jul 2010. ISSN 1879-0445. doi: 10.1016/j.cub.2010.05.069. URL http://www.ncbi.nlm.nih.gov/pubmed/20598886http://linkinghub.elsevier.com/retrieve/pii/S0960982210007748.

Alexandra Reichenbach, Angela Costello, Peter Zatka-Haas, and Jörn Diedrichsen. Mechanisms of responsibility assignment during redundant reaching movements. *Journal of neurophysiology*, 109(44):2021–8, 2013. ISSN 1522-1598. doi: 10.1152/jn.01052.2012. URL http://jn.physiology.org/content/early/2013/01/23/jn.01052.2012.

Shoko Kasuga and Daichi Nozaki. Cross talk in implicit assignment of error information during bimanual visuomotor learning. *Journal of neurophysiology*, 106(3):1218–26, sep 2011. ISSN 1522-1598. doi: 10.1152/jn.00278.2011. URL http://www.ncbi.nlm.nih.gov/pubmed/21653713.

Reza Shadmehr and John W. Krakauer. A computational neuroanatomy for motor control. *Experimental Brain Research*, 185(3):359–381, 2008. ISSN 00144819. doi: 10.1007/s00221-008-1280-5.

Emanuel Todorov. Stochastic optimal control and estimation methods adapted to the noise characteristics of the sensorimotor system. *Neural computation*, 17(5):1084–1108, 2005. ISSN 0899-7667. doi: 10.1162/0899766053491887.

W. Li and E. Todorov. Iterative linearization methods for approximately optimal control and estimation of non-linear stochastic system. *International Journal of Control*, 80(9):1439–1453, sep 2007. ISSN 0020-7179. doi: 10.1080/00207170701364913. URL http://www.tandfonline.com/doi/abs/10.1080/00207170701364913.

F. Crevecoeur, R.J. Sepulchre, J.-L. Thonnard, and P. Lefèvre. Improving the state estimation for optimal control of stochastic processes subject to multiplicative noise. *Automatica*, 47(3):591–596, mar 2011. ISSN 00051098. doi: 10.1016/j.automatica.2011.01.026. URL http://linkinghub.elsevier.com/retrieve/pii/S0005109811000410.

Emanuel Todorov and Michael I Jordan. Optimal feedback control as a theory of motor coordination. *Nature neuroscience*, 5(11):1226–35, nov 2002. ISSN 1097-6256. doi: 10.1038/nn963. URL http://www.ncbi.nlm.nih.gov/pubmed/12404008.

Joseph Y Nashed, Frédéric Crevecoeur, and Stephen H Scott. Influence of the behavioral goal and environmental obstacles on rapid feedback responses. *Journal of neurophysiology*, 108(4):999–1009, aug 2012. ISSN 1522-1598. doi: 10.1152/jn.01089.2011. URL http://www.ncbi.nlm.nih.gov/pubmed/22623483.

J. Andrew Pruszynski and Stephen H. Scott. Optimal feedback control and the long-latency stretch response. *Experimental brain research*, 218(3):341–59, may 2012. ISSN 1432-1106. doi: 10.1007/s00221-012-3041-8. URL http://link.springer.com/10.1007/s00221-012-3041-8http://www.ncbi.nlm.nih.gov/pubmed/22370742.

Jörn Diedrichsen. Optimal task-dependent changes of bimanual feedback control and adaptation. *Current biology : CB*, 17(19):1675–9, oct 2007. ISSN 0960-9822. doi: 10.1016/j.cub.2007.08.051. URL http://www.pubmedcentral.nih.gov/articlerender.fcgi?artid=2230536{&}tool=pmcentrez{&}rendertype=abstract.

Jörn Diedrichsen and Noreen Dowling. Bimanual coordination as task-dependent linear control policies. *Human movement science*, 28(3):334–47, jun 2009. ISSN 1872-7646. doi: 10.1016/j.humov.2008.10.003. URL http://www.ncbi.nlm.nih.gov/pubmed/19131136.

Yuki Ueyama. Mini-max feedback control as a computational theory of sensorimotor control in the presence of structural uncertainty. *Frontiers in computational neuroscience*, 8(September):119, 2014. ISSN 1662-5188. doi: 10.3389/fncom.2014.00119. URL http://journal.frontiersin.org/Journal/10.3389/fncom.2014.00119/abstract.

Tyler Cluff, Frédéric Crevecoeur, and Stephen H. Scott. A perspective on multisensory integration and rapid perturbation responses. *Vision Research*, 110(PB):215–222, 2015. ISSN 18785646. doi: 10.1016/j.visres.2014.06.011. URL http://dx.doi.org/10.1016/j.visres.2014.06.011.

Neville Hogan. Impedance Control: An Approach to Manipulation: Part II—Implementation. *Journal of Dynamic Systems, Measurement, and Control*, 107(1):8, 1985. ISSN 00220434. doi: 10.1115/1.3140713. URL http://dynamicsystems.asmedigitalcollection.asme.org/article.aspx?articleid=1403621http://dynamicsystems.asmedigitalcollection.asme.org/article.aspx?articleid=1403623.

E Burdet, R Osu, D W Franklin, T E Milner, and M Kawato. The central nervous system stabilizes unstable dynamics by learning optimal impedance. *Nature*, 414(6862):446–9, nov 2001. ISSN 0028-0836. doi: 10.1038/35106566. URL http://www.ncbi.nlm.nih.gov/pubmed/11719805.

J Andrew Pruszynski, Isaac Kurtzer, Timothy P Lillicrap, and Stephen H Scott. Temporal evolution of "automatic gain-scaling". *Journal of neurophysiology*, 102(2):992–1003, aug 2009. ISSN 0022-3077. doi: 10.1152/jn.00085.2009. URL http://jn.physiology.org/cgi/doi/10.1152/jn.00085.2009http://www.ncbi.nlm.nih.gov/pubmed/19439680http://www.pubmedcentral.nih.gov/articlerender.fcgi?artid=PMC2724331.

Frédéric Crevecoeur and Stephen H. Scott. Beyond Muscles Stiffness: Importance of State-Estimation to Account for Very Fast Motor Corrections. *PLoS Computational Biology*, 10(10):e1003869, oct 2014. ISSN 1553-7358. doi: 10.1371/journal.pcbi.1003869. URL http://dx.plos.org/10.1371/journal.pcbi.1003869.

E. Burdet, R. Osu, D. W. Franklin, T. Yoshioka, T. E. Milner, and M. Kawato. A method for measuring endpoint stiffness during multi-joint arm movements. *Journal of biomechanics*, 33(12):1705–9, dec 2000. ISSN 0021-9290. doi: 10.1016/S0021-9290(00)00142-1. URL http://www.ncbi.nlm.nih.gov/pubmed/11006397.

Stephen H. Scott. A Functional Taxonomy of Bottom-Up Sensory Feedback Processing for Motor Actions. *Trends in Neurosciences*, xx:1–15, 2016. ISSN 01662236. doi: 10.1016/j.tins.2016.06.001. URL http://linkinghub.elsevier.com/retrieve/pii/S0166223616300522.

Karl J. Astrom. *Introduction to Stochastic Control Theory*, volume 70 of *Mathematics in Science and Engineering*. Elsevier, jan 1970. ISBN 9780120656509. doi: 10.1016/S0076-5392(09)X6015-7. URL http://epubs.siam.org/doi/abs/10.1137/1014021http://linkinghub.elsevier.com/retrieve/pii/S0076539209X60157.

Tamer Başar and Pierre Bernhard. *H infinity -Optimal Control and Related Minimax Design Problems*. Birkhäuser Boston, Boston, MA, 2008. ISBN 978-0-8176-4756-8. doi: 10.1007/978-0-8176-4757-5. URL http://link.springer.com/10.1007/978-0-8176-4757-5.

James B. Rawlings and David Q. Mayne. *Model Predictive Control : Theory and Design*. 2012. ISBN 978-0-975-93770-9.

Ian E. Brown, Ernest J. Cheng, and Gerald E. Loeb. Measured and modeled properties of mammalian skeletal muscle. II. The effects of stimulus frequency on force-length and force-velocity relationships. *Journal of Muscle Research and Cell Motility*, 20(7):627–643, 1999. ISSN 01424319. doi: 10.1023/A:1005585030764.

Elise H E Walker and Eric J Perreault. Arm dominance affects feedforward strategy more than feedback sensitivity during a postural task. *Experimental brain research*, apr 2015. ISSN 1432-1106. doi: 10.1007/s00221-015-4271-3. URL http://www.ncbi.nlm.nih.gov/pubmed/25850407.

Christopher N Schabowsky, Joseph M Hidler, and Peter S Lum. Greater reliance on impedance control in the nondominant arm compared with the dominant arm when adapting to a novel dynamic environment. *Experimental brain research*, 182(4):567–77, oct 2007. ISSN 1432-1106. doi: 10.1007/s00221-007-1017-x. URL http://www.ncbi.nlm.nih.gov/pubmed/17611744.

Paul L Gribble, Lucy I Mullin, Nicholas Cothros, and Andrew Mattar. Role of cocontraction in arm movement accuracy. *Journal of neurophysiology*, 89(5):2396–2405, 2003. ISSN 0022-3077. doi: 10.1152/jn.01020.2002.

Debashis Kushary, A. C. Davison, and D. V. Hinkley. Bootstrap Methods and Their Application. *Cambridge University Press*, 42(2):216, 1997. ISSN 00401706. doi: 10.2307/1271471. URL http://www.jstor.org/stable/1271471?origin=crossref.

Alexander Adam, C J De Luca, and Zeynep Erim. Hand dominance and motor unit firing behavior. *Journal of neurophysiology*, 80(3):1373–82, sep 1998. ISSN 0022-3077. URL http://www.ncbi.nlm.nih.gov/pubmed/9744946.

S. T. Albert and R. Shadmehr. The Neural Feedback Response to Error As a Teaching Signal for the Motor Learning System. *Journal of Neuroscience*, 36(17):4832–4845, 2016. ISSN 0270-6474. doi: 10.1523/

JNEUROSCI.0159-16.2016. URL http://www.jneurosci.org/cgi/doi/10.1523/JNEUROSCI.0159-16.2016.

Jinsung Wang and Robert L. Sainburg. Interlimb transfer of visuomotor rotations depends on handedness. *Experimental Brain Research*, 175(2):223–230, 2006. ISSN 00144819. doi: 10.1007/s00221-006-0543-2.

Christian Stockinger, Benjamin Thürer, Anne Focke, and Thorsten Stein. Intermanual transfer characteristics of dynamic learning: direction, coordinate frame, and consolidation of interlimb generalization. *Journal of Neurophysiology*, page jn.00727.2015, 2015. ISSN 0022-3077. doi: 10.1152/jn.00727.2015. URL http://jn.physiology.org/content/early/2015/09/25/jn.00727.2015.abstract?papetoc{%}5Cnhttp://jn.physiology.org/lookup/doi/10.1152/jn.00727.2015.

Olivier White and Jörn Diedrichsen. Flexible Switching of Feedback Control Mechanisms Allows for Learning of Different Task Dynamics. *PLoS ONE*, 8 (2), 2013. ISSN 19326203. doi: 10.1371/journal.pone.0054771.

James R. Lackner and Paul DiZio. Motor control and learning in altered dynamic environments. *Current Opinion in Neurobiology*, 15(6):653–659, dec 2005. ISSN 09594388. doi: 10.1016/j.conb.2005.10.012. URL http://linkinghub.elsevier.com/retrieve/pii/S0959438805001613.

Paul R Davidson, Daniel M Wolpert, Stephen H Scott, and J Randall Flanagan. Common Encoding of Novel Dynamic Loads Applied to the Hand and Arm. *The Journal of Neuroscience*, 25(22):5425–5429, jun 2005. ISSN 0270-6474. doi: 10.1523/JNEUROSCI.0429-05.2005. URL http://search.ebscohost.com/login.aspx?direct=true{%}7B{&}{%}7Ddb=psyh{%}7B{&}{%}7DAN=2005-06015-012{%}7B{&}{%}7Dsite=ehost-live{%}5Cnhttp://flanagan@post.queensu.ca.

J. Kluzik, J. Diedrichsen, R. Shadmehr, and A. J. Bastian. Reach Adaptation: What Determines Whether We Learn an Internal Model of the Tool or Adapt the Model of Our Arm? *Journal of Neurophysiology*, 100(3):1455–1464, 2008. ISSN 0022-3077. doi: 10.1152/jn.90334.2008. URL http://jn.physiology.org/cgi/doi/10.1152/jn.90334.2008.

M Desmurget, M Jordan, C Prablanc, and M Jeannerod. Constrained and unconstrained movements involve different control strategies. *Journal of neurophysiology*, 77(3):1644–1650, 1997. ISSN 0022-3077.

Christopher Scharver, James Patton, Robert Kenyon, and Eric Kersten. Comparing adaptation of constrained and unconstrained movements in three dimensions. *Proceedings of the 2005 IEEE 9th International Conference on Rehabilitation Robotics*, 2005(Icorr):434–439, 2005. doi: 10.1109/ICORR.2005.1501136.

Luis D. Lledó, Jorge A. Díez, Arturo Bertomeu-Motos, Santiago Ezquerro, Francisco J. Badesa, José M. Sabater-Navarro, and Nicolás García-Aracil. A comparative analysis of 2D and 3D tasks for virtual reality therapies based on robotic-assisted neurorehabilitation for post-stroke patients. *Frontiers in Aging Neuroscience*, 8(AUG):1–16, 2016. ISSN 16634365. doi: 10.3389/fnagi.2016.00205.

Jacob E. Schaffer and Robert L. Sainburg. Interlimb differences in coordination of unsupported reaching movements. *Neuroscience*, 350:54–64, 2017. ISSN 18737544. doi: 10.1016/j.neuroscience.2017.03.025. URL http://dx.doi.org/10.1016/j.neuroscience.2017.03.025.

Yasuo Kawakami, Kimitaka Nakazawa, Toshiro Fujimoto, Daichi Nozaki, Mitsumasa Miyashita, and Tetsuo Fukunaga. Specific tension of elbow flexor and extensor muscles based on magnetic resonance imaging. *European Journal of Applied Physiology and Occupational Physiology*, 68(2):139–147, feb 1994. ISSN 03015548. doi: 10.1007/BF00244027. URL http://link.springer.com/10.1007/BF00244027.

Stephan P. Swinnen, Kris Jardin, and Ruud Meulenbroek. Between-limb asynchronies during bimanual coordination: Effects of manual dominance and attentional cueing. *Neuropsychologia*, 34(12):1203–1213, dec 1996. ISSN 00283932. doi: 10.1016/0028-3932(96)00047-4. URL http://www.sciencedirect.com/science/article/pii/0028393296000474http://linkinghub.elsevier.com/retrieve/pii/0028393296000474.

Ian O'Sullivan, Etienne Burdet, and Jörn Diedrichsen. Dissociating variability and effort as determinants of coordination. *PLoS computational biology*, 5(4):e1000345, apr 2009. ISSN 1553-7358. doi: 10.1371/journal.pcbi.1000345. URL http://www.pubmedcentral.nih.gov/articlerender.fcgi?artid=2661023{&}tool=pmcentrez{&}rendertype=abstract.

P N Sabes, M I Jordan, and D M Wolpert. The role of inertial sensitivity in motor planning. *The Journal of neuroscience : the official journal of the Society for Neuroscience*, 18(15):5948–57, aug 1998. ISSN 0270-6474. URL http://www.ncbi.nlm.nih.gov/pubmed/9671681.

Ignasi Cos, Benoit Girard, and Paul Cisek. A Modelling Perspective on the Role of Biomechanics on Motor Decision-Making. *NeuroComp / KEOpS'12 workshop*, pages 1–6, 2012. URL http://www.isir.upmc.fr/files/2012ACTN2714.pdf.

Ignasi Cos, Mehdi Khamassi, and Benoı̂t Girard. Modelling the learning of biomechanics and visual planning for decision-making of motor actions. *Journal of Physiology-Paris*, 107(5):399–408, nov 2013. ISSN 09284257. doi: 10.1016/j.jphysparis.2013.07.004. URL http://linkinghub.elsevier.com/retrieve/pii/S0928425713000430.

John M. Hollerbach and Tamar Flash. Dynamic interactions between limb segments during planar arm movement. *Biological Cybernetics*, 44(1):67–77, may 1982. ISSN 0340-1200. doi: 10.1007/BF00353957. URL http://link.springer.com/10.1007/BF00353957.

P L Gribble and D J Ostry. Compensation for interaction torques during single- and multijoint limb movement. *Journal of neurophysiology*, 82(5):2310–26, nov 1999. ISSN 0022-3077. URL http://www.ncbi.nlm.nih.gov/pubmed/10561408.

Natalia Dounskaia, J. A. Goble, and W. Wang. The role of intrinsic factors in control of arm movement direction: implications from directional preferences. *Journal of Neurophysiology*, 105(3):999–1010, mar 2011. ISSN 0022-3077. doi: 10.1152/jn.00630.2010. URL http://jn.physiology.org/content/105/3/999.shorthttp://jn.physiology.org/cgi/doi/10.1152/jn.00630.2010.

Natalia Dounskaia, Wanyue Wang, Robert L Sainburg, and Andrzej Przybyla. Preferred directions of arm movements are independent of visual perception of spatial directions. *Experimental Brain Research*, 232(2):575–586, feb 2014. ISSN 0014-4819. doi: 10.1007/s00221-013-3766-z. URL http://www.ncbi.nlm.nih.gov/pubmed/24258530http://link.springer.com/10.1007/s00221-013-3766-z.

Wanyue Wang, Travis Johnson, Robert L Sainburg, and Natalia Dounskaia. Interlimb differences of directional biases for stroke production. *Experimental Brain Research*, 216(2):263–274, jan 2012. ISSN 0014-4819. doi: 10.1007/s00221-011-2927-1. URL http://www.pubmedcentral.nih.gov/articlerender.fcgi?artid=3697123{&}tool=pmcentrez{&}rendertype=abstracthttp://link.springer.com/10.1007/s00221-011-2927-1.

Andrew Fitzgibbon, Maurizio Pilu, and RB Fisher. Direct least square fitting of ellipses. *IEEE Transactions on Pattern Analysis and Machine Intelligence*, 21(5):476–480, may 1999. ISSN 01628828. doi: 10.1109/34.765658. URL http://ieeexplore.ieee.org/xpls/abs{_}all.jsp?arnumber=765658http://ieeexplore.ieee.org/lpdocs/epic03/wrapper.htm?arnumber=765658.

E. F. Camacho and C. Bordons. *Model Predictive control*. Advanced Textbooks in Control and Signal Processing. Springer London, London, 2007. ISBN 978-1-85233-694-3. doi: 10.1007/978-0-85729-398-5. URL http://link.springer.com/10.1007/978-0-85729-398-5.

M. Dimitriou, D. M. Wolpert, and D. W. Franklin. The Temporal Evolution of Feedback Gains Rapidly Update to Task Demands. *Journal of Neuroscience*, 33(26):10898–10909, jun 2013. ISSN 0270-6474. doi:

10.1523/JNEUROSCI.5669-12.2013. URL http://www.jneurosci.org/cgi/doi/10.1523/JNEUROSCI.5669-12.2013.

Daniel J Goble and Susan H Brown. Upper limb asymmetries in the matching of proprioceptive versus visual targets. *Journal of neurophysiology*, 99(6): 3063–74, jun 2008. ISSN 0022-3077. doi: 10.1152/jn.90259.2008. URL http://www.ncbi.nlm.nih.gov/pubmed/18436632.

Britne a Shabbott and Robert L Sainburg. Differentiating between two models of motor lateralization. *Journal of neurophysiology*, 100(2):565–575, 2008. ISSN 0022-3077. doi: 10.1152/jn.90349.2008.

Jeffrey A. Saunders and David C. Knill. Humans use continuous visual feedback from the hand to control fast reaching movements. *Experimental brain research*, 152(3):341–52, oct 2003. ISSN 0014-4819. doi: 10.1007/s00221-003-1525-2. URL http://www.ncbi.nlm.nih.gov/pubmed/12904935.

Jeffrey A Saunders and David C Knill. Visual feedback control of hand movements. *The Journal of neuroscience : the official journal of the Society for Neuroscience*, 24(13):3223–34, mar 2004. ISSN 1529-2401. doi: 10.1523/JNEUROSCI.4319-03.2004. URL http://www.ncbi.nlm.nih.gov/pubmed/15056701.

David W. Franklin and Daniel M. Wolpert. Specificity of reflex adaptation for task-relevant variability. *The Journal of neuroscience : the official journal of the Society for Neuroscience*, 28(52):14165–14175, dec 2008. ISSN 0270-6474. doi: 10.1523/JNEUROSCI.4406-08.2008. URL http://www.jneurosci.org/cgi/doi/10.1523/JNEUROSCI.4406-08.2008.

Stephen H. Scott, Tyler Cluff, Catherine R. Lowrey, and Tomohiko Takei. Feedback control during voluntary motor actions. *Current Opinion in Neurobiology*, 33:85–94, aug 2015. ISSN 09594388. doi: 10.1016/j.conb.2015.03.006. URL http://linkinghub.elsevier.com/retrieve/pii/S0959438815000574http://www.ncbi.nlm.nih.gov/pubmed/25827274.

James Gordon, Maria Felice Ghilardi, Scott E. Cooper, and Claude Ghez. Accuracy of planar reaching movements - II. Systematic extent errors resulting from inertial anisotropy. *Experimental Brain Research*, 99(1):112–130, 1994. ISSN 00144819. doi: 10.1007/BF00241416.

Reza Shadmehr, Helen J. Huang, and Alaa A. Ahmed. A Representation of Effort in Decision-Making and Motor Control. *Current biology : CB*, 26(14): 1929–34, jul 2016. ISSN 1879-0445. doi: 10.1016/j.cub.2016.05.065. URL http://www.ncbi.nlm.nih.gov/pubmed/27374338.

Stephen H Scott, Paul L Gribble, Kirsten M Graham, and D William Cabel. Dissociation between hand motion and population vectors from neural activity in motor cortex. *Nature*, 413(6852):161–165, sep 2001. ISSN 00280836. doi: 10.1038/35093102. URL http://www.ncbi.nlm.nih.gov/pubmed/11557980http://www.nature.com/doifinder/10.1038/35093102.

Timothy P Lillicrap and Stephen H Scott. Preference distributions of primary motor cortex neurons reflect control solutions optimized for limb biomechanics. *Neuron*, 77(1):168–79, jan 2013. ISSN 1097-4199. doi: 10.1016/j.neuron.2012.10.041. URL http://www.ncbi.nlm.nih.gov/pubmed/23312524.

Ethan A Heming, Timothy P. Lillicrap, Mohsen Omrani, Troy M. Herter, J. Andrew Pruszynski, and Stephen H. Scott. Primary motor cortex neurons classified in a postural task predict muscle activation patterns in a reaching task. *Journal of Neurophysiology*, page jn.00971.2015, 2016. ISSN 0022-3077. doi: 10.1152/jn.00971.2015. URL http://jn.physiology.org/lookup/doi/10.1152/jn.00971.2015.

Paul Cisek. Making decisions through a distributed consensus. *Current opinion in neurobiology*, 22(6):927–36, dec 2012. ISSN 1873-6882. doi: 10.1016/j.conb.2012.05.007. URL http://dx.doi.org/10.1016/j.conb.2012.05.007http://www.ncbi.nlm.nih.gov/pubmed/22683275.

Daniel M. Wolpert and Michael S. Landy. Motor control is decision-making. *Current opinion in neurobiology*, 22(6):996–1003, dec 2012. ISSN 1873-6882. doi: 10.1016/j.conb.2012.05.003. URL http://dx.doi.org/10.1016/j.conb.2012.05.003http://linkinghub.elsevier.com/retrieve/pii/S0959438812000827http://www.ncbi.nlm.nih.gov/pubmed/22647641http://www.pubmedcentral.nih.gov/articlerender.fcgi?artid=PMC3434279.

Vincent S. Huang, Adrian Haith, Pietro Mazzoni, and John W. Krakauer. Rethinking Motor Learning and Savings in Adaptation Paradigms: Model-Free Memory for Successful Actions Combines with Internal Models. *Neuron*, 70 (4):787–801, 2011. ISSN 08966273. doi: 10.1016/j.neuron.2011.04.012. URL http://dx.doi.org/10.1016/j.neuron.2011.04.012.

Jean-Jacques Orban de Xivry and Philippe Lefèvre. Formation of model-free motor memories during motor adaptation depends on perturbation schedule. *Journal of Neurophysiology*, 113(7):2733–2741, 2015. ISSN 0022-3077. doi: 10.1152/jn.00673.2014. URL http://jn.physiology.org/content/113/7/2733.abstract.

J.-J. Orban de Xivry, Sarah E. Criscimagna-Hemminger, and Reza Shadmehr. Contributions of the Motor Cortex to Adaptive Control of Reaching Depend on the Perturbation Schedule. *Cerebral Cortex*, 21(7):1475–1484, jul 2011.

ISSN 1047-3211. doi: 10.1093/cercor/bhq192. URL https://academic.oup.com/cercor/article-lookup/doi/10.1093/cercor/bhq192.

R S Johansson and G Westling. Roles of glabrous skin receptors and sensorimotor memory in automatic control of precision grip when lifting rougher or more slippery objects. *Experimental brain research*, 56(3):550–64, 1984. ISSN 0014-4819. doi: 10.1007/BF00237997. URL http://www.ncbi.nlm.nih.gov/pubmed/6499981.

J. Randall JR Flanagan and AlanM. AM Wing. Modulation of grip force with load force during point-to-point arm movements. *Experimental Brain Research*, 95(1):131–143, jul 1993. ISSN 0014-4819. doi: 10.1007/BF00229662. URL http://link.springer.com/content/pdf/10.1007/BF00229662.pdfhttp://link.springer.com/10.1007/BF00229662http://link.springer.com/article/10.1007/BF00229662.

J. Randall Flanagan and a M Wing. The stability of precision grip forces during cyclic arm movements with a hand-held load. *Experimental brain research. Experimentelle Hirnforschung. Expérimentation cérébrale*, 105(3):455–64, jan 1995. ISSN 0014-4819. URL http://www.ncbi.nlm.nih.gov/pubmed/7498399.